



MARMARA UNIVERSITY
INSTITUTE FOR GRADUATE STUDIES
IN PURE AND APPLIED SCIENCES



**CENTRIFUGAL PUMP DESIGN AND
PERFORMANCE OPTIMIZATION USING
LOSS CORRELATIONS**

OĞUZCAN MERCAN

MASTER THESIS

Department of Mechanical Engineering

Thesis Supervisor

Assoc. Prof. Dr. Emre ALPMAN

Thesis CO- Supervisor

Prof. Dr. Erkan AYDER

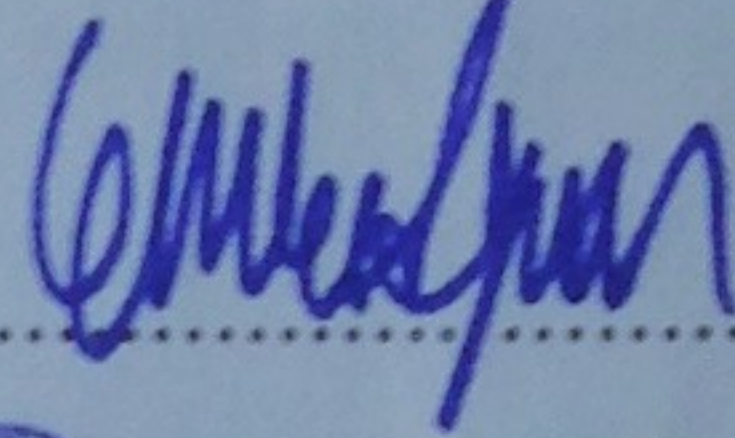
ISTANBUL, 2018

MARMARA UNIVERSITY
INSTITUTE FOR GRADUATE STUDIES IN PURE AND
APPLIED SCIENCES

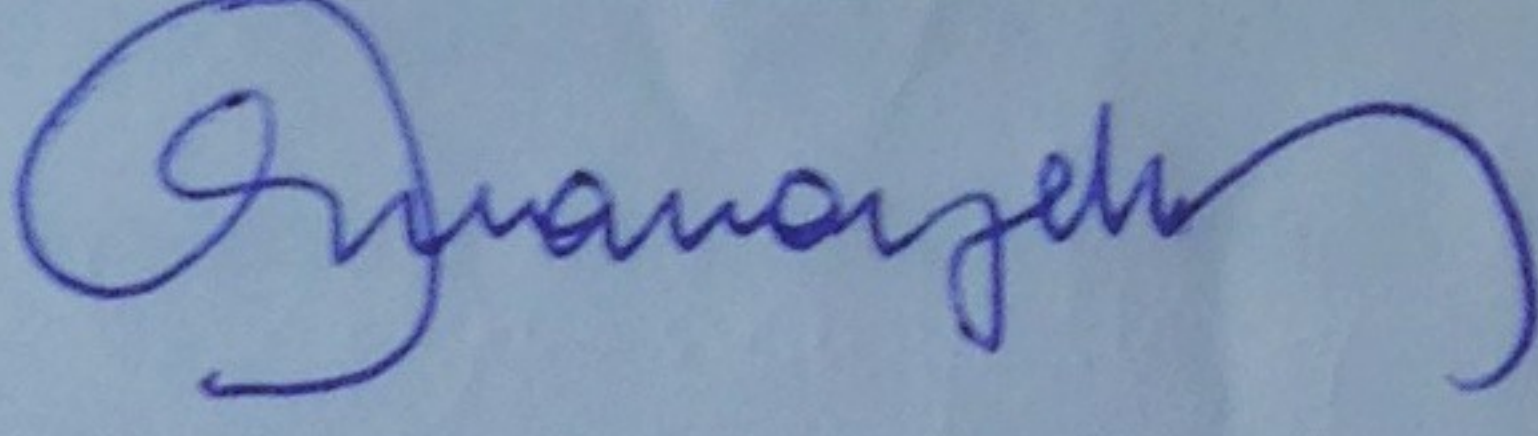
Oğuzcan Mercan, a Master of Science student of Marmara University Institute for Graduate Studies in Pure and Applied Sciences, defended his thesis entitled “**Centrifugal Pump Design and Performance Optimization Using Loss Correlations**”, on December 04, 2018 and has been found to be satisfactory by the jury members.

Jury Members

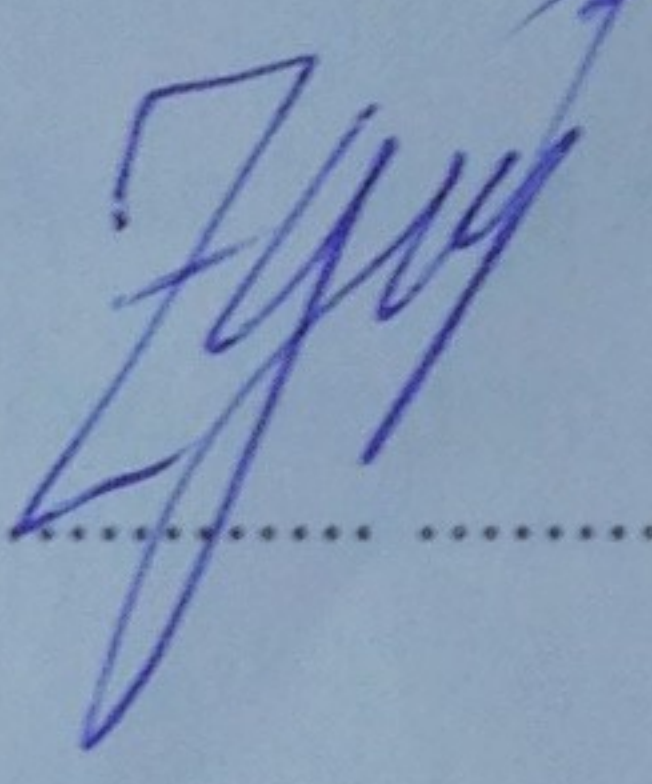
Assoc. Prof. Dr. Emre ALPMAN (Advisor)

Marmara University 

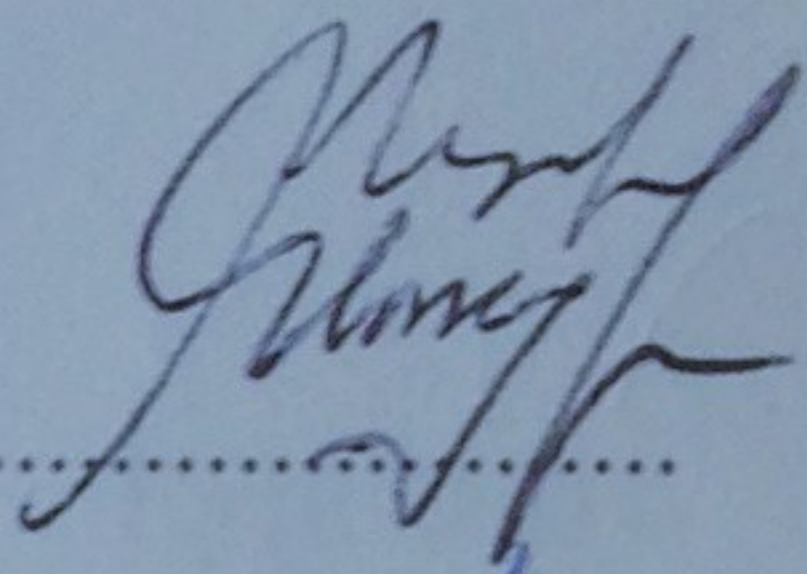
Prof. Dr. Erkan AYDER (Co-Advisor)

Istanbul Technical University 

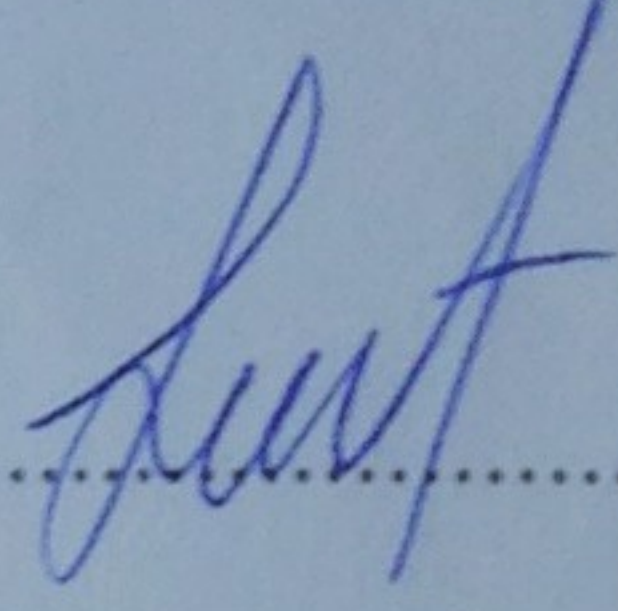
Prof. Dr. Zafer GÜL (Jury Member)

Marmara University 

Assoc. Prof. Mustafa YILMAZ (Jury Member)

Marmara University 

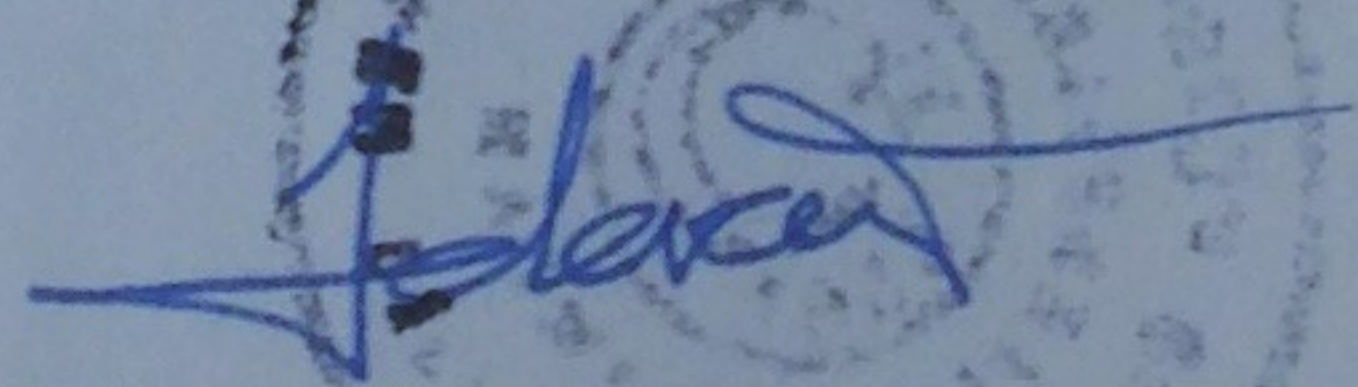
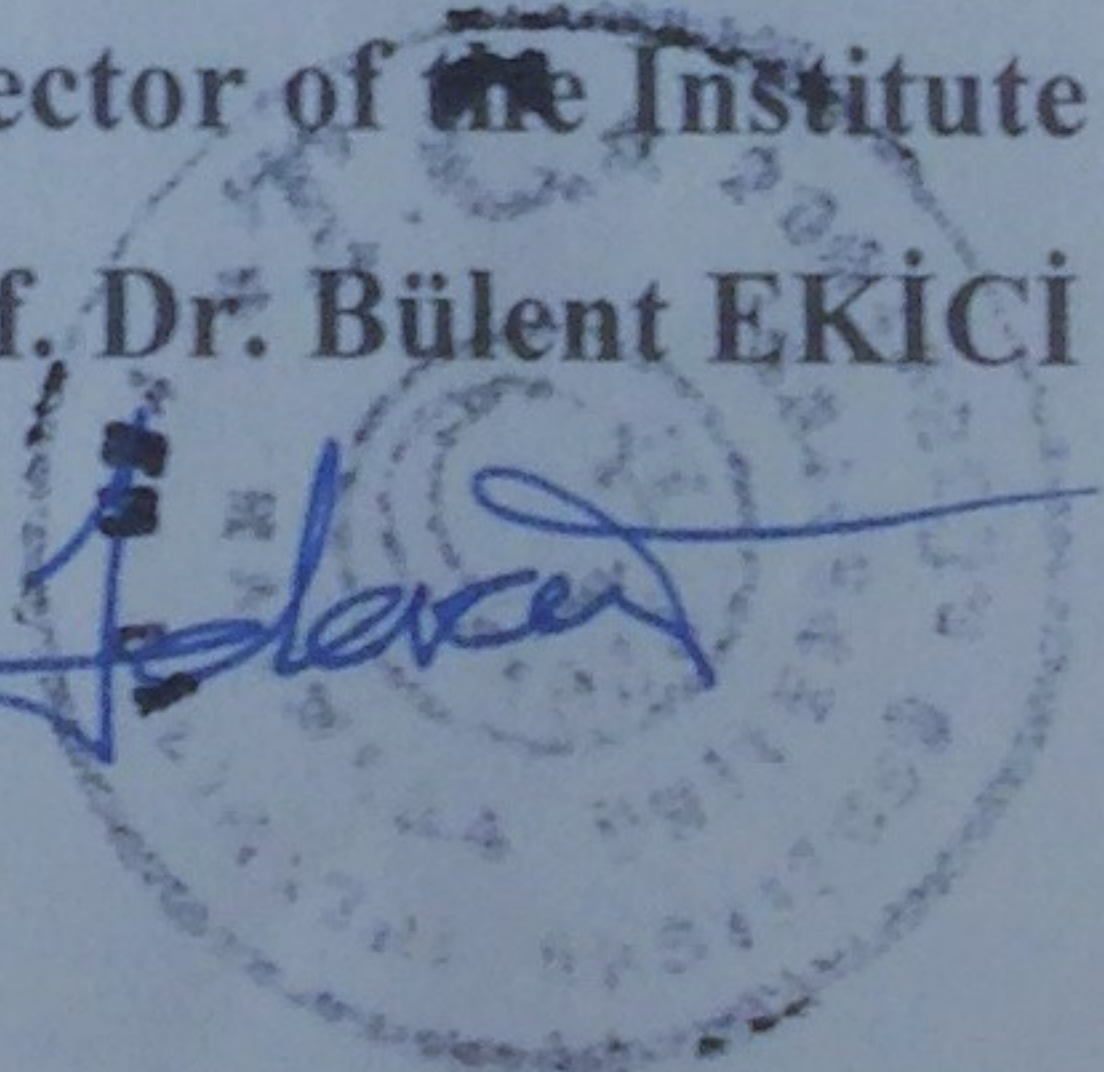
Asst. Prof. Dr. Levent KAVURMACIOĞLU (Jury Member)

Istanbul Technical University 

APPROVAL

Marmara University Institute for Graduate Studies in Pure and Applied Sciences Executive Committee approves that Oğuzcan Mercan be granted the degree of Master of Science in Department of Mechanical Engineering, Mechanical Engineering Program on 05.12.2018.... (Resolution no: 2018/29-46)

Director of the Institute
Prof. Dr. Bülent EKİCİ

Acknowledgment

It would have not been possible to write this master thesis without the help and support of the kind people around me, to only some of whom it is possible to give particular mention here.

Above all, I would like to thank my wife Esin for her personal support and great patience at all times. My parents who have given their unequivocal support throughout, as always, for which my mere expressions of thanks likewise does not suffice.

This thesis would not have been possible without the help, support, guidance, positive attitude and patience of my supervisor, Prof. Dr. Erkan Ayder not to mention his advice and unsurpassed knowledge of centrifugal pumps. The good advice and support of my supervisor Assoc. Prof. Dr. Emre Alpman has been invaluable on academic level for which I am extremely grateful.

I would like to express my gratitude to the management of Miksan Motor A. S., Turkey for permission of the data used in this thesis and for unlimited support and peaceful ambience throughout the study.

Oğuzcan Mercan

Eylül 2018

Table of Contents

| | |
|--|------|
| Acknowledgement | i |
| Özet | iv |
| Abstract | v |
| Symbols | vi |
| Abbreviations | viii |
| List of figures | ix |
| List of tables | xii |
| 1. Introduction | 1 |
| 2. Pump Theory | 3 |
| 2.1. Design parameters | 3 |
| 2.1.1. Design of impeller | 6 |
| 2.1.2. Design of volute | 12 |
| 2.2. Loss Models | 13 |
| 2.2.1. Theoretical Head | 15 |
| 2.2.2. Slip factor | 16 |
| 2.2.3. Inlet Loss | 17 |
| 2.2.4. Impeller Loss | 17 |
| 2.2.4.1. Mismatching loss..... | 17 |
| 2.2.4.2. Impeller friction loss | 18 |
| 2.2.4.3. Impeller blade loading loss | 19 |
| 2.2.5. Volute Loss | 19 |
| 2.2.5.1. Volute mismatching loss | 19 |
| 2.2.5.2. Volute friction loss | 20 |
| 2.2.5.3. Diffusor loss | 20 |
| 2.2.6. Disk Friction Loss | 21 |
| 2.2.7. Resulting Head | 22 |
| 2.3. Code Implementation | 22 |
| 2.4. CFD Analysis and Pre-processing Steps | 24 |
| 2.4.1. Solid Modeling | 24 |

| | | |
|--------|---|----|
| 2.4.2. | Meshing | 26 |
| 2.4.3. | Solver Settings | 28 |
| 2.5. | Experimental setup and procedure | 30 |
| 2.5.1. | Test Setup | 30 |
| 2.5.2. | Experimental Procedure | 31 |
| 2.5.3. | Data Processing and Calculations | 32 |
| 3. | Results and Discussion..... | 33 |
| 3.1. | Predictions with the Loss Correlation | 33 |
| 3.2. | Experimental Results | 38 |
| 3.3. | CFD Results | 40 |
| 3.3.1. | CFD Results of Pump-1 | 41 |
| 3.3.2. | CFD Results of Pump-2 | 47 |
| 3.3.3. | CFD Results of Pump-3 | 51 |
| 4. | Conclusion | 55 |
| | References | 56 |
| | Appendices | 59 |

ÖZET

KAYIP KORELASYONLARI YARDIMIYLA SANTRİFÜJ POMPA TASARIMI VE OPTİMİZASYONU

Bu çalışmada, kayıp korelasyonları kullanılarak bir santrifüj pompanın performansının hesaplanması için bir tahmin yöntemi geliştirilmiştir. Yöntem, pompanın ön tasarımında elde edilen ana boyutları kullanıp enerji kayıplarını hesaplayarak basma yüksekliğinin ve verimin debi ile değişimlerini belirlemektedir. Geliştirilen yöntem ayrıca tasarımcıya pompa içinde oluşan enerji kayıplarını ve miktarlarını göstererek hangi büyüklüklerde değişiklikler yapılması gerektiği hakkında bir fikir vermektedir. Akım makinalarının tasarımında hızlı araçlara sahip olmak önemlidir. Günümüzde gelişmiş olan mühendislik araçları başlıca katı modelleme, Sonlu Eleman Metodu (SEM), akış analizi vb. amaçlara yöneliktir. Akış analizi amaçlı yazılımlar pompa tasarım süreçlerinin önemli bir parçasıdır. Tasarımcının ön boyutları belirledikten sonra uzun ve zahmetli uğraşlar gerektiren Hesaplamalı Akışkanlar Dinamiği (HAD) adımının öncesinde hızlı performans tahmini yapan araçlara sahip olması çok arzu edilen bir durumdur. Pompa tasarımında bu adım korelasyonlara dayanan bir yöntemin kullanılması olabilir. Bu çalışmada santrifüj pompaların H_m-Q ve $\eta-Q$ performans eğilimlerini kayıp korelasyonlarını kullanarak belirleyen bir yöntem geliştirilmiş, deneysel ve HAD sonuçları ile sınanmıştır.

ABSTRACT

CENTRIFUGAL PUMP DESIGN AND PERFORMANCE OPTIMIZATION USING LOSS CORRELATIONS

In this study, a theoretical prediction method has been applied to calculate the performance of a centrifugal pump using energy loss correlations. The method calculates the energy losses and determines variation of the delivery head and the efficiency with the flow rate using the basic dimensions obtained in the pump's primary design. By showing the energy losses inside the pump the developed method also presents designer an idea of which dimension modifications are needed. After determining the main dimensions, it is highly desirable that the designer has tools to make quick performance prediction before the Computational Fluid Dynamics (CFD) step, which is a long and laborious task. In pump design, such a quick design tool can be obtained using correlations. In this study, a method of determining the H_m - Q and η - Q performance prediction of centrifugal pumps by using loss correlations was developed and tested with experimental and CFD results.

Symbols

A: Area (m^2)

a: distance between blades (m)

b: height (m)

c: absolute velocity (m/s)

D: diameter (m)

e: blade thickness (m)

g: gravitational acceleration (m^2/s)

H: head (m)

l: length (m)

n: rotational speed (rpm)

r: radius (m)

Re: Reynold's number (-)

Q: flow rate (m^3/s)

u: circumferential velocity (m/s)

w: relative velocity (m/s)

z: number of blades (-)

β : blade angle ($^\circ$)

σ : slip factor (-)

τ : blade blockage factor (-)

v: viscosity (m/s^2)

ξ : friction factor (-)

Losses (m)

ΔH_0 : inlet loss

ΔH_{i1} : impeller mismatching loss

ΔH_{i2} : impeller friction loss

ΔH_{i3} : impeller diffusion loss

ΔH_{v1} : volute mismatching loss

ΔH_{v2} : volute friction loss

ΔH_d : diffusor loss

ΔH_{df} : disk friction loss

Subscripts

0: pump inlet

1: impeller blade leading edge

2: impeller blade trailing edge

3: volute cutwater

4: volute throat

5: diffusor outlet

i: impeller

m: meridional component

th: theoretical value

u: circumferential component

v: volute

Abbreviations

BC: Boundary Conditions

BEP: Best Efficiency Point

CFD: Computational Fluid Dynamics

cSt: Centistoke

LE: Leading Edge

MRF: Multiple Reference Frame

TE: Trailing Edge

List of Figures

| | |
|--|----|
| Figure 2.1. Definitions of directions..... | 3 |
| Figure 2.2. Effect of the specific speed on the design of centrifugal pump impellers | 4 |
| Figure 2.3. Radial section of the impeller | 6 |
| Figure 2.4. Velocity triangle of impeller inlet (LE) | 7 |
| Figure 2.5. Velocity coefficients vs specific speed | 8 |
| Figure 2.6. Pressure coefficients vs specific speed | 9 |
| Figure 2.7. Velocity triangle of impeller outlet (TE) | 10 |
| Figure 2.8. Sectional view of the volute..... | 13 |
| Figure 2.9. Reduction of theoretical Euler head due to losses | 14 |
| Figure 2.10. Meridional and orthogonal section of a centrifugal pump | 14 |
| Figure 2.11. Velocity triangles at impeller inlet and outlet | 15 |
| Figure 2.12. Interface of the calculation software | 23 |
| Figure 2.13. Interface of the loss calculation window | 23 |
| Figure 2.14. CAD model of impeller and volute assembly | 25 |
| Figure 2.15. Fluid domains in Design Modeler | 25 |
| Figure 2.16. Sectional view of generated mesh | 27 |
| Figure 2.17. Detailed view of interface between impeller and volute | 27 |
| Figure 2.18. Detailed view of layer compression | 28 |
| Figure 2.19. Skewness quality of the mesh | 28 |
| Figure 2.20. Turbulence model settings of the analysis | 29 |
| Figure 2.21. Inlet and outlet conditions of the pump | 29 |
| Figure 2.22. Section of centrifugal pump | 30 |
| Figure 2.23. Display of pump test stand | 32 |
| Figure 3.1. Flowchart of the prediction software | 33 |

| | |
|---|----|
| Figure 3.2. Calculation on main dimensions of Pump-1 | 34 |
| Figure 3.3. Calculation on main dimensions of Pump-2 | 34 |
| Figure 3.4. Calculation on main dimensions of Pump-3 | 35 |
| Figure 3.5. Predicted losses of impeller and volute at design point and off-design conditions of Pump-1 | 35 |
| Figure 3.6. Predicted losses of impeller and volute at design point and off-design conditions of Pump-2 | 36 |
| Figure 3.7. Predicted losses of impeller and volute at design point and off-design conditions of Pump-3 | 36 |
| Figure 3.8. Theoretical Q-H curve, total loss and actual Q-H curve of Pump-1 | 37 |
| Figure 3.9. Loss components of predicted Pump-1 | 37 |
| Figure 3.10. Theoretical Q-H curve, total loss and actual Q-H curve of Pump-2 | 38 |
| Figure 3.11. Theoretical Q-H curve, total loss and actual Q-H curve of Pump-3 | 38 |
| Figure 3.12. Experimental H-Q results of Pump-1 | 39 |
| Figure 3.13. Experimental H-Q results of Pump-2 | 39 |
| Figure 3.14. Experimental H-Q results of Pump-3 | 40 |
| Figure 3.15. Convergence plots of nominal flow rate analysis for Momentum and Mass (left) and Turbulence (right)..... | 40 |
| Figure 3.16. y^+ values at the impeller blades..... | 41 |
| Figure 3.17. Distribution of static (left) and total (right) pressure in mid-plane for nominal flow rate of 600 l/min | 42 |
| Figure 3.18. Distribution of static (left) and total (right) pressure in mid-plane for the flow rate of 390 l/min | 42 |
| Figure 3.19. Distribution of static (left) and total (right) pressure in mid-plane for the flow rate of 850 l/min | 43 |
| Figure 3.20. Static pressure distribution on the mid-section of Pump-1..... | 44 |
| Figure 3.21. Total pressure distribution on the mid-section of Pump-1 | 44 |

| | |
|---|----|
| Figure 3.22. Relative velocity distribution on the mid-section of Pump-1..... | 45 |
| Figure 3.23. Delivery head vs flow rate graph of Pump-1 CFD results | 45 |
| Figure 3.24. Impeller head, pump head and volute losses of Pump-1 CFD results | 46 |
| Figure 3.25. Results comparison of Pump-1..... | 46 |
| Figure 3.26. Comparison of loss results of Pump-1..... | 47 |
| Figure 3.27. Static pressure distribution on the mid-section of Pump-2..... | 48 |
| Figure 3.28. Total pressure distribution on the mid-section of Pump-2 | 48 |
| Figure 3.29. Relative velocity distribution on the mid-section of Pump-2..... | 49 |
| Figure 3.30. Delivery head vs flow rate graph of Pump-2 CFD results | 49 |
| Figure 3.31. Comparison of loss results of Pump-2..... | 50 |
| Figure 3.32. Sectional view of Pump-2 | 50 |
| Figure 3.33. Static pressure distribution on the mid-section of Pump-3..... | 51 |
| Figure 3.34. Total pressure distribution on the mid-section of Pump-3 | 52 |
| Figure 3.35. Relative velocity distribution on the mid-section of Pump-3..... | 52 |
| Figure 3.36. Delivery head vs flow rate graph of Pump-3 CFD results | 53 |
| Figure 3.37. Comparison of loss results of Pump-3..... | 53 |
| Figure 3.38. Impeller of experimental Pump-3 and predicted and CFD Pump-3..... | 54 |

List of Tables

| | |
|---|----|
| Table 2.1. Skewness values and the corresponding cell quality | 26 |
| Table 2.2. Main dimension of the test pump | 31 |
| Table 3.1. CFD results at certain flow rates for Pump-1 | 43 |
| Table 3.2. CFD results at certain flow rates for Pump-2 | 48 |
| Table 3.3. CFD results at certain flow rates for Pump-3 | 51 |
| Table 3.4. Comparison of results at certain flow rates | 54 |

1. INTRODUCTION

The flow inside the pump is three-dimensional and highly complicated. Such complicated flows can be successfully simulated using computational fluid dynamics (CFD) [1-4]. For a pump designer it is important to predict the pump performance characteristics without performing the time consuming and challenging CFD calculations during the design stage. However, the model employed should sufficiently capture the basic physical features of pump flows. Therefore, it is important to understand the flow physics inside the impeller to make the design changes for reducing the losses and for running the impeller with higher efficiency. The design of centrifugal pumps can still be considered as a classic topic today. There are well known books on this topic by Pfleiderer [5], Gülich [6] and Tuzson [7].

Off-design performance prediction of centrifugal pumps is still quite uncertain. There are many different loss correlations in the literature that can be used for off-design conditions. Pump characteristics can be predicted up to certain accuracy by its geometry and proper loss models. Hamkins [8] method uses, in most aspects, the well accepted principles currently. The only uncertain part consists of the evaluation of the blade loading losses in the impeller [9]. Wiesner [10] developed a formula for the prediction of slip factors and compared it with measurements on compressors and pumps [11] which is based on the calculation of Busemann [12]. Wiesner reviewed all available methods for calculating the value of slip factor and compared the predictions with values obtained from tests. He concluded that Busemann's procedure was still the most generally applicable predictor for determining the slip factor of centrifugal impellers [12]. A modified form of the Wiesner's equation is used for correlating the data which is mostly applied for pumps [13]. Blade loading losses are calculated here by Pearsall [14] according to the adjustment for centrifugal pumps improved by Myles [15].

The determination meridional shape of the impeller is one of the most crucial design steps and it is mainly based on the experience. The specific speed is also related with meridional shape. The other geometrical dimensions such as impeller diameter, exit width, inlet and outlet blade angles can be determined through the one dimensional turbomachinery theory and can be modified later on. After this, the losses occurring on various occasions on the impeller will be examined and the conformity of the calculated

impeller with the design values will be compared. In this study, a modified impeller geometry is designed by examining the losses of an impeller geometry whose main dimensions are calculated in accordance with the design values. A computer code written in JavaFx programming language is developed and used for this purpose. Predictions obtained using the proposed model are compared with CFD calculations. All the simulations have been performed with ANSYS CFX software package [16-19] that utilizes the finite volume method for the solution of the steady 3D incompressible Navier-Stokes equations.

The purpose of this thesis is to develop a pump performance prediction code using theoretical and empirical energy loss equations from the literature. Mathematical models of loss correlations are examined in the next section. Experimental and CFD results of the three different pumps are examined and compared to the results of programming code of the same pumps at the third chapter. Finally, comparison of losses is examined and the predicted values and performance curves obtained by CFD analysis, experiment and programming code.

2. PUMP THEORY

The purpose of this chapter is to explain the theoretical basis of energy conversion in a centrifugal pump.

When the pump operates, energy is transferred to the shaft in the form of mechanical energy. It is converted to flow work (related to static pressure) and kinetic energy in the impeller. The process is described through Euler's pump equation which is described in this chapter. The pump equation can be explained and a theoretical loss-free head and power consumption can be calculated via velocity triangles for the flow in the impeller inlet and outlet. Definitions of impeller direction is shown in Figure 2.1.

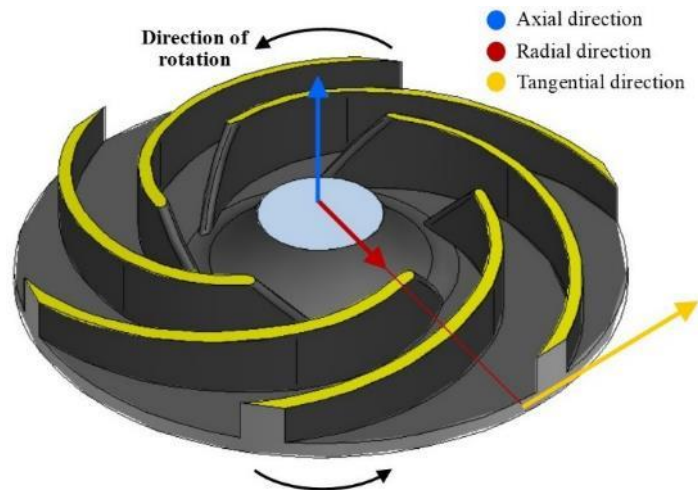


Figure 2.1. Definitions of directions

2.1. Design Parameters

It is usually sufficient to know the three characteristic dimensions in the design calculation of a centrifugal pump.

H_m : Delivery Head (m)

Q : Flow rate (m^3/s)

n : Rotational speed (rpm)

The specific speed n_q is a parameter derived from a dimensional analysis from flow rate Q , delivery head H_m , rotational speed n , at best efficiency point (BEP), which allows a

comparison of impellers of various pump sizes. The specific speed can also be used to classify the optimum impeller design as shown in the Figure 2.2 below.

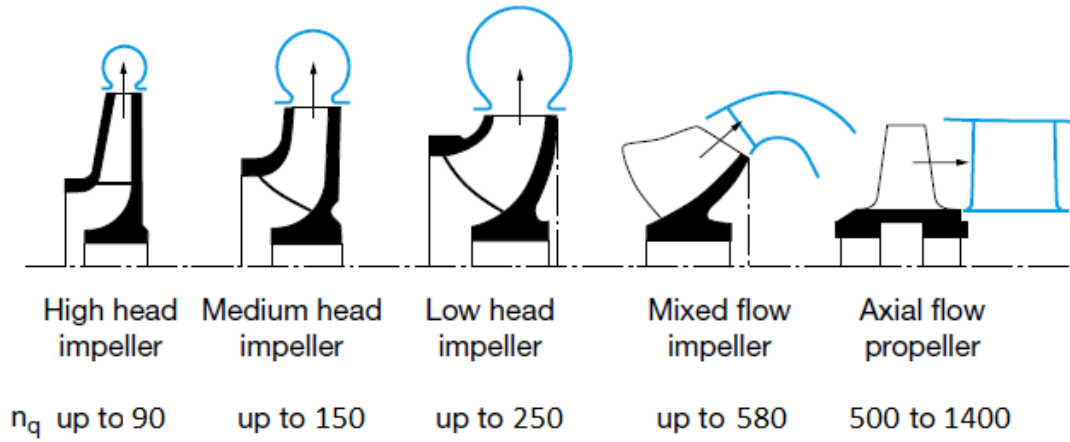


Figure 2.2. Effect of the specific speed on the radial section of centrifugal pump impellers [20]

There are several definitions for specific speed in the literature. However, to be consistent throughout this study, the expression (dimensionless specific speed) in Eq. 2.1 is used, [21]:

$$n_q = 3.65 \cdot n \frac{\sqrt{Q}}{H_m^{3/4}} \quad (2.1)$$

Pumps with low specific speed, called low n_q pumps, have a radial outlet with large outlet diameter, D_2 compared to inlet diameter, D_1 . The head curves are relatively flat, and the power curve has a positive slope in the entire flow area.

On the contrary, pumps with high specific speed, so-called high n_q pumps, have an increasingly axial outlet, with small outlet diameter D_2 , compared to the width, b . Head curves are typically descending and have a tendency to create saddle points. Performance curves decrease when flow increases.

In this study, design optimization of radial impellers is aimed and as a result, range of specific speed is limited between 40 and 180.

Nominal inlet diameter D_0 (m) can be calculated by Equation 2.2 [21].

$$D_0 = 4.5 \cdot \sqrt[3]{\frac{Q}{n}} \quad (2.2)$$

Hydraulic and volumetric efficiencies are calculated after the specific speed and nominal diameter are obtained. The head of pump has been directly influenced by the hydraulic efficiency. Therefore, the right efficiency has to be selected to regard the reduction in head. The volumetric efficiency of the pump has been taken into account since there is an outflow through the clearance between impeller and volute. Hydraulic and volumetric efficiencies are obtained from the Equation 2.3 and 2.4 [21].

$$\eta_h = 1 - \frac{0.42}{(\log D_0 - 0.172)^2} \quad (2.3)$$

$$\eta_v = \frac{1}{1 + 0.68 \cdot n_q^{-2/3}} \quad (2.4)$$

The mechanical efficiency of large pumps is around 99.5 % or even above. In contrast, the mechanical losses of small pumps below 5 kW can use up a considerable portion of the coupling power [6]. Therefore mechanical efficiency η_m of the pump can be selected to be 97% for this calculation. Then overall efficiency of the pump can be calculated from Equation 2.5.

$$\eta = \eta_h \cdot \eta_v \cdot \eta_m \quad (2.5)$$

The density of pumped fluid (ρ), flow rate (Q), delivery head (H) and the overall efficiency are sufficient to calculate the required power N_i (W) of the pump shaft.

$$N_i = \frac{\rho \cdot g \cdot H \cdot Q}{\eta} \quad (2.6)$$

Shaft diameter d_s that stands the consisted torque safely can be evaluated according to efficiency and power. The material and allowable stress τ_{al} should be determined to calculate the shaft diameter. Structural steel is chosen for the shaft material in this calculation. Equation (2.7) is used for the shaft diameter [21]:

$$d_s = \sqrt[3]{\frac{16 \cdot N_i / \omega}{\pi \cdot \tau_{al}}} = 3.65 \cdot \sqrt[3]{\frac{N_i}{n \cdot \tau_{al}}} \quad (2.7)$$

where d_s is in m, N_i is in W, n is in rpm, and τ_{al} in N/m². Shaft diameter should be selected larger than the calculated value to handle the transmitted torque and easily

reducibility. Standard shaft diameter size should be also considered while selecting pump shaft diameter. Hub diameter D_h of the impeller can be chosen as [21].

$$D_h = (1.2 \sim 1.5) \cdot d_s \quad (2.8)$$

2.1.1. Design of impeller

The most important component of a pump is the impeller that transfers energy to the flow. Thus, it should be the first part to be designed. Then outputs of the impeller calculation determines the inputs of volute. Radial section of the impeller is shown in Figure 2.3.

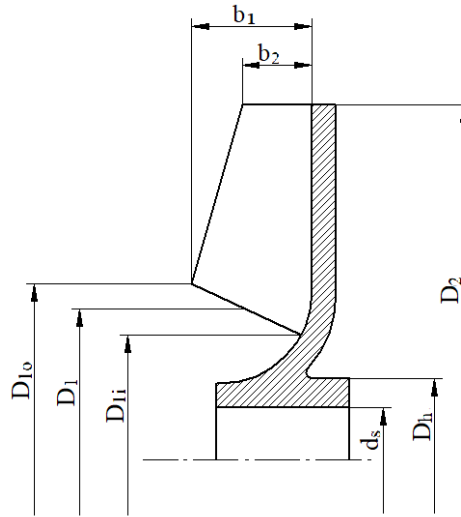


Figure 2.3. Radial section of the impeller

Impeller design starts with the determination of the specific speed according to Equation 2.1. Inlet diameter of the impeller D_1 should be chosen slightly smaller than D_0 . For this purpose, the coefficient of Schulz σ_s in equation 2.9 can be selected between 0.90~0.95 [21].

$$D_1 = \sigma_s \cdot D_0 \quad (2.9)$$

Impeller inlet outer diameter D_{1o} can be selected 3~4mm larger than D_0 [21].

$$D_{1o} = D_0 + (3 \sim 4)mm \quad (2.10)$$

Then inlet inner diameter D_{1i} becomes

$$D_{li} = 2 \cdot D_1 - D_{1o} \quad (2.11)$$

Since D_0 and D_h is known, absolute velocity at impeller inlet c_0 (m/s) can be found from the basic calculation from the flow rate over area.

$$c_0 = \frac{Q}{\pi \cdot (D_0^2 - D_h^2) / 4} \quad (2.12)$$

Absolute velocity c_1 on the inlet of the impeller can be calculated as the formula [21]

$$c_1 = (1.05 \sim 1.1) \cdot c_0 \quad (2.13)$$

α_1 and β_1 represent the angles of the absolute and relative velocities at the inlet of the impeller shown in the Figure 2.4. The fluid flow to the impeller inlet is mostly axial and it is assumed non-swirling, meaning $\alpha_1=90^\circ$. Then the circumferential component of the absolute inflow velocity is zero;

$$c_1 = c_{m1} \quad (2.14)$$

and

$$c_{u1}=0 \quad (2.15)$$

The velocity triangle at the impeller inlet (LE) can be seen in Figure 2.4 which shows the relation between the relative and absolute velocities. The velocity triangle is described by three vectors: the peripheral (circumferential) velocity, u which is multiplication of angular velocity ω , and impeller radius r ; the relative velocity w and the absolute velocity c which is obtained through the vectorial addition of u and w .

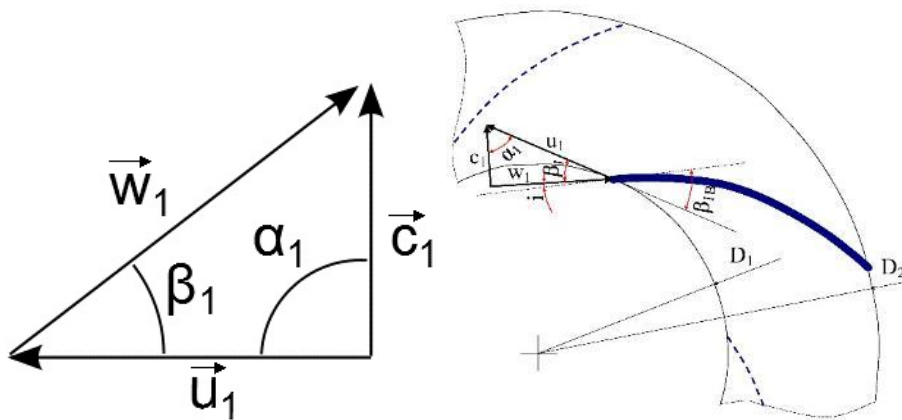


Figure 2.4. Velocity triangle of impeller inlet (LE)

c_{m1} value should be checked by the velocity coefficient k_{cm1} from the Figure 2.5. which can be used to find the velocity coefficients k_{cm1} , k_{cm2} , and k_{u2} as a function of specific speed.

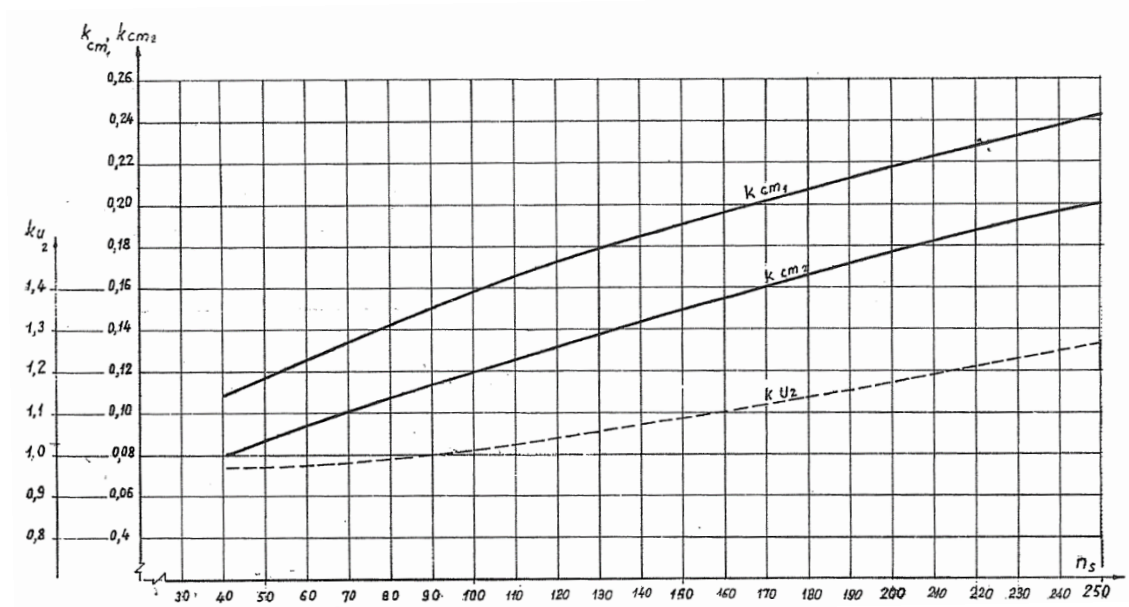


Figure 2.5. Velocity coefficients vs specific speed [21]

Alternative equation for the calculation of c_{m1} is given below. Resulting c_{m1} values from the Equation 2.16 and 2.17 should be closer.

$$c_{m1c} = k_{cm1} \sqrt{2 \cdot g \cdot H_m} \quad (2.16)$$

Tangential component of the velocity triangle u_1 (m/s) at the impeller inlet may easily be calculated by knowing the rotational speed n of the impeller, by the following relation:

$$u_1 = \frac{\pi D_1 n}{60} \quad (2.17)$$

Flow angle β_{10} can be found as

$$\beta_{10} = \arctan \frac{c_{m1}}{u_1} \quad (2.18)$$

The difference between blade angle β_{10} and flow angle β_1 is known as incidence:

$$i_1 = \beta_{10} - \beta_1$$

The blade inlet angle can be calculated by adding an incidence angle of 3° to 7° to the flow angle [21]. Then flow angle β_1 becomes

$$\beta_1 = \beta_{10} + i \quad (2.19)$$

It is important to take into account the effect of blade blockage τ_1 because of blade thickness while calculating the inlet blade angle. It has a significant effect since the decrease in the area of the flow passage caused by finite number of blades leads to an accelerated flow through the blades. Therefore, blockage τ_1 will be calculated later.

Blade width can be calculated by the Equation 2.20

$$b_1 = \frac{Q}{\pi D_1 \tau_1 c_{m1}} \quad (2.20)$$

Blade blockage τ_1 at the impeller inlet would be considered 0.6~0.7 for the first estimation [21] and will be replaced for the further equations.

In order to calculate the outer diameter of the impeller, D_2 , the pressure coefficient and u_2 has to be obtained. Pressure coefficient can be found by Figure 2.6 which shows the graph of coefficients as a function of specific speed.

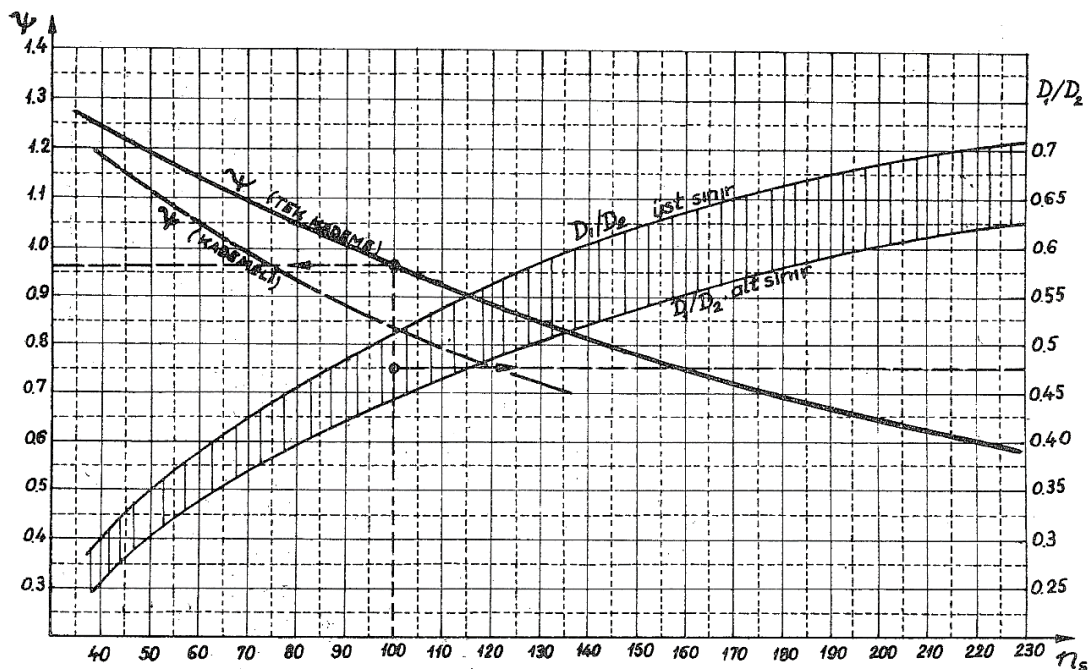


Figure 2.6. Pressure coefficients vs. specific speed [21]

After the proper pressure coefficient is selected from the graph, tangential component of the velocity can be calculated by the following relation

$$u_2 = \sqrt{\frac{2g \cdot H_m}{\psi}} \quad (2.21)$$

Tangential velocity at the impeller outlet can be controlled by the equation below containing velocity coefficient k_{u2} which is obtained from Figure 2.5.

$$u_{2c} = k_{u2} \sqrt{2g \cdot H_m} \quad (2.22)$$

Since u_2 is known, it is possible to calculate impeller outer diameter D_2 by the following equation;

$$D_2 = \frac{60 \cdot u_2}{\pi n} \quad (2.23)$$

where n is in rpm, and u_2 is in m/s, results as D_2 in m. Outer diameter of the impeller has the primary effect on the head of the pump. Since the needed head may not be reached because of losses, it should be selected higher than the calculated value using Equation 2.23.

The absolute velocity, c , can be decomposed into meridional and tangential components with subscripts m and u . c_{m2} can be obtained from the equation below. The velocity triangle at the impeller outlet (TE) is displayed in Figure 2.7 which shows the relation between the relative and absolute velocities.

$$c_{m2} = k_{cm2} \sqrt{2g \cdot H_m} \quad (2.24)$$

$$c_{u2} = \frac{g \cdot H_m}{u_2 \cdot \eta_h} \quad (2.25)$$

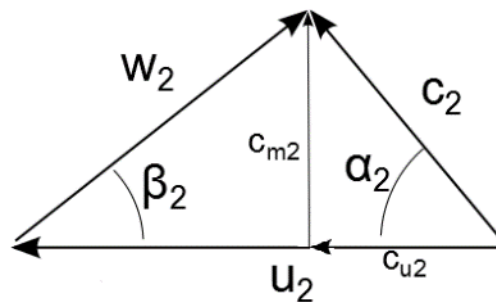


Figure 2.7. Velocity triangle of impeller outlet (TE)

Flow angle β_2 can be found via trigonometric equation given in Equation (2.26) which can be easily seen from the velocity triangle Figure 2.7.

$$\beta_2 = \tan^{-1} \left(\frac{c_{m2}}{u_2 - c_{u2}} \right) \quad (2.26)$$

However, the constructive angle β_2 , which is the wing angle due to the cascade wing, must be greater than the angle β_2 calculated from the deviation of Δc_u . In other words, if it is required that the fluid to leave the impeller with β_2 angle, we have to choose β_{2k} blade exit angle larger than β_2 taking into account the deviation. Then equation for β_{2k} becomes;

$$\beta_{2k} = \tan^{-1} \left(\frac{c_{m2}}{u_2 - c_{u2k}} \right) \quad (2.26)$$

and c_{u2k} is

$$c_{u2k} = K \cdot c_{u2} \quad (2.27)$$

where K is the deviation coefficient

$$K = 1 + \frac{1.2(1 + \sin \beta_{2k})}{Z} \cdot \frac{1}{1 - \left(\frac{D_1}{D_2} \right)^2} \quad (2.28)$$

Number of blades, Z , is another parameter that has an important role in the impeller design. There are various methods to calculate the number of blades in literature. Optimization of the blade number is well accepted consideration. Friction loss and blockage will be low if the number of blades is low; but, it may cause separation in the flow. On the other hand, if the number of blades is higher, then there is more frictional loss and blockage; however, the flow would be guided better to prevent separation.

As previously explained, the construction of β_{2k} at the blade exit is predicted before the required β_{2k} angle, and then it has to be checked whether it provides the relevant correlations. If it does not, iterations are continued until the selected β_{2k} blade angle calculated at the end of the process reach values close to each other.

The sequence of operations can be summarized as follows

- β_{2k} blade angle has to be selected closed to β_2

- The number of blades is calculated according to this selected β_{2k} value

$$Z = 6.5 \frac{D_2 + D_1}{D_2 - D_1} \cdot \sin \frac{\beta_1 + \beta_{2k}}{2} \quad (2.29)$$

- K deviation coefficient is calculated according to Equation 2.28
- c_{u2k} is calculated according to Equation 2.27
- β_{2ki} is calculated according to Equation 2.26

β_{2k} value found is compared with the selected β_{2k} value and the process is repeated until there is 2-3° difference between them [21].

The blade outlet width is also a significant parameter together with the blade number and the blade outlet angle that affects the needed pump head. Although the larger the width, the pump head is higher and flow separation has to be avoided. Blade outlet width can be calculated by the equation in Formula 2.30 below.

$$b_2 = \frac{Q}{\pi D_2 \tau_2 c_{m2}} \quad (2.30)$$

where τ_2 is blade blockage at the impeller outlet and is calculated from formula

$$\tau_2 = 1 - \frac{Z \cdot e}{\pi D_2 \sin \beta_{2k}} \quad (2.31)$$

where e is the blade thickness.

In the same way, the inlet blockage includes corrected number of blades flow can be calculated as equation below

$$\tau_1 = 1 - \frac{Z \cdot e}{\pi D_1 \sin \beta_1} \quad (2.32)$$

If the previously selected τ_1 value differs from the value found by calculation (actual value) then impeller inlet width b_1 has to be corrected to the actual τ_1 value.

2.1.2. Design of volute

The impeller often discharges directly into the volute, which is a spiral-shaped flow passage usually of circular or trapezoidal cross section [7]. The volute cross sectional areas are usually designed to produce at design point of the pump constant velocity and

pressure along the periphery of the impeller [22]. Cross section of volute increases gradually around the impeller periphery, starting from the volute tongue and ending at the volute throat shown in Figure 2.8. The volute tongue directs the total flow, collected from around the impeller, through the throat to the pump exit flange. The gradually increasing volute flow cross sections are calculated from the flow rate and from an average velocity at the volute cross section center. The usual flow model assumes that the impeller outlet tangential velocity decreases in proportion to the radius to maintain constant angular momentum. The volute cross section A as a function of the circumferential angle θ counted from the tongue becomes [7]

$$A = \frac{(\theta / 2\pi)Q}{(C_{u2}R_2 / R)} \quad (2.33)$$

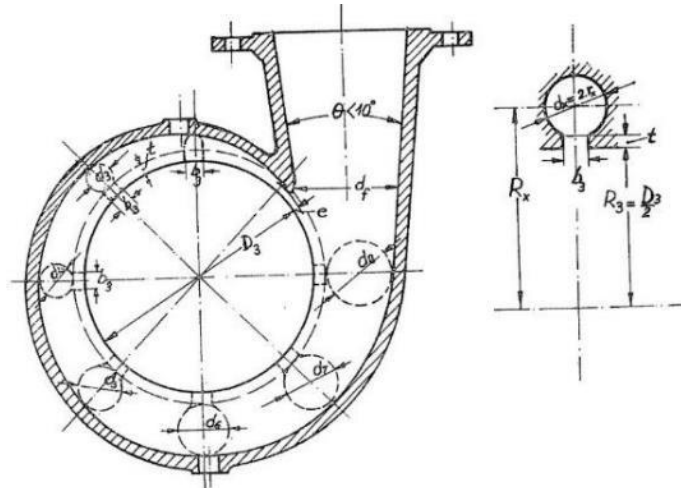


Figure 2.8. Sectional view of the volute [21]

When the flow rate is greater than the design flow rate, the flow generally accelerates in the volute, and the pressure tends to decrease in the circumferential direction. When the flow rate is less than the design flow rate, the volute velocity tends to decrease, and the pressure increases circumferentially around the impeller. Because of this pressure increase or decrease, a transverse pressure force appears on the impeller at off-design conditions [7].

2.2. Loss Models

Since neither the hydraulic losses nor the effect of recirculation can be accurately calculated in advance, a prediction of the characteristics is only possible using empirical

methods [6]. Main hydraulic losses in a centrifugal pump are friction losses, impeller and volute mismatching losses, and disk friction loss. The losses cause reduction in the theoretical head shown in Figure 2.9.

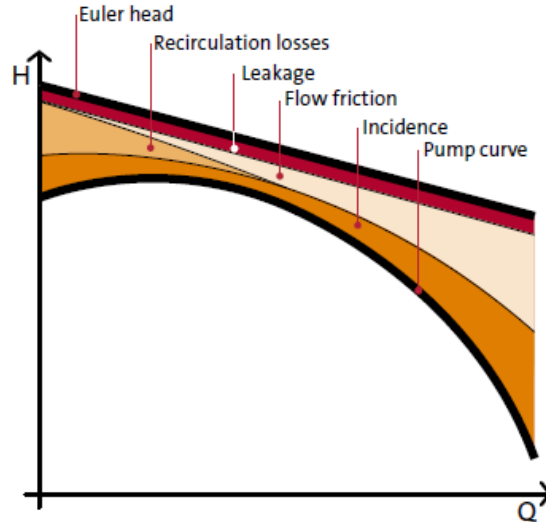


Figure 2.9. Reduction of theoretical Euler head due to losses [23]

Conventional one-dimensional prediction methods are based on an estimation of a theoretical head delivered by the pump from which several losses are subtracted. The theoretical head comes from the velocity triangles at inlet and outlet of the impeller, taking into account the slip of the flow with respect to the blades. The losses traditionally are broken down into components associated with the inlet of the pump, the impeller and the volute. A number of reference points are considered to determine these losses, as shown in Figure 2.10.

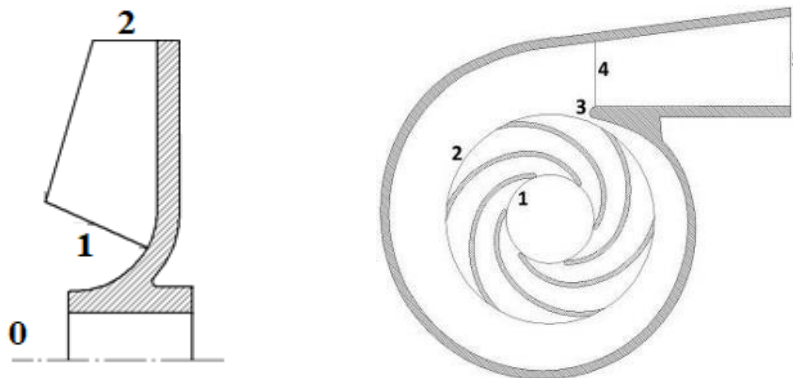


Figure 2.10. Meridional and orthogonal section of a centrifugal pump

The points indicated in the Figure (2.10) are

0: pump inlet

1: impeller inlet

2: impeller outlet

3: volute cutwater

4: volute throat

5: diffusor outlet

2.2.1. Theoretical Head

Expression of the theoretical head (H_m) is calculated from Euler's pump equation, which gives the conservation of angular momentum across the impeller. No pre-rotation or non-swirling inflow is considered here. Therefore, the fluid enters the impeller axially. The angular momentum of the fluid entering the impeller would then have to be subtracted from, or added to, the angular momentum of the fluid leaving the impeller, in order to calculate the theoretical hydraulic head [6,7]. Without pre-rotation the theoretical hydraulic head is given by the expression

$$H_{th} = \frac{u_2 \cdot c_{u2}}{g} \quad (2.34)$$

Where u_2 is the blade speed at the outlet of the impeller; c_{u2} is the circumferential component of absolute velocity at outlet as shown in Figure 2.11.

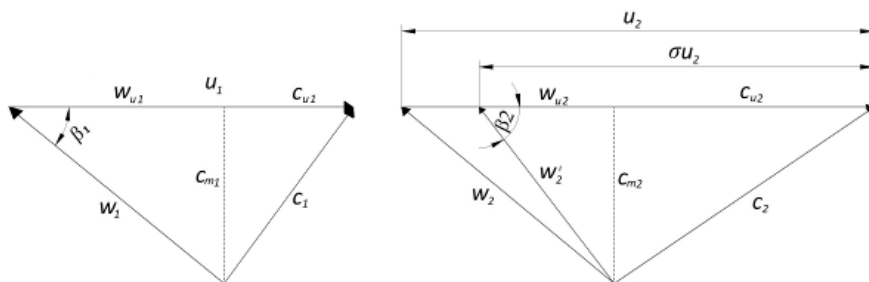


Figure 2.11. Velocity triangles at impeller inlet and outlet

2.2.2. Slip factor

The slip phenomenon has a strong influence on the working condition of centrifugal pumps. From a theoretical point of view, no valid solution has been given today for calculating the slip factor in the general case of an arbitrary impeller, several methods have been proposed by a large number of authors, Stodola [24], Busemann, Stanitz [25], Wiesner, Backström [26] etc. comparisons with experimental results have been done without showing a clear connection between the slip and the flow in the impeller [27].

Stodola [24] was the first that describes the expression for slip velocity in 1927. Busemann developed what has been termed a more exact theoretical solution which requires rather extensive mathematical treatment [11]. He proposed a remarkable slip factor prediction method that was sensitive to the blade radius ratio which is the radial distance of the blade leading edge from the axis divided by that of the blade trailing edge [26].

A commonly used expression for the slip factor of radial bladed impellers ($\beta = 0^\circ$) is one proposed by Stanitz, based on numerical solution of flow fields in impellers with radius ratio 0.445 [26].

Wiesner [11] obtained an empirical formula which is given in equation (2.35). This is a universally accepted formula that predicts the slip factor, σ . The formula includes the relation of outlet blade angle β_2 , and number of blades, Z .

$$\sigma = \left[1 - \frac{\sqrt{\sin(\beta_2)}}{Z^{0.7}} \right] \left[1 - \left(\frac{\frac{r_1}{r_2} - \epsilon}{1 - \epsilon} \right)^3 \right] \quad (2.35)$$

where ϵ is the blade solidity defined as

$$\epsilon = e^{-8.16 \frac{\sin(\beta_2)}{Z}} \quad (2.36)$$

which limits the formula by the ratio of inlet and outlet radius of the impeller has to be equal or larger than ϵ . If $r_1/r_2 < \epsilon$, then second term of the equation in Formula (2.35) is excluded from the calculation.

Tangential component of the absolute velocity c_{u2} can be found by extracting tangential component of the relative velocity w_{u2} from the peripheral velocity u_2 , by taking into account of slip factor as σu_2 . Relation between w_{u2} and c_{m2} can be found easily from the Figure 2.11.

$$c_{u2} = \sigma u_2 - \frac{c_{m2}}{\tan \beta_2} \quad (2.37)$$

However, the actual head and flow rate performance curve tend to a significant deviation from the corresponding Euler behavior due to slip since c_{u2} decreases relatively.

2.2.3. Inlet Loss

Inlet loss is usually 10% of the inlet kinetic energy for the end-suction pumps [7] which is calculated by the relation below:

$$\Delta H_0 = 0.10 \frac{c_0^2}{2g} \quad (2.38)$$

where c_0 is the pump inlet velocity.

2.2.4. Impeller Loss

Main losses in the impeller are caused by mismatching of the flow at inlet, friction and blade loading.

2.2.4.1. Mismatching loss

Mismatching loss is defined as

$$\Delta H_{i1} = \mu \frac{c_{u1}^2}{2g} \quad (2.39)$$

where μ is called the reduction factor which is generally accepted as 0.65 [9,21].

Equation (2.39) shows that mismatching of impeller is caused by the presence of the tangential component of the absolute velocity, c_{u1} . According to inlet velocity triangle given in the Figure 2.11, c_{u1} can be found from Equation (2.40).

$$c_{u1} = u_1 - \frac{c_{m1}}{\tan(\beta_1)} \quad (2.40)$$

c_{m1} is the meridional component of the absolute velocity which can be expressed by the definition given in Equation:

$$c_{m1} = \frac{Q}{\pi D_1 b_1 \tau_1} \quad (2.41)$$

Where Q is the volumetric flow rate, D_1 is the inlet diameter, b_1 is inlet height and τ_1 is blade blockage factor defined as:

$$\tau_1 = 1 - \frac{e.Z}{\pi D_1 \sin(\beta_1)} \quad (2.42)$$

2.2.4.2. Impeller friction loss

Impeller friction loss can be described as

$$\Delta H_{i2} = \xi \frac{L_i}{D_h} \frac{w_1^2}{2g} \quad (2.43)$$

where L_i is mean length described below

$$L_i = \frac{D_2 - D_1}{2 \sin\left\{\frac{(B_1 + B_2)}{2}\right\}} \quad (2.44)$$

and D_h is the main hydraulic diameter calculated by the ratio of sum of impeller inlet area $a_1 b_1$ and outlet area $a_2 b_2$ to circumference of impeller inlet and outlet.

$$a_1 = \frac{\pi D_1 \sin \beta_1}{Z} \quad (2.45)$$

and

$$a_2 = \frac{\pi D_2 \sin \beta_2}{Z} \quad (2.46)$$

$$D_h = \frac{2(a_1 b_1 + a_2 b_2)}{(a_1 + b_1 + a_2 + b_2)} \quad (2.47)$$

Friction factor ξ is calculated by the formula below

$$\xi = \{1.138 + 2 \log(D_h - k)\}^{-2} \quad (2.48)$$

where k is the roughness which can be taken 2.6×10^{-4} (m) for cast iron material.

2.2.4.3. Impeller blade loading loss

Blade loss calculation of centrifugal impellers is adapted from the classical Lieblein diffusion factor method by Myles [15]. Diffusion factor can be calculated by

$$D_f = 1 - \frac{w_2}{w_1} + \frac{(u_1 - c_{u1}) - (u_2 - c_{u2})}{2s w_1} \quad (2.49)$$

where s is the solidity described as

$$s = \frac{Z}{2\pi \sin\{(\beta_1 + \beta_2)/2\}} \ln\left(\frac{r_2}{r_1}\right) \quad (2.50)$$

Blade loading loss is defined as

$$\Delta H_{i3} = D_f \frac{w_2^2}{2g} \quad (2.51)$$

Diffusion factor can become negative due to acceleration especially low flow rates. When the factor is negative, blade loading loss is accepted to be zero.

2.2.5. Volute Loss

Losses in the volute are caused by mismatching of the impeller and volute, and friction.

2.2.5.1. Volute mismatching loss

Mismatching loss can be described as the formula by Hamkins [8].

$$\Delta H_{v1} = \frac{1}{2} \left(\frac{D_2 c_{u2} - D_4 c_{u4}}{D_3} \right)^2 \quad (2.52)$$

Equation (19) is only valid for $D_2 c_{u2} > D_4 c_{u4}$.

If the angular momentum at the outlet of the impeller is equal to the angular momentum to volute throat angular momentum, then the expression equals to zero. Therefore, mismatching loss at design point becomes zero.

2.2.5.2. Volute friction loss

Volute friction loss can be described by the equation of Worster [28] below:

$$\Delta H_{v2} = \xi \frac{A_v c_4^2}{A_4 2g} \quad (2.53)$$

where A_v is the volute surface area

$$A_v = \frac{\pi D_4^2}{4} \left[1 + \left(\frac{2\pi}{\ln \frac{r_3 + r_4}{r_3}} \right)^2 \right]^{0.5} + 2\pi \left[\frac{r_4 (2r_3 + r_4)}{2 \ln \frac{r_3 + r_4}{r_3}} - r_2^2 \right] \quad (2.54)$$

and A_4 is the throat area

$$A_4 = \frac{\pi D_4^2}{2} \quad (2.55)$$

Friction factor can be described as [9]

$$\xi = \left\{ 1.89 + 1.62 \log \left(\frac{L_v}{k} \right) \right\}^{-2.5} \quad (2.56)$$

where k is the roughness which can be taken 2.6×10^{-4} (m) for cast iron material. L_v is a length that stands for a mean streamline in the volute which is given below [9]

$$L_v = \frac{r_3 - r_2 + \pi r_4}{\sin \alpha_2} \quad (2.57)$$

where α_2 is the volute divergence angle.

2.2.5.3. Diffusor Loss

Discharge of the volute can be modelled as conical diffusor. Loss can be calculated as

$$\Delta H_d = K \frac{c_4^2 - c_5^2}{2g} \quad (2.58)$$

Where K is the loss coefficient which is the ratio of diffusor length to area.

2.2.6. Disk Friction Loss

Disk friction power loss is caused by the friction between the rotating faces of the impeller and the fluid. Power loss can be expressed by Pearsall formula [14] given in Equation (2.59):

$$P_{df} = \frac{C\zeta u_2^3 r_2^2}{2} \quad (2.59)$$

where C is the torque coefficient defined below

$$C = 0.15 \text{Re}^{-0.2} \quad (2.60)$$

and Re is the Reynold's number,

$$\text{Re} = \frac{u_2 D_2}{\nu} \quad (2.61)$$

Approximately 30% of the disk power is returned as useful work according to Hamkins [8]. Then head rise due to disk pumping can be described as

$$\Delta H_{df} = 0.3 \frac{P_{df}}{\zeta Q g} \quad (2.62)$$

2.2.7. Resulting Head

Resulting head can be calculated by subtracting impeller and volute losses from theoretical head and disk pumping gain:

$$H = \Delta H_{th} - \Delta H_0 - \Delta H_{i1} - \Delta H_{i2} - \Delta H_{i3} - \Delta H_{v1} - \Delta H_{v2} - \Delta H_d + \Delta H_{df} \quad (2.63)$$

2.3. Code Implementation

This section will describe the implementation details for pump design and performance prediction software.

Java is one most popular programming languages on the globe and is supported on at least 3 billion devices [29] in 2013. Programs are converted and stored as Java Virtual Machine (JVM) bytecode and are then executed on a given host using its JVM via Java

Runtime Environment (JRE). This allows the same “binary” to be executed in different platform with no modification.

Java FX [30] is an open-source Java library that allows programmers to create applications that interact with the user via user interfaces (e.g., buttons, checkboxes, tabs, etc.). The library provides insight into user actions, such as clicking on a button or tuning a scrollable, and gives the programmer the ability to trigger certain functionalities in the program.

The pump design and performance optimization software has been implemented on Java 1.8 using Java FX. A couple of different user interfaces have been built in order to collect input from the users and show the outputs in an easily conceivable way. Via the program, a user is able to perform a couple of operations, each will be shown as a separate flow in this section.

Eclipse which is an integrated development environment (IDE) is used in computer programming. The user interface has been created and edited using the Scene Builder software which is integrated with JavaFx.

The application first asks the user to enter flow rate (Q), delivery head (H), and pump speed in design point. Using the equations between 2.1 and 2.33, the application performs the initial calculations for the design point, which are then optimized by the user via the interface. In order to see the effects of modifications on the design, the user has to press the update calculate button that can also further be modified if needed. If needed, the user can press the draw button to visualize the impeller blade profile, which are printed using Bezier curves. Modifications can be made on the printed profile by keeping the inlet and outlet blade angles constant. The user can investigate the volute section by using the upper tabs. Part of calculations up until this step can be found in Appendix A.1. Moreover, the Java FX code for the interface is partially given in Appendix A.2. Interface of the software is shown in the Figure 2.12. Yellow text boxes are editable and can be modified further calculations.

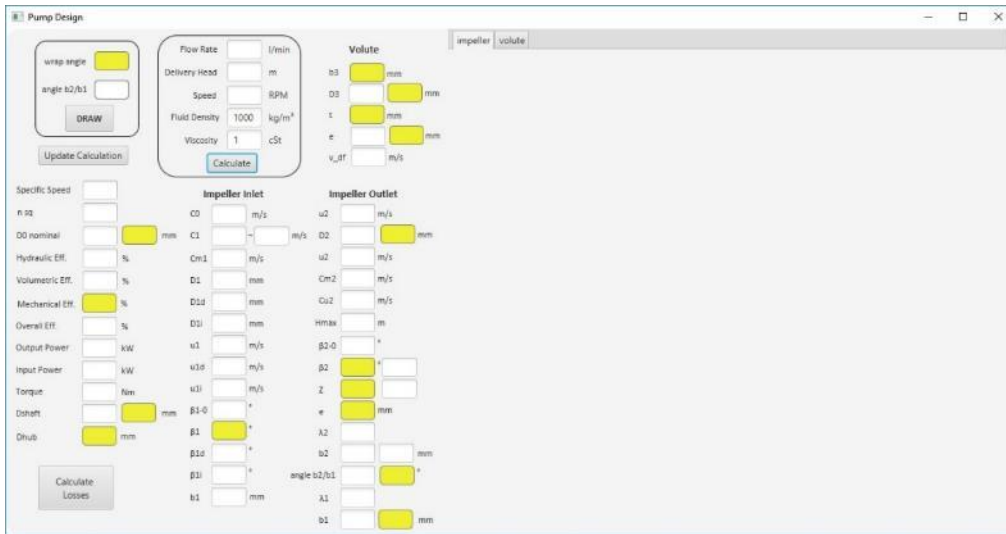


Figure 2.12. Interface of the calculation software

‘Calculate Losses’ button executes the loss calculation of the designed impeller and volute. Then a new pop-up window opens which shows the losses of impeller and volute for the design point and the off-design points. Thus delivery head at design point and off-design conditions are obtained. If the final results are below the desired values, then the design has been modified by returning to the previous window. As a result, the user ends the operation by obtaining the performance curve of the designed pump from the loss values. Loss calculation codes can be found in Appendix A.1. The JavaFx code for the interface of loss calculation is in Appendix A.3. Interface of the software is shown in the Figure 2.13.

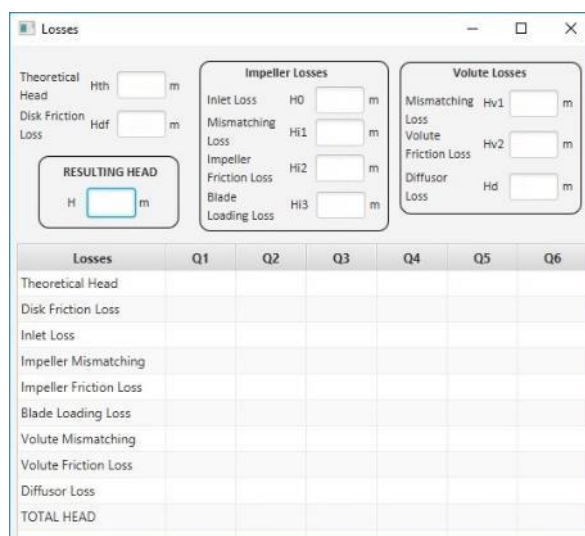


Figure 2.13. Interface of the loss calculation window

2.4. CFD Analysis and Pre-processing Steps

The set of equations together with the Navier-Stokes Equations, conservation of mass and energy that are partial differential equation system, were derived in the early nineteenth century and have no known general analytical solution but can be discretized and solved numerically [16]. Therefore, capacity of the computer which solves these equations plays a very important role on the quality of the results and determines duration of analysis. The computer operated the calculation in this thesis has Intel® Core™ i7-7500 CPU operating at 2.7 GHz and of 12 GB RAM with a 64 bit Windows 10 operating system. The capacity of the computer can be accepted as sufficient to run CFD analysis in this study.

There are a number of different solution methods that are used in CFD codes. The most common, and the one on which CFX is based, is known as the finite volume technique. In this technique, the region of interest is divided into small sub-regions, called control volumes. The equations are discretized and solved iteratively for each control volume. As a result, an approximation of the value of each variable at specific points throughout the domain can be obtained. In this way, one derives a full picture of the behavior of the flow [16].

2.4.1. Solid Modeling

3D solid parts of impeller and volute have to be created to analyze the pump performance. Fluid volume inside the volute can be modified by using CFX module, but using CAD software enables revising the impeller and volute to be more suitable for CFD analyses. Because solid models include manufacturing details such as fillets, chamfers or small surfaces which are not necessary for CFD calculations. Nevertheless, CFD software cannot compute these details due to meshing errors. If the quality of the mesh is low, then the solution step of the analysis cannot converge. Eventually, the designer has to simplify the 3D solid data as much as possible in order to prevent errors in CFD analyses. Removing these details do not affect the accuracy of analysis compared to real performance. In this study, Solid Edge ST9 is used for solid modeling. For the fluid volume, backside of the volute and impeller is closed by planar surface to create closed fluid domain. Other small details have to be removed from the CAD

geometry. Impeller is also simplified for the analysis. Shaft hole and keyway are closed completely and small fillets are removed. Assembly of the impeller and volute is created shown in Figure 2.14. Mechanical parts such as washer and nut are not included in the design even they are in direct contact with fluid. Improper features, surfaces, edges etc. are removed for CFD analysis. Then the file is imported to the next software of ANSYS DesignModeler to extract fluid domain and check final surface and edge quality.

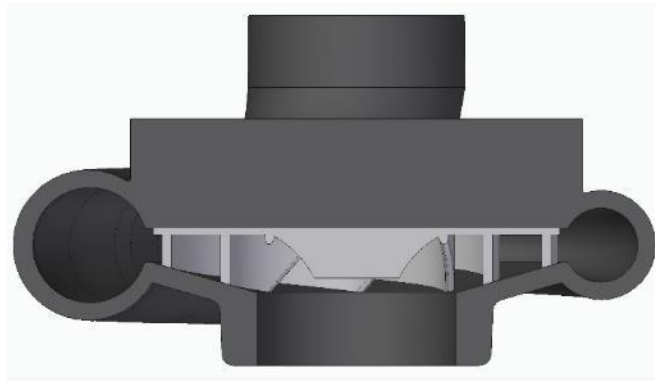


Figure 2.14. CAD model of impeller and volute assembly

First step in DesignModeler is to create fluid domain from the interior part of solid models. Then pump inlet is extended three times the diameter and pump outlet is extended five times the diameter to eliminate the effects of boundary conditions on the fluid flow. Finally, whole model is divided to three parts which are inlet, impeller (rotating part) and volute (outlet) shown in Figure 2.15. Impeller domain is rotated during CFD analysis. Thus, rotating part can be separated from the stationary parts.

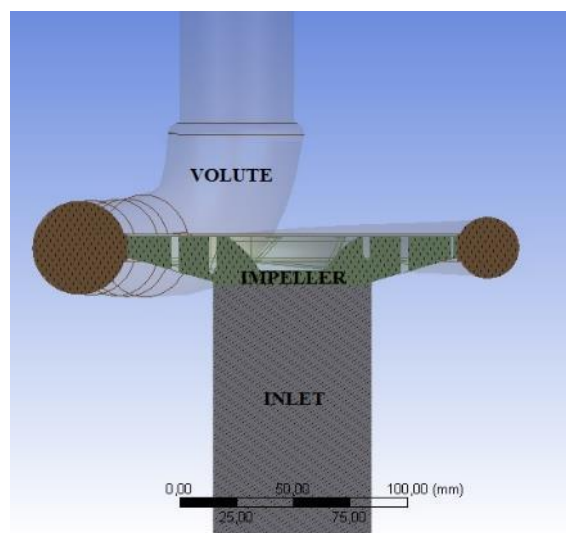


Figure 2.15. Fluid domains in Design Modeler

2.4.2. Meshing

Meshing is dividing the parts into small elements. The corner of each element, where calculation is performed, is called node. The quality of the mesh should be high to have better accuracy in solutions; however, finer meshes increase element number and duration of analysis takes longer. As a result, there is a balanced level of mesh size that gives tolerable results.

Skewness is one of the primary quality measures for a mesh. Skewness determines how close to ideal (equilateral or equiangular) a face or cell is. The following Table 2.1 lists the range of skewness values and the corresponding cell quality [17].

Table 2.1. Skewness values and the corresponding cell quality [17]

| Value of Skewness | Cell Quality |
|-------------------|--------------|
| 1 | degenerate |
| 0.9 — <1 | bad (sliver) |
| 0.75 — 0.9 | poor |
| 0.5 — 0.75 | fair |
| 0.25 — 0.5 | good |
| >0 — 0.25 | excellent |
| 0 | equilateral |

According to the definition of skewness, a value of 0 indicates an equilateral cell (best) and a value of 1 indicates a completely degenerate cell (worst) [17].

Default values of meshing is applied for the geometry. The coarse mesh is assigned to the inlet and outlet extension pipes with a cell size of 8 mm. This is sufficient since inlet and outlet pipes do not have a critical role for the fluid flow as volute or impeller. Then, a mesh size of 2 mm is applied to the impeller domain. Face sizing of 0.5 mm is used to the blades and interiors of the impeller. Because interiors are the common faces between the inlet to impeller and impeller to volute. Therefore, element size should be higher for the accuracy of the analysis. Inflation is applied for the all domains which is useful for CFD boundary layer resolution. First layer thickness of 0.05 mm is selected for the

inflation option. 10 layers of inflation with a growth rate of 1.2 is used. Sectional view of generated mesh is show in Figure 2.16.

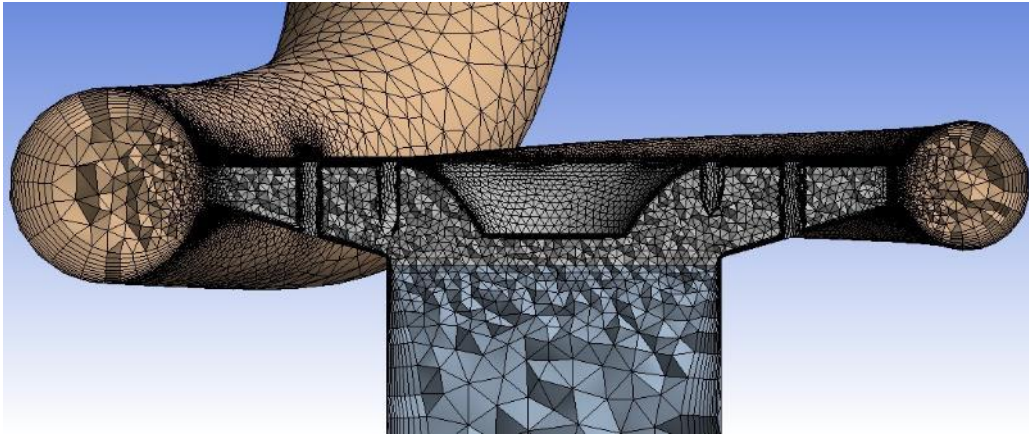


Figure 2.16. Sectional view of generated mesh

Detailed view of the interior of impeller and volute is shown in Figure 2.17.

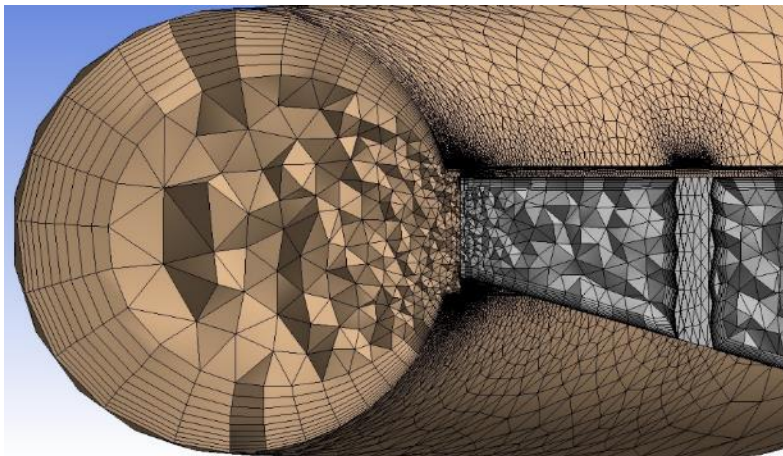


Figure 2.17. Detailed view of interface between impeller and volute

Total height of the layers differs due to the max element size of the domains. Therefore, layer compression method is selected to preserve 10 layers for the whole geometry. This method controls the growth rate of the layers and increase the frequency of the layers if necessary. Figure 2.18 shows the transitions between the layers of inlet, impeller and volute domain.

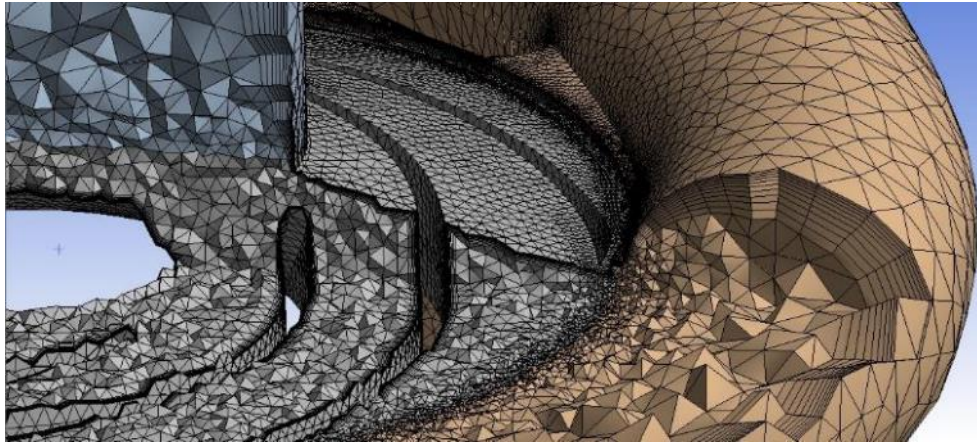


Figure 2.18. Detailed view of layer compression

Nearly 2.7 million elements were used and intensity of the grid is increased in the vicinity of the impeller. In the same way, boundary layer mesh (inflation) was applied to the model geometry. The quality of the resulting grid was checked with the quality skewness parameter. The maximum skewness value was 0.9 for the entire geometry. It was observed that the number of elements above 0.85 was very small as shown in Figure 2.19. Therefore, quality of grid structure accepted.

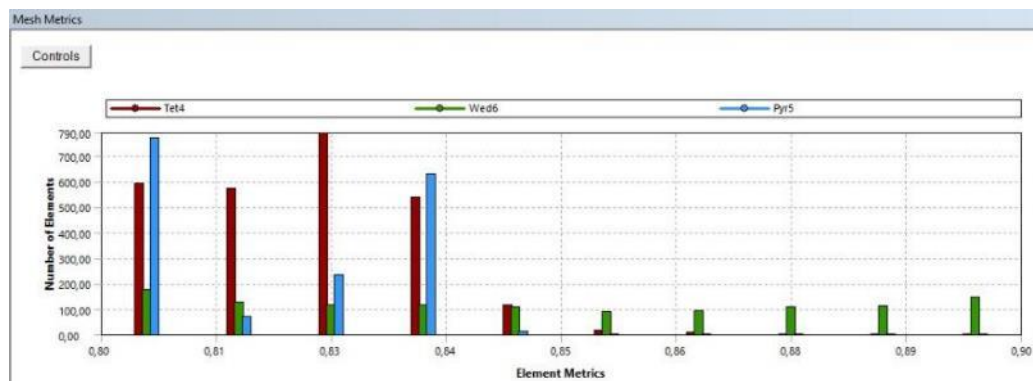


Figure 2.19. Skewness quality of the mesh

2.4.3. Solver Settings

ANSYS CFX was used as solver for the flow analysis. The equations solved are the three-dimensional Reynolds-averaged Navier-Stokes equations. The fluid is incompressible and the rotation of the impeller was performed with MRF (Multiple Reference Frame) feature of the solver. MRF allows the analysis of situations involving domains that are rotating relative to one another [18]. The angular velocity, ω , is defined as 303.7 rad/s (2900 rpm) through the impeller (rotating) domain motion.

The Shear Stress Transport model was used as the turbulence model shown in Figure 2.20. The $k-\omega$ based SST model accounts for the transport of the turbulent shear stress and gives highly accurate predictions of the onset and the amount of flow separation under adverse pressure gradients [2,3,18]. The analysis carried out with the modification of boundary conditions.

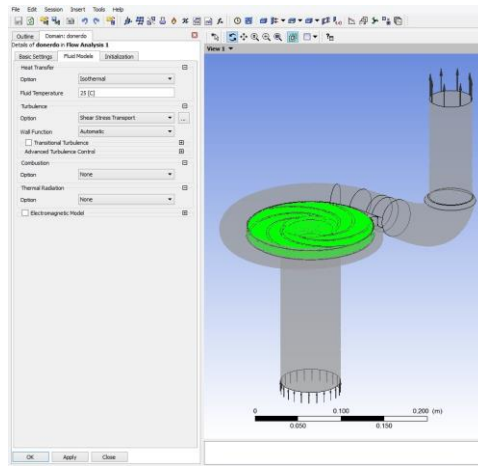


Figure 2.20. Turbulence model settings of the analysis

The mass flow rate and the flow direction normal to the boundary are given at the inlet. Static pressure of 0 Pa (atmospheric pressure) was defined at the pump outlet as shown in Figure 2.21 a and b. Turbulence intensity is specified as medium intensity (5%) which is the recommended option if the turbulence information is unknown [19].

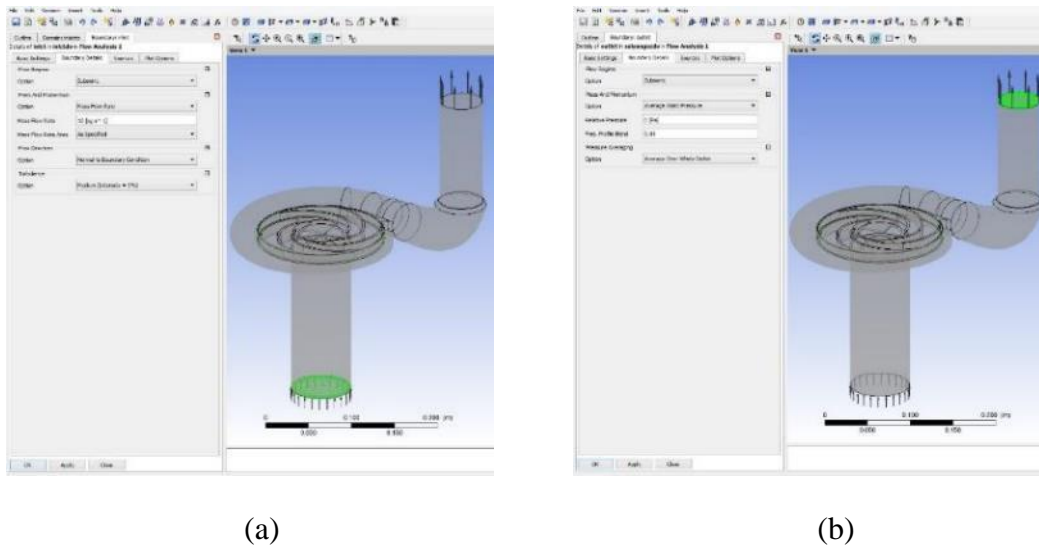


Figure 2.21. (a) Inlet and (b) outlet conditions of the pump

2.5. Experimental setup and procedure

2.5.1. Test Setup

Pump is installed to a tank with the dimensions of 300 cm x 75 cm x 60 cm. Pump-1 outlet is connected to G2 T-pipe, Pump-2 is connected to G1½ T-pipe and Pump-3 is connected to G1¼ T-pipe to measure the pressure without any losses. Pressure at the discharge is measured from T-pipes by using a digital manometer. Then pumps are connected to the pipeline by a flexible hydraulic pipe. Then magnetic flow meter of nominal size DN 80 is installed to the pipeline. 3-inch ball valve is installed at a distance of 100 cm ahead of pipeline to adjust the flow rate. Electric motor is monitored by a digital Wattmeter to measure electrical consumption and current. The pump is operated by supplying 400V – 50Hz mains electricity. The tank is filled with emulsion of 3% of coolant and water at a viscosity of 1 cSt.

Immersed Pump-1 that is used in the study is shown in Figure 2.22. All three pumps have open impeller. Pump-1 has circular shape cross-section, Pump-2 and Pump-3 have trapezoidal cross-section volute.

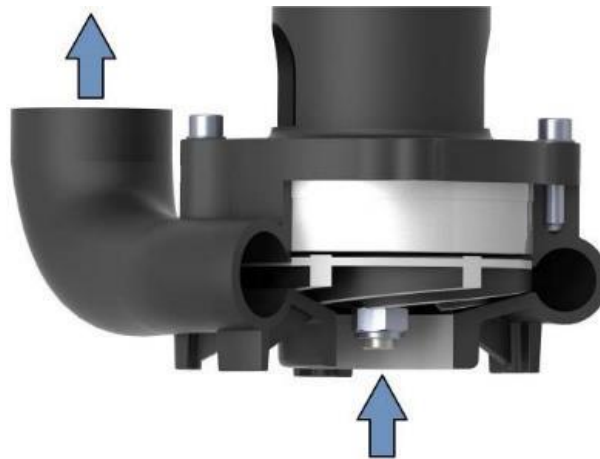


Figure 2.22. Section of centrifugal pump

Main dimensions and sectional view of the impeller and volute is shown in the Table 2.2.

Table 2.2. Main dimensions of test pump

| PUMP-1 | | | PUMP-2 | | | PUMP-3 | | |
|----------------|-------|-------|----------------|-------|-------|----------------|-------|-------|
| Symbol | Value | Unit | Symbol | Value | Unit | Symbol | Value | Unit |
| D ₁ | 65 | mm | D ₁ | 48 | mm | D ₁ | 35 | mm |
| D ₂ | 142 | mm | D ₂ | 106 | mm | D ₂ | 94 | mm |
| b ₁ | 19.75 | mm | b ₁ | 24.5 | mm | b ₁ | 17.5 | mm |
| b ₂ | 9.9 | mm | b ₂ | 15.6 | mm | b ₂ | 12.1 | mm |
| β_1 | 22 | ° | β_1 | 16 | ° | β_1 | 26 | ° |
| β_2 | 26 | ° | β_2 | 24 | ° | β_2 | 38 | ° |
| z | 6 | - | z | 5 | - | z | 5 | - |
| e | 5 | mm | e | 3.5 | mm | e | 3 | mm |
| n | 2900 | rpm | n | 2900 | rpm | n | 2900 | rpm |
| Q | 600 | l/min | Q | 300 | l/min | Q | 120 | l/min |

2.5.2. Experimental Procedure

Pump tests are performed according to EN ISO 9906-2012. Pump is immersed to the tank and pressure is measured only on the pump outlet since the pump is immersed to the fluid. Pressure has to be measured as much as closer to the pump outlet to prevent pressure loss due to elbows and piping itself. Also pressure has to be measured same port as pump outlet by connecting T-pipe. Then pump is connected to the piping by a flexible hydraulic pipe. Pressure is measured by a digital manometer.

The pump is operated by supplying 400V – 50Hz mains electricity. Electrical panel is required to monitor voltage, current and power consumption. Trapped air is evacuated by the valve on the pressure gauge before collecting the data.

Flow rate is measured by an electromagnetic flowmeter and is monitored by its screen. Flow rate is adjusted by closing the valve and pressure values are received from the gauge starting at fully open position to closed position with varying pressure points. Display of test stand is shown in Figure 2.23.

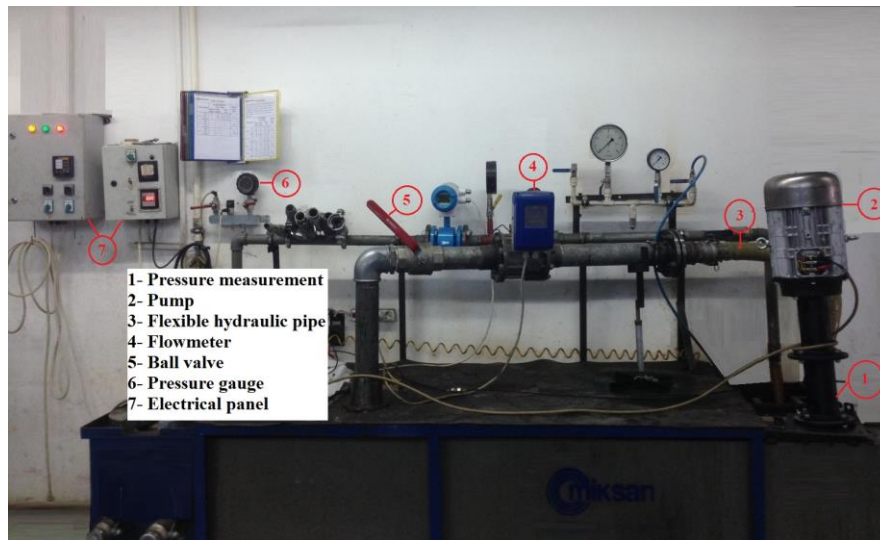


Figure 2.23. Display of pump test stand

2.5.3. Data Processing and Calculations

Collected data of varying pressure points are written to MS Excel® tables. Units of all the data are entered in measured form (bar for pressure, l/min for flow rate and kW for power consumption). Then, equations are entered to calculate the efficiency. Motor efficiency which is already known, is entered for the calculation of pump overall efficiency by the ratio of required fluid power to electrical power consumption that results pump-electrical motor assembly overall efficiency. Thus, all the required values are entered into the table. As a result, pump characteristic curves of hydraulic performance, power consumption and efficiency are plotted using collected and calculated data.

3. RESULTS AND DISCUSSION

3.1. Predictions with the Loss Correlation

Using the loss models explained above, a computer program was developed to predict the performance of a centrifugal pump using JavaFX software. The program structure is described in the flowchart shown in Figure 3.1.

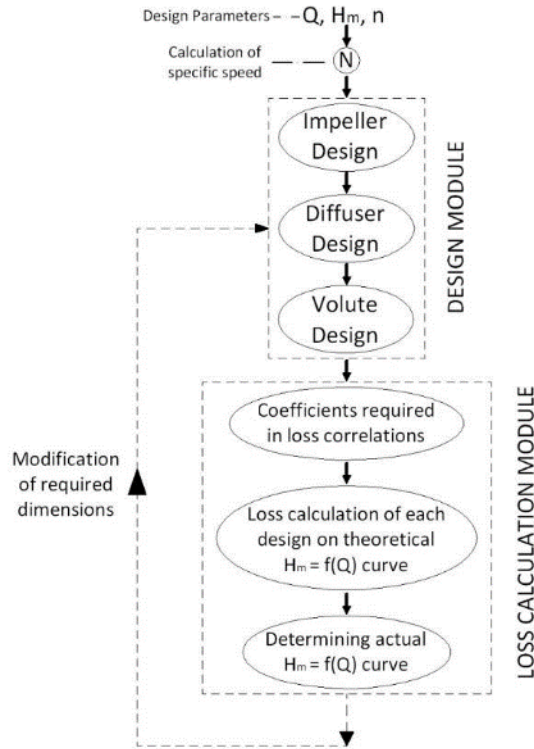


Figure 3.1. Flowchart of the prediction software

The main design parameters are flow rate Q , delivery head H_m , and rotational speed n . These constitute the inputs of the program. Then the program calculates the main dimensions of the impeller and volute (Figure 3.2 to Figure 3.4). The calculations can be modified by making necessary changes on the impeller and volute geometry. Finally loss models are applied for the final geometry to get H-Q graph of the pump.



Figure 3.2. Calculation on main dimensions of Pump-1



Figure 3.3. Calculation on main dimensions of Pump-2

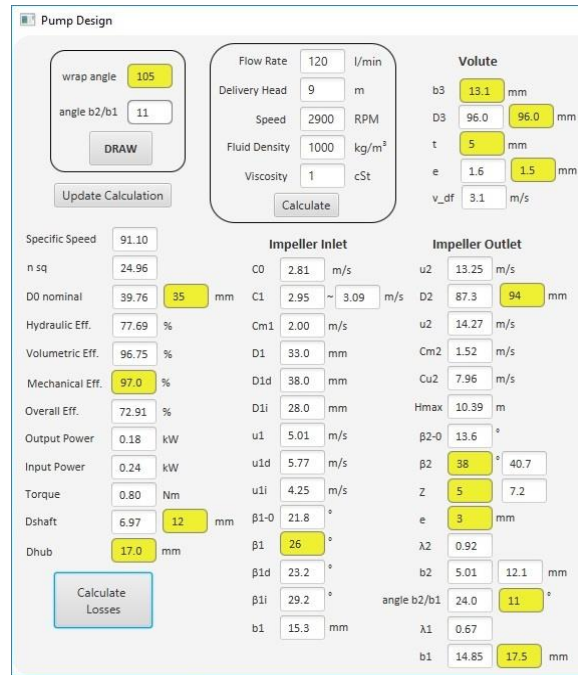


Figure 3.4. Calculation on main dimensions of Pump-3

The calculations can be repeated for each design until the desired pump performance is achieved.

Loss models are applied for the design and off-design points. The results obtained for different flow rates can be found in the Figure3.5 to Figure 3.7.

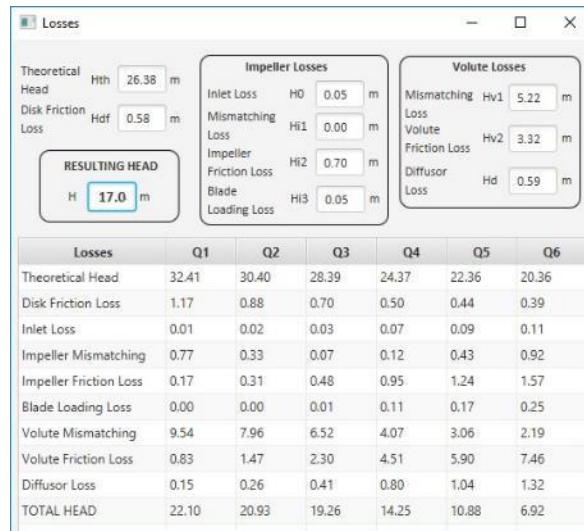


Figure 3.5. Predicted losses of impeller and volute at design point and off-design conditions of Pump-1

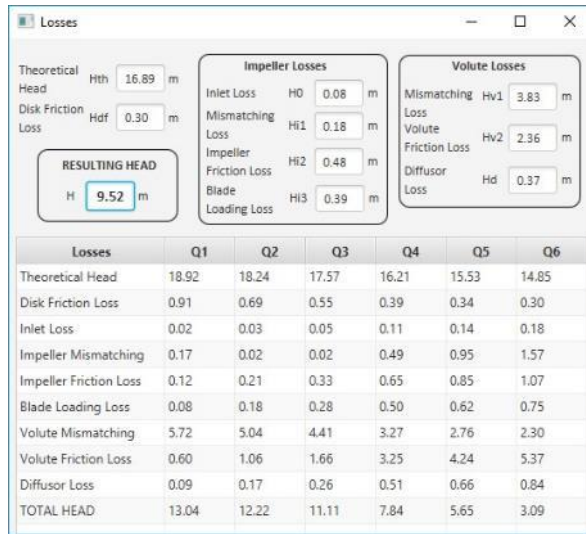


Figure 3.6. Predicted losses of impeller and volute at design point and off-design conditions of Pump-2

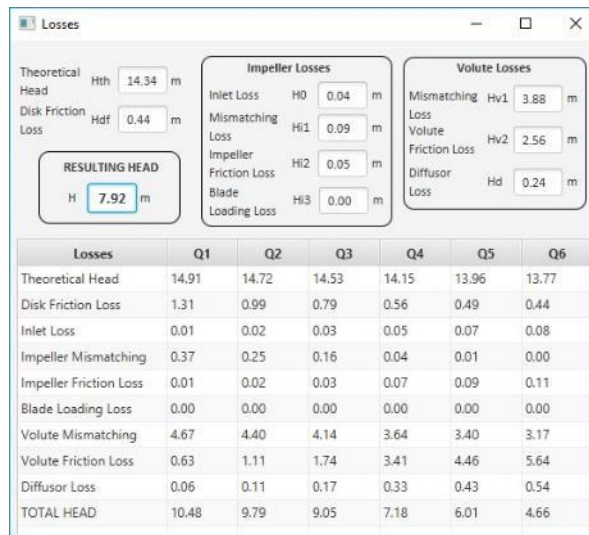


Figure 3.7. Predicted losses of impeller and volute at design point and off-design conditions of Pump-3

Figure 3.8 shows the theoretical head-curve, the total loss, and the resulting head-curve of Pump-1 which has the same geometries of impeller and volute for experimental, CFD and theoretical prediction. Head losses increase at higher flow rates as expected and the theoretical head discharge curve (Euler head) which is almost a straight line, creates the actual head curve by subtracting the losses. BEP has the minimum head loss which can be seen in Figure 3.8.

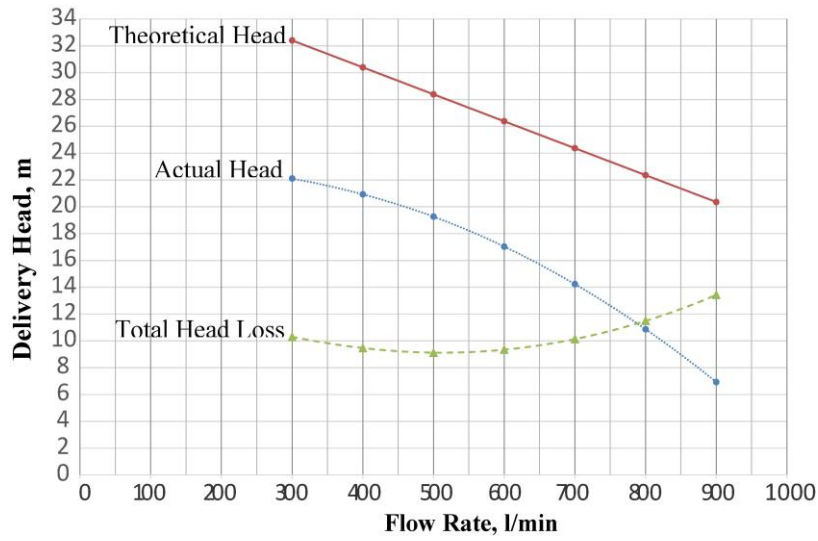


Figure 3.8. Theoretical H-Q curve, total loss and actual H-Q curve of Pump-1

Figure 3.9 shows the different loss components of the designed Pump-1. Friction losses of both impeller and volute (i.e., ΔH_{i2} , ΔH_{v2}) have a significant effect for high flow rates. Mismatching losses (i.e., ΔH_{i1} , ΔH_{v1}) are dominant for low flow rates. Volute losses obviously (i.e., ΔH_{v1} , ΔH_{v2}) have higher effect on the predicted pump performance.

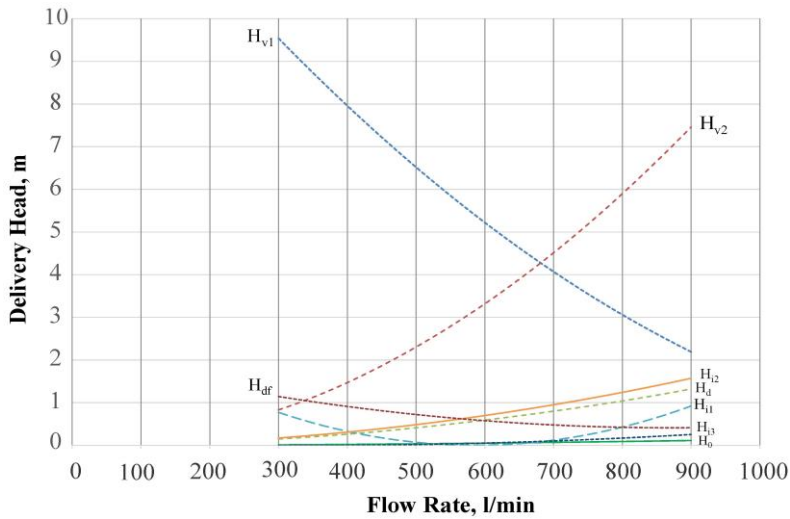


Figure 3.9. Loss components of predicted Pump-1

Figure 3.10 shows the theoretical head-curve, the total loss, and the resulting head-curve of Pump-2. Head losses increase at higher flow rates same as Pump-1. Minimum head loss occurs at low flow rate.

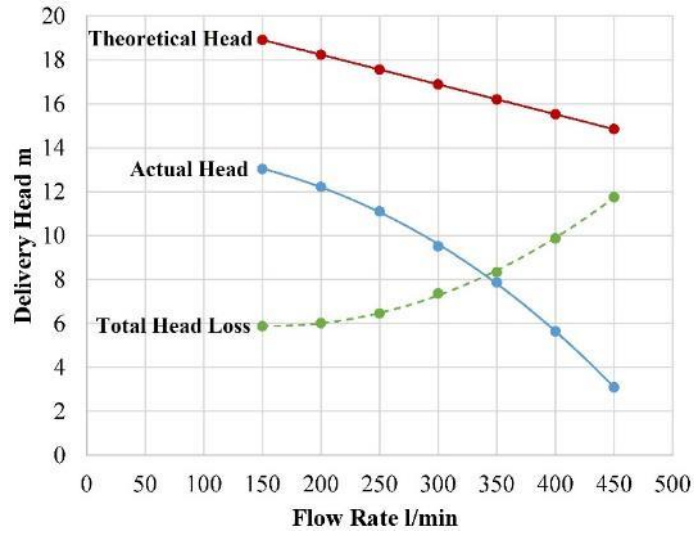


Figure 3.10. Theoretical H-Q curve, total loss and actual H-Q curve of Pump-2

Figure 3.11 shows the theoretical head-curve, the total loss, and the resulting head-curve of Pump-3. Head losses increase at higher flow rates same as Pump-1 and Pump-2. Minimum head loss occurs at low flow rate similarly in Pump-2.

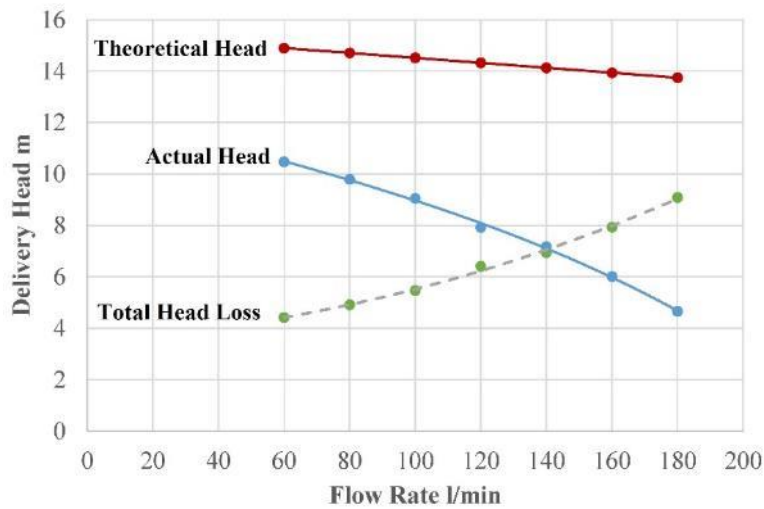


Figure 3.11. Theoretical H-Q curve, total loss and actual H-Q curve of Pump-3

3.2. Experimental Results

The measured H-Q characteristics of the Pump-1 is presented in the Figure 3.12. Delivery head is measured 15.85m at the design point of 600 l/min. The full report can be seen in Appendix B.1.

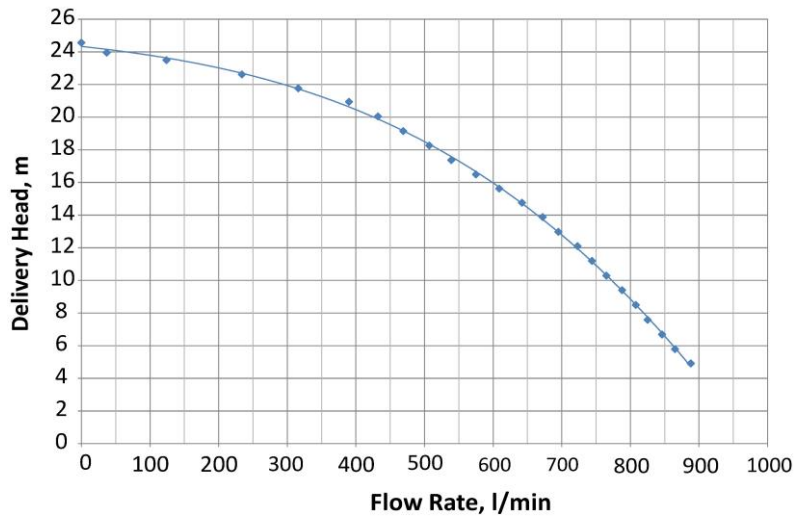


Figure 3.12. Experimental H-Q results of Pump-1

The measured H-Q characteristics of the Pump-2 is presented in the Figure 3.13. Delivery head is measured 8.99m at the design point of 300 l/min. The full report can be seen in Appendix B.2.

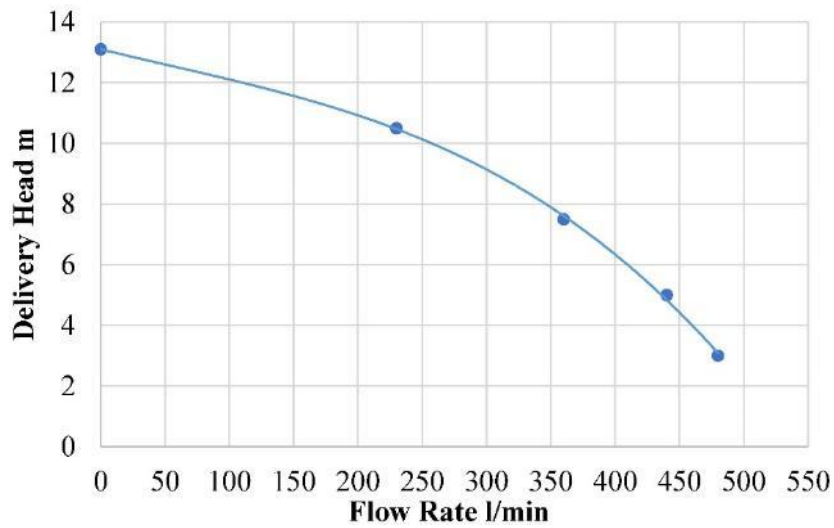


Figure 3.13. Experimental H-Q results of Pump-2

The measured H-Q characteristics of the Pump-3 is presented in the Figure 3.14. Delivery head is measured 7.9 m at the design point of 120 l/min. The full report can be seen in Appendix B.3.

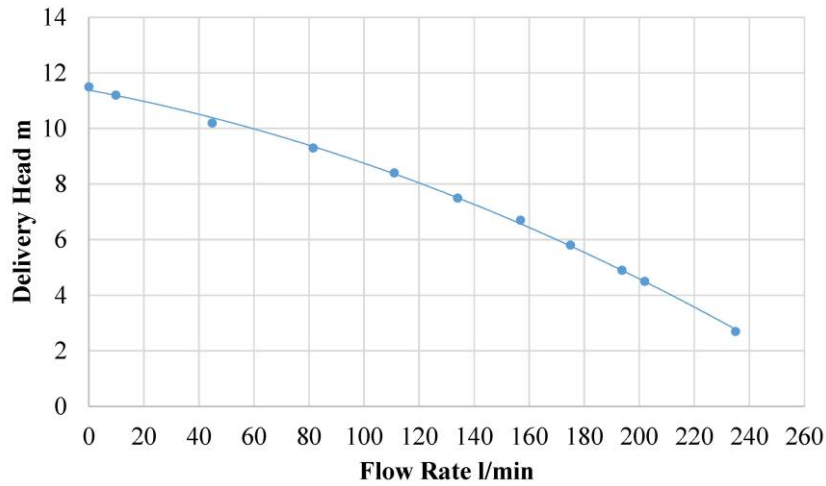


Figure 3.14. Experimental H-Q results of Pump-3

3.3. CFD Results

Throughout this analysis, the total pressure at the pump inlet and outlet were checked. Also static pressure distribution of the mid-plane of the pumps are examined. Moreover, the shaft power is calculated from the torque value on the blade. Then the pump efficiency is calculated by the help of the power, flow and pressure transferred to the flow.

Approximately 450 iterations are run to reach the convergence criteria of residuals. Residual type of RMS (root mean square) is selected. Target RMS residual value is $1e-06$ for all solutions. Convergence plots for nominal flow rate analysis are illustrated in Figure 3.15.

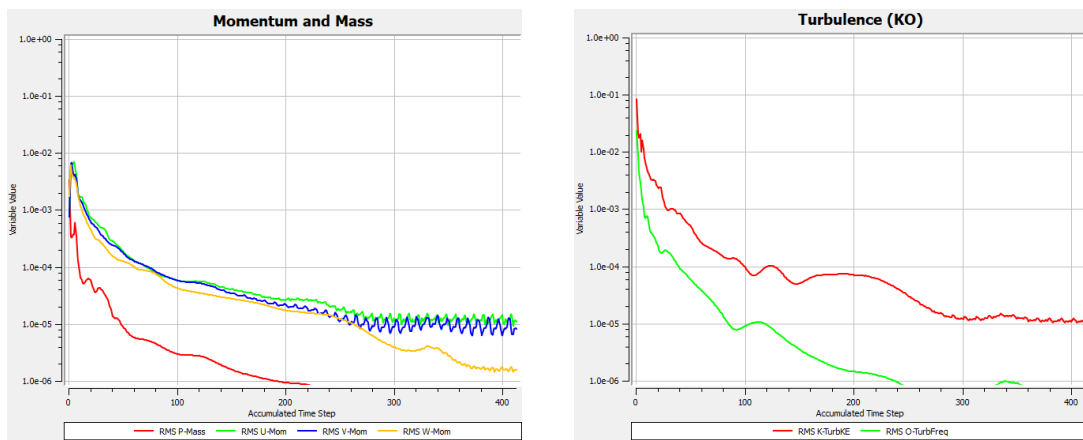


Figure 3.15. Convergence plots of nominal flow rate analysis for Momentum and Mass (left) and Turbulence (right)

A Low-Reynolds number $k-\omega$ model would require a near wall resolution of at least $y^+ < 2$ [19]. The y^+ values at the blades are less than 2 hence it shows the boundary layer is captured which is shown in the Figure 3.16.

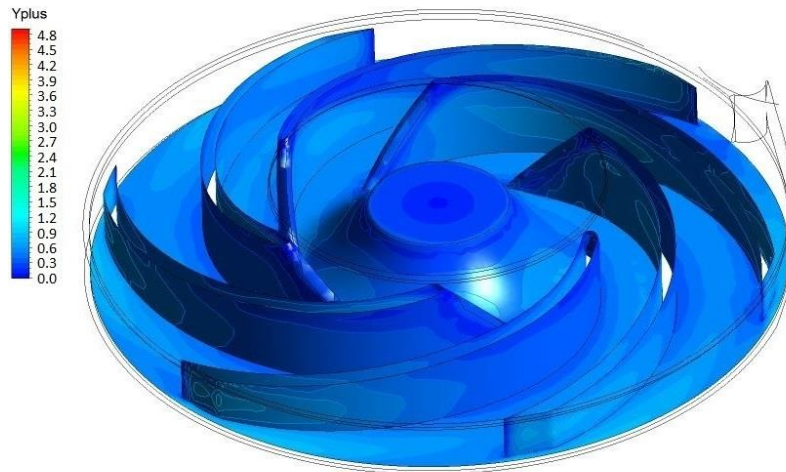


Figure 3.16. y^+ values at the impeller blades

3.3.1. CFD Results of Pump-1

To illustrate the pressure distribution obtained at the impeller exit, total and static pressures are plotted at the mid-plane of the pump in Fig. 3.17 to Fig. 3.19 for three representative flowrates. Figure 3.17 shows the distribution of static pressure in mid-plane of the impeller and the volute for the nominal flow rate (600 l/min). The distribution of the pressure is very similar and evenly distributed for all channels in the impeller. Pressure is gradually increasing through the blades and there is basically no pressure gradient in the volute. There is an increase in total pressure from the back of the tongue to the exit, which is reflected in the velocity component values. It is expected that the radial velocity would increase towards the impeller for the best efficiency point. The difference regarding the magnitude of the total pressure due to the term of kinetic energy which is added on the static pressure.

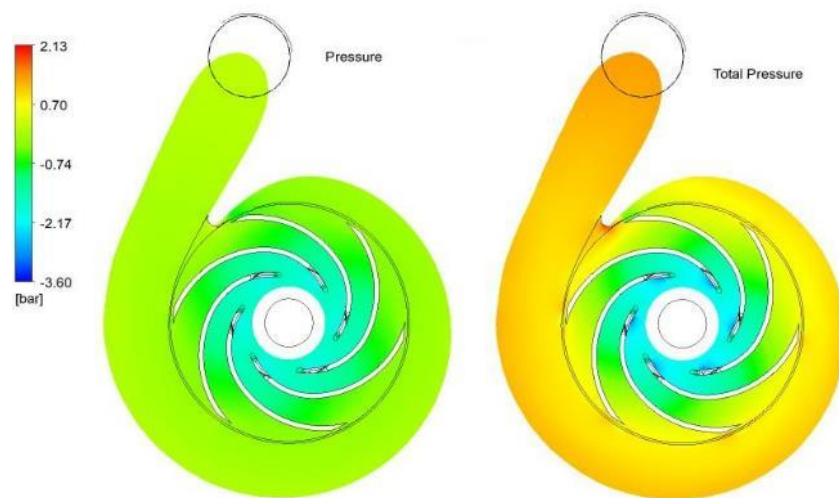


Figure 3.17. Distribution of static (left) and total (right) pressure in mid-plane for nominal flow rate of 600 l/min

Figure 3.18 shows the distribution of static pressure in mid plane of the impeller and the volute for 65% of the nominal flow rate (390 l/min). Pressure is increasing in the volute in circumferential direction. Pressure distribution in the impeller channels is not equal due to the pressure differential in the volute. Total pressure in the volute is very similar to the static pressure due to the low flow rate and velocity. Total pressure of the impeller is lower than the static pressure which shows increase in the losses.

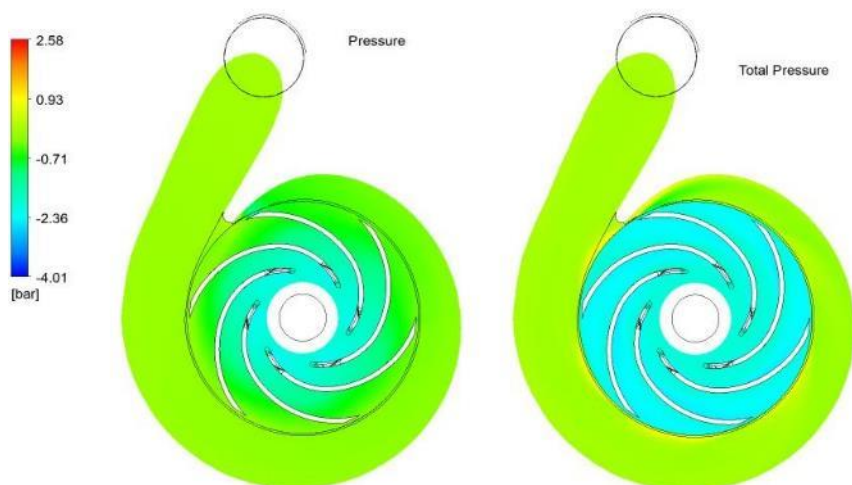


Figure 3.18. Distribution of static (left) and total (right) pressure in mid-plane for the flow rate of 390 l/min

Figure 3.19 shows the distribution of static pressure in mid plane of the impeller and the volute for 140% of the nominal flow rate (850 l/min). Pressure is increasing in the volute in circumferential direction. Pressure distribution in the impeller channels is not equal due to the pressure differential in the volute. There is a reduction in total pressure which indicates an increase in the pump losses at the high flow rate.

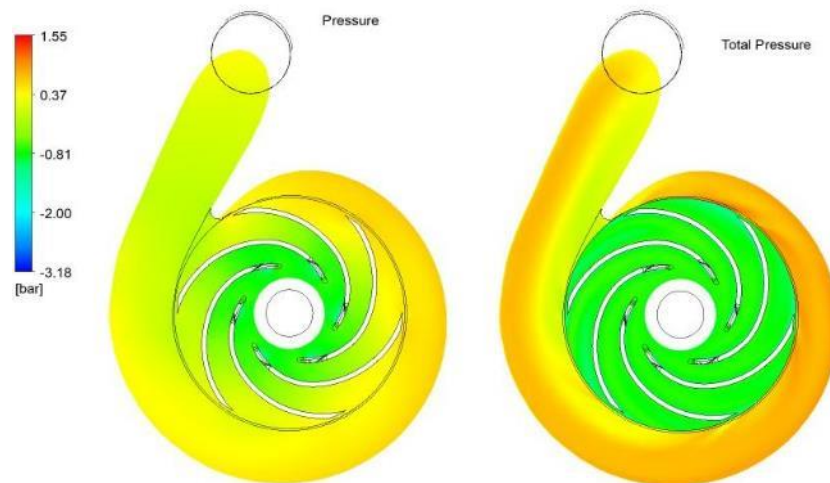


Figure 3.19. Distribution of static (left) and total (right) pressure in mid-plane for the flow rate of 850 l/min

Analyses are performed for 3 different flow rates and calculated pump head values are shown in Table 3.1.

Table 3.1. CFD Results at certain flow rates for Pump-1

| Flow rate (l/min) | ΔP (bar) | H (m) |
|-------------------|------------------|-------|
| 390 | 2.03 | 20.71 |
| 600 | 1.82 | 18.56 |
| 850 | 1.1 | 11.22 |

The total and static pressure variations within the pump for the three flow rates studied are shown in Figure 3.20 and Figure 3.21. The pressure increases gradually from the tongue to the volute exit for flow rates lower than design point. When the flow rate

approaches the nominal value, the pressure distribution becomes more uniform. For flow rates higher than design flow rate, the pressure reaches its highest value behind the tongue and starts to decrease around the circumference of the impeller, taking its minimum value just behind the tongue.

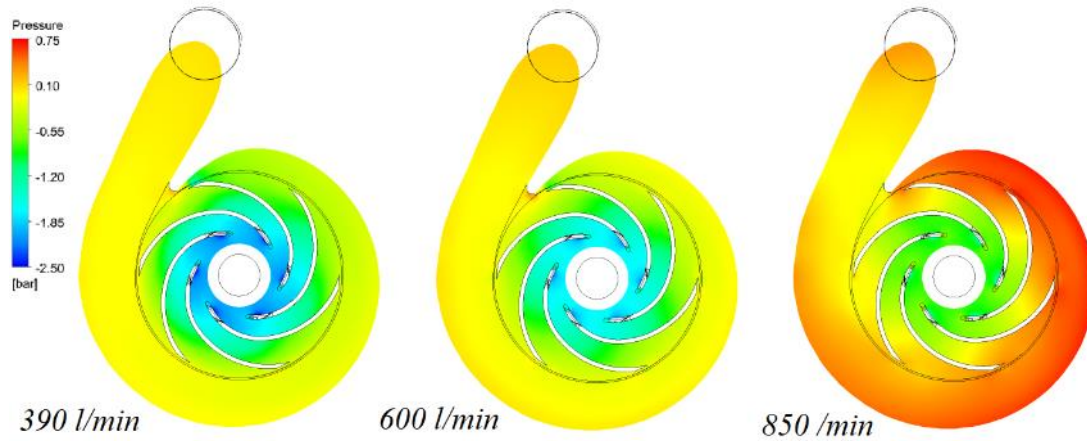


Figure 3.20. Static pressure distribution on the mid-section of Pump-1 (bar)

A considerable proportion of the fluid energy at the impeller tip is kinetic energy and its efficient transformation into static pressure is important. The kinetic energy present at the impeller outlet is converted into static pressure in the volute casing. The volute cross sectional areas are usually designed to produce at design point of the pump constant velocity and pressure along the periphery of the impeller. Loss models have been developed as adiabatic head (enthalpy) losses which is strictly valid for incompressible flow, only. Decrease in the pump discharge total pressure indicates an entropy rise at constant enthalpy which also shows increase in the pump losses.

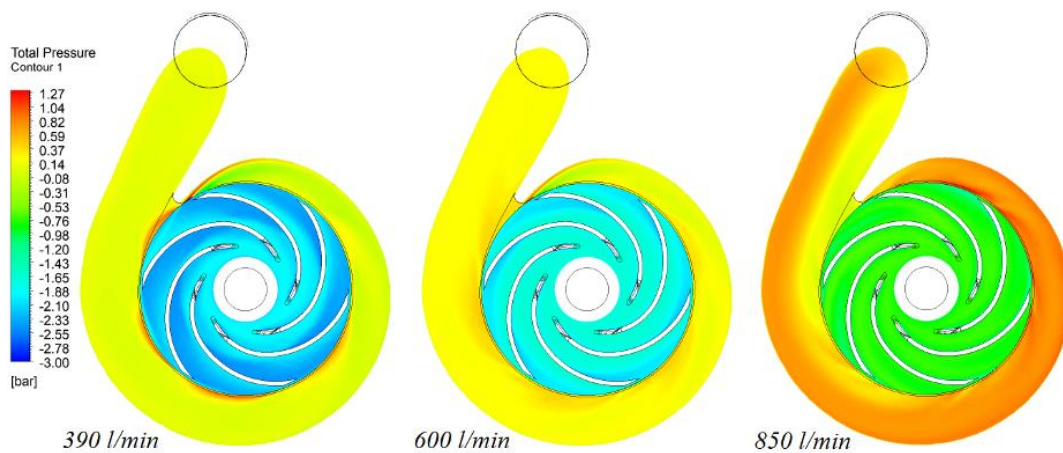


Figure 3.21. Total pressure distribution on the mid-section of Pump-1 (bar)

Figure 3.22 shows a vector plot of the relative velocity in the mid plane of the impeller and volute. It can be clearly seen that the relative velocity increases as the fluid moves towards to the discharge of the impeller. The velocity distribution becomes the most uniform at the design volume flow rate, similar to the pressure distribution. Small recirculation zones can be seen in the impeller channels of the flow rate of 390 l/min. Flow velocities are very low in these channels where the volute pressure is the largest.

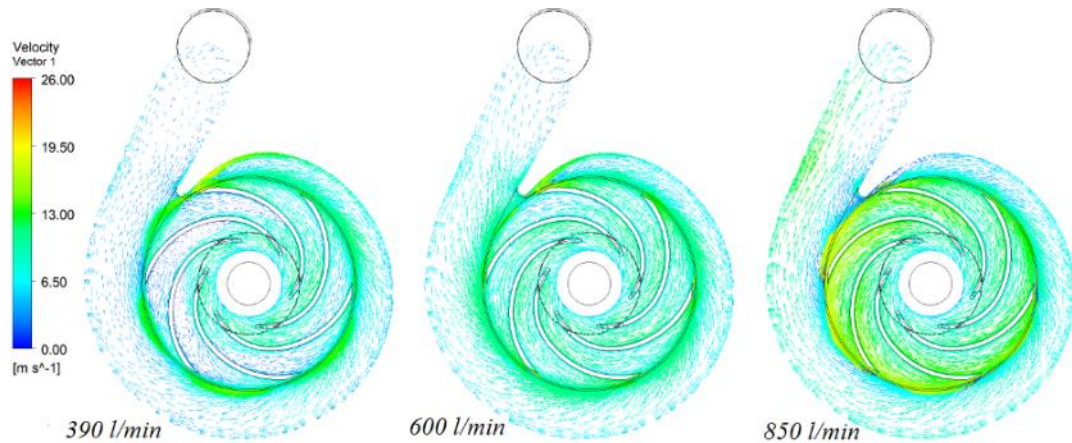


Figure 3.22. Relative velocity distribution on the mid-section of Pump-1 (m/s)

CFD result of pump-1 delivery head versus flow rate of three points is presented in the Figure 3.23.

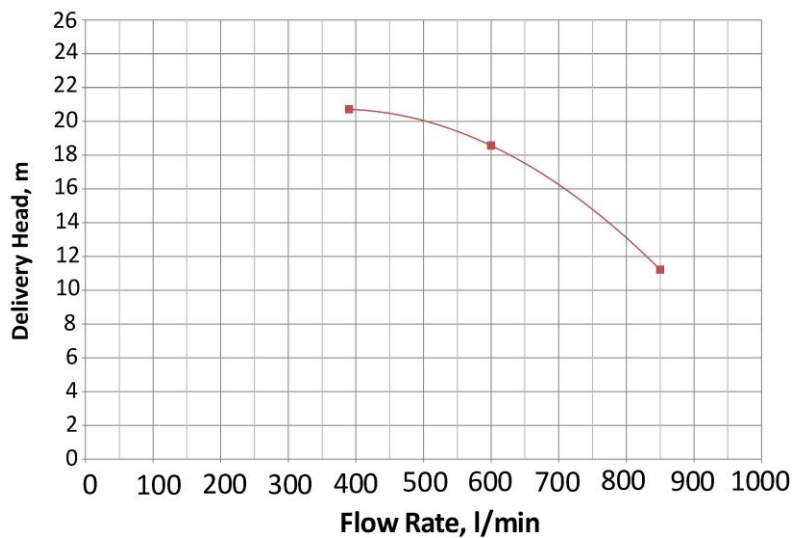


Figure 3.23. Delivery head (m) vs. flow rate graph of Pump-1 CFD results

Pressure difference between rotating domain inlet and outlet gives the delivery head by impeller while the pressure loss between the impeller exit and the volute outlet is the volute loss. Relation between CFD results is shown in Figure 3.24.

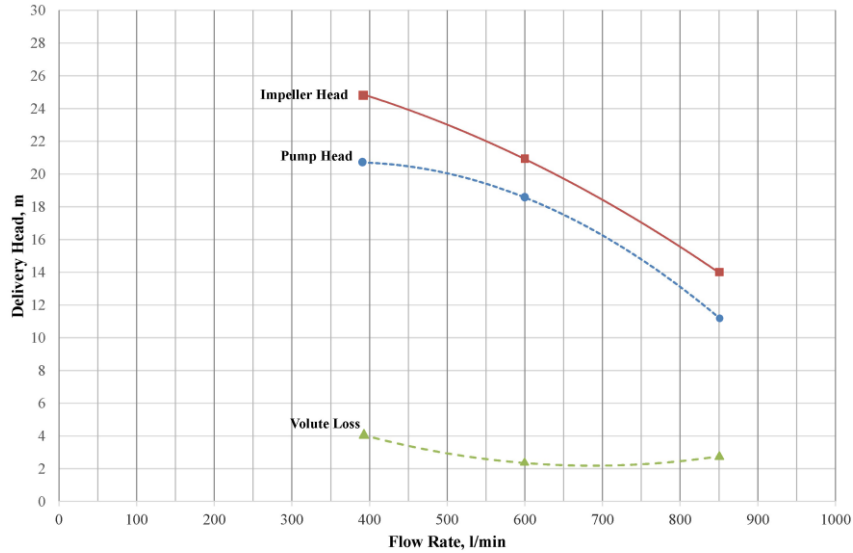


Figure 3.24. Impeller head, pump head and volute losses of Pump-1 CFD results

Comparison of H-Q graph between theoretical prediction, experimental and CFD results of Pump-1 are shown in Figure 3.25.

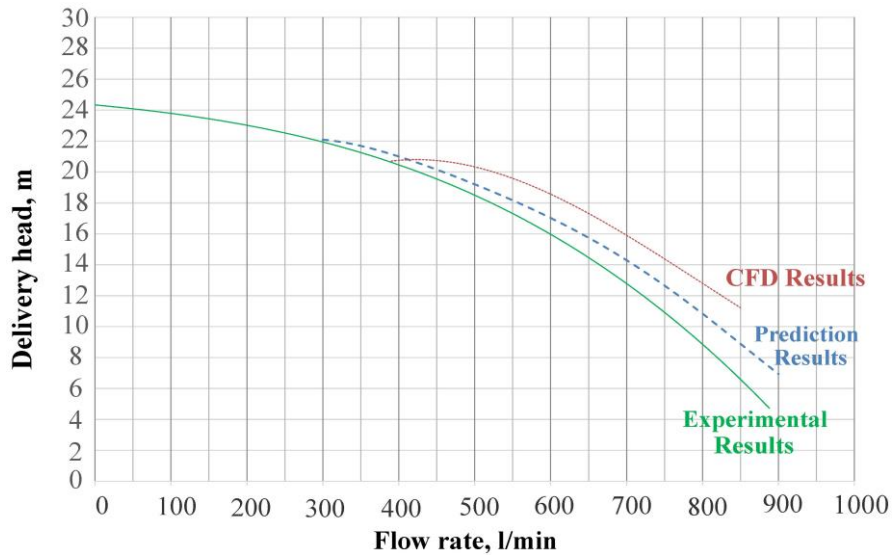


Figure 3.25. Result comparison of Pump-1

At low flow rates both CFD results and theoretical predictions show excellent agreement with the experimental data however, considerable discrepancies are observed as the flow rate increases. It is interesting to note that despite the visible discrepancies,

the theoretical predictions are in better agreement with the measurement at high flow rates compared to the CFD results.

Volute losses by CFD and theoretical prediction results are compared in the Figure 3.26 below. Here, theoretical predictions yield higher volute losses compared to the CFD predictions. Since MRF modeling is used for CFD calculations, MRF ignores the relative motions of the zones with respect to each other and does not account for fluid dynamic interaction between stationary and rotating components. For this reason MRF is often referred to as the “frozen rotor” approach. The drawbacks of the model include inadequate prediction of physics for local flow values and sensitivity of the results to the relative position of the rotor and stator for tightly coupled components [16]. For this reason, the position of the impeller relative to the volute affects CFD loss calculations.

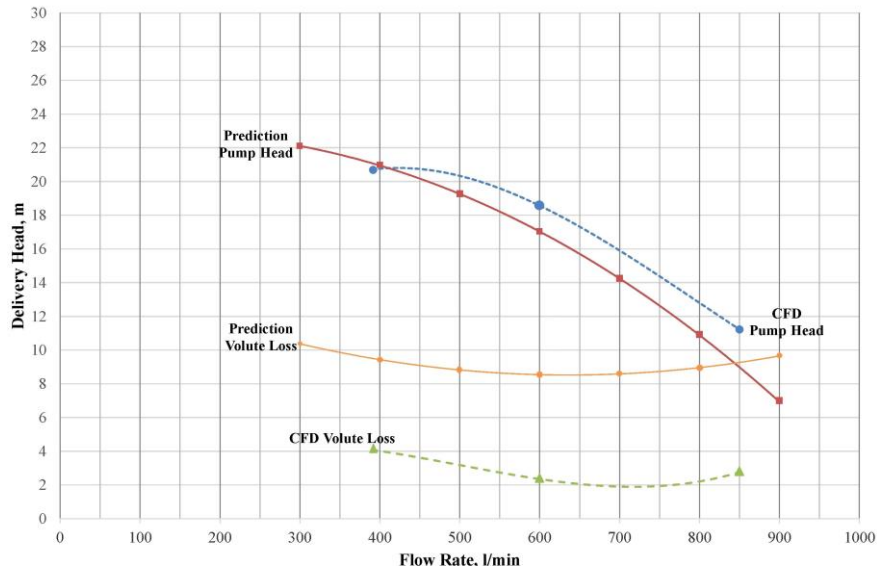


Figure 3.26. Comparison of loss results of Pump-1

3.3.2. CFD Results of Pump-2

Analyses are performed for 3 different flow rates and calculated pump head values are shown in Table 3.2.

Table 3.2. CFD Results at certain flow rates for Pump-2

| Flow rate (l/min) | ΔP (bar) | H (m) |
|-------------------|------------------|-------|
| 150 | 1.03 | 10.51 |
| 300 | 0.86 | 8.77 |
| 450 | 0.64 | 6.53 |

The total and static pressure variation within the pump for the three flow rates studied is shown in Figure 3.27 and Figure 3.28. Figure 3.27 shows the distribution of static pressure in mid plane of the impeller. Volute of the pump is below the impeller with trapezoidal cross-sectional shape. There is a small gap between the impeller and the volute that fluid passes through. The distribution of the pressure is very similar and evenly distributed for all channels in the impeller. Pressure is gradually increasing through the blades.

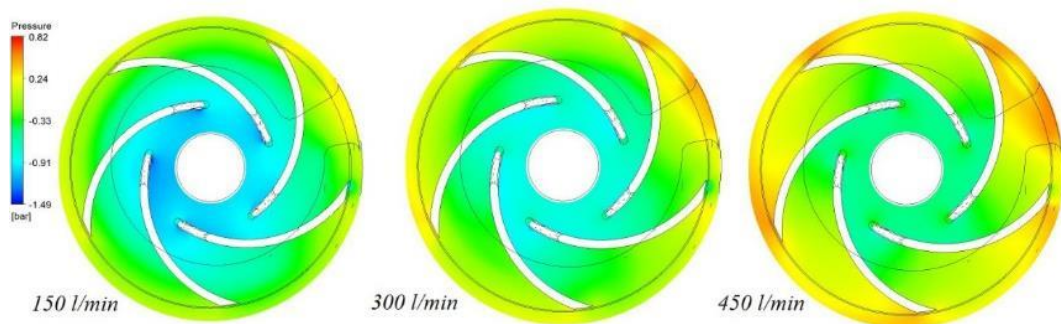


Figure 3.27. Static pressure distribution on the mid-section of Pump-2 (bar)

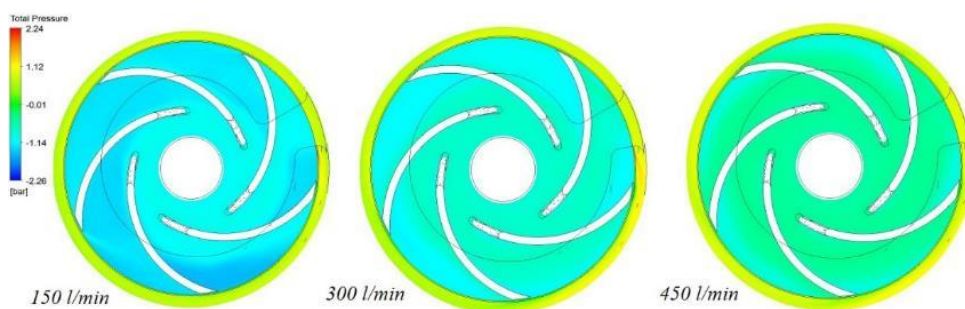


Figure 3.28. Total pressure distribution on the mid-section of Pump-2 (bar)

At design point, the distribution of the pressure is very similar and evenly distributed for all channels in the impeller. Pressure is gradually increasing through the blades and there is basically no pressure gradient in the gap and volute. Total pressure is gradually increasing from left to right as the flow rate increases.

Figure 3.29 shows a vector plot of the relative velocity in the mid plane of the impeller and gap. The velocity distribution becomes the most uniform at the design volume flow rate, similar to the pressure distribution. Small recirculation zones can be seen in the impeller channels of the flow rate of 150 l/min. Flow velocities are very low in these channels.

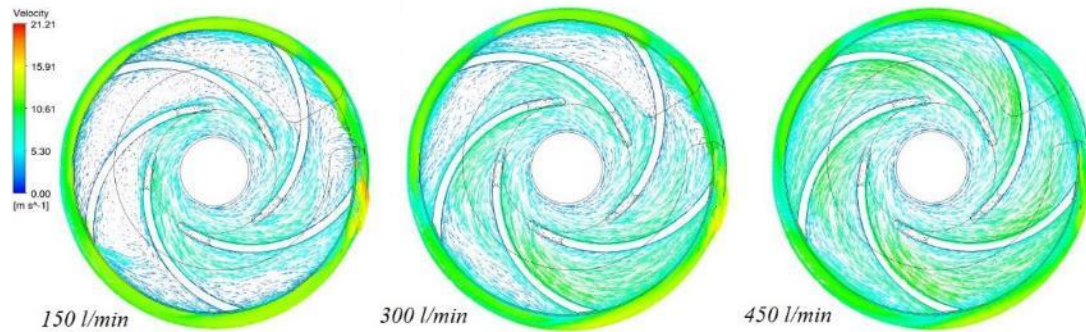


Figure 3.29. Relative velocity distribution on the mid-section of Pump-2 (m/s)

CFD result of pump-2 delivery head versus flow rate is presented in the Figure 3.30.

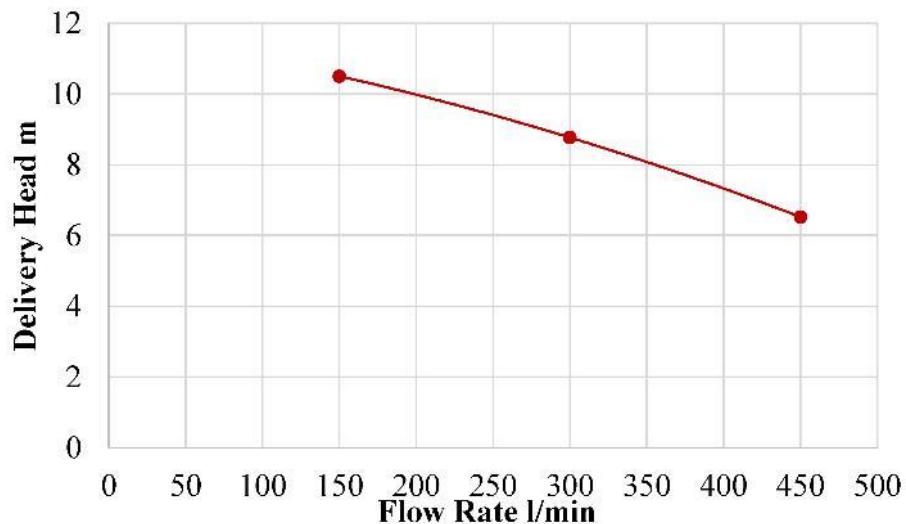


Figure 3.30. Delivery head (m) vs. flow rate graph of Pump-2CFD results

Comparison of H-Q graph between theoretical prediction, experimental and CFD results of Pump-2 are shown in Figure 3.31.

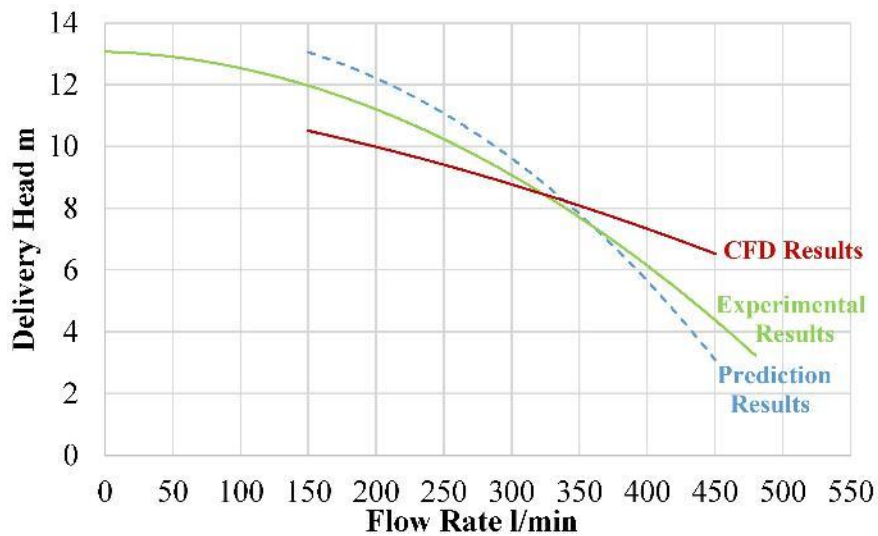


Figure 3.31. Comparison of loss results of Pump-2

At design point, both CFD results and theoretical predictions show excellent agreement with the experimental data however, considerable discrepancies are observed at off-design conditions. It is interesting to note that despite the visible discrepancies, the theoretical predictions are in better agreement with the measurement at low flow rates compared to the CFD results. The discrepancies may occur due to the geometry of volute has trapezoidal shape and flow passas through the gap without a tongue. Sectional view of Pump-2 is shown Figure 3.32.

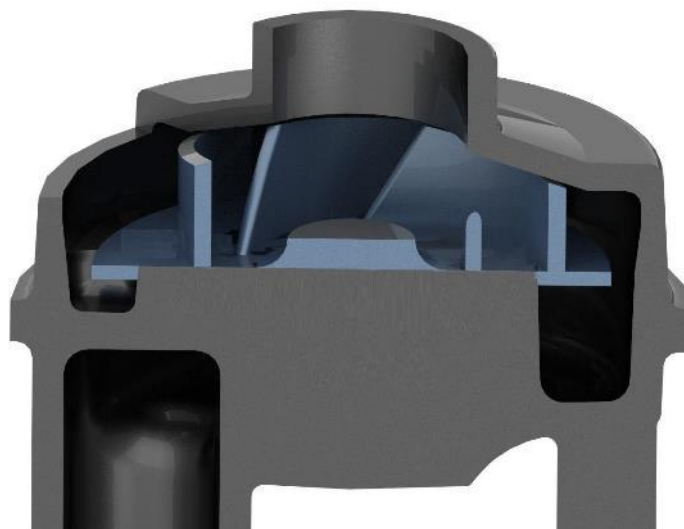


Figure 3.32. Sectional view of Pump-2

3.3.3. CFD Results of Pump-3

Analyses are performed for 3 different flow rates and calculated pump head values are shown in Table 3.3.

Table 3.3. CFD Results at certain flow rates for Pump-3

| Flow rate (l/min) | ΔP (bar) | H (m) |
|-------------------|------------------|-------|
| 60 | 0.96 | 9.79 |
| 120 | 0.73 | 7.46 |
| 180 | 0.43 | 4.39 |

The total and static pressure variation within the pump for the three flow rates studied is shown in Figure 3.33 and Figure 3.34. The pressure increases gradually from the tongue to the volute exit for flow rates lower than design point. When the flow rate approaches the nominal value, the pressure distribution becomes more uniform. For flow rates higher than design flow rate, the pressure reaches its highest value behind the tongue and starts to decrease around the circumference of the impeller, taking its minimum value just behind the tongue. Figure 3.33 shows the distribution of static pressure in mid plane of the impeller. Volute of the pump is at the top of the impeller with trapezoidal cross-sectional shape. The distribution of the pressure is very similar and evenly distributed for all channels in the impeller. Pressure is gradually increasing through the blades.

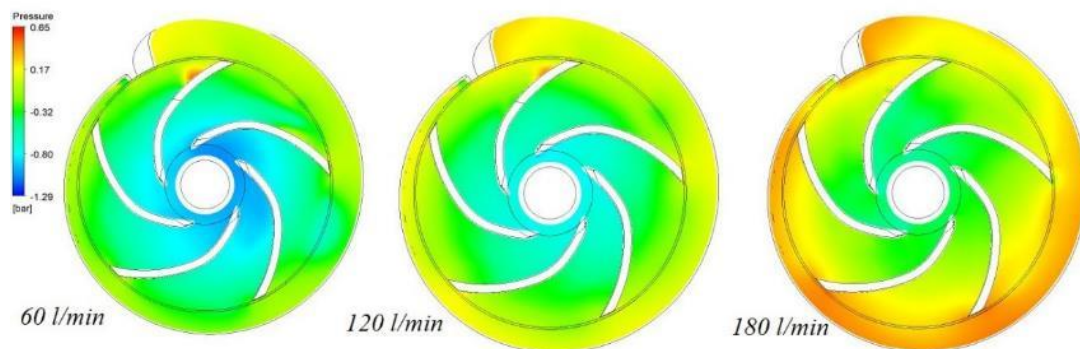


Figure 3.33. Static pressure distribution on the mid-section of Pump-3 (bar)

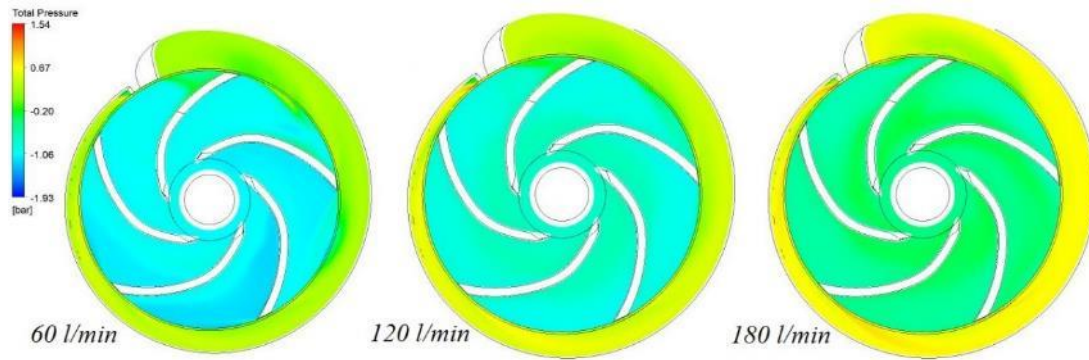


Figure 3.34. Total pressure distribution on the mid-section of Pump-3 (bar)

At design point (120 l/min), the distribution of the pressure is very similar and evenly distributed for all channels in the impeller. Pressure is gradually increasing through the blades and there is basically no pressure gradient volute.

Figure 3.35 shows a vector plot of the relative velocity in the mid plane of the impeller and volute. The velocity distribution becomes the most uniform at the design volume flow rate, similar to the pressure distribution. Small recirculation zones can be seen in the impeller channels of the flow rate of 60 l/min. Flow velocities are very low in these channels where the volute pressure is the largest.

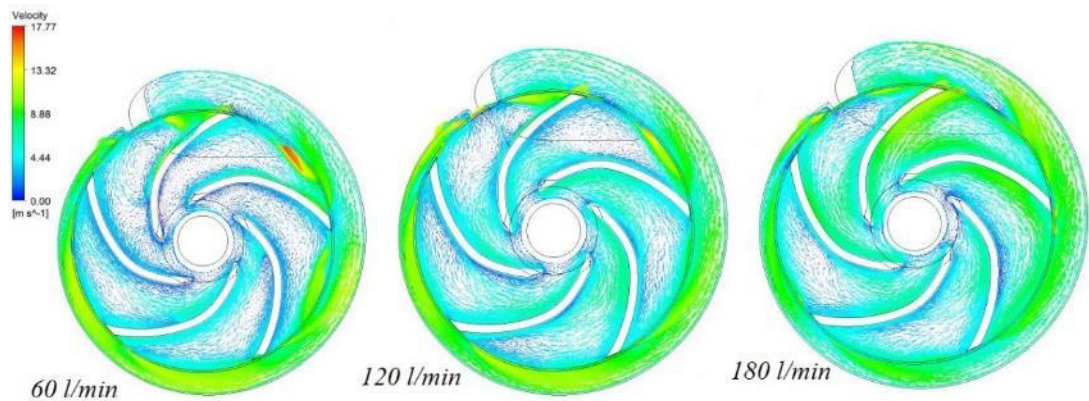


Figure 3.35. Relative velocity distribution on the mid-section of Pump-3 (m/s)

CFD result of Pump-3 delivery head versus flow rate is presented in the Figure 3.36.

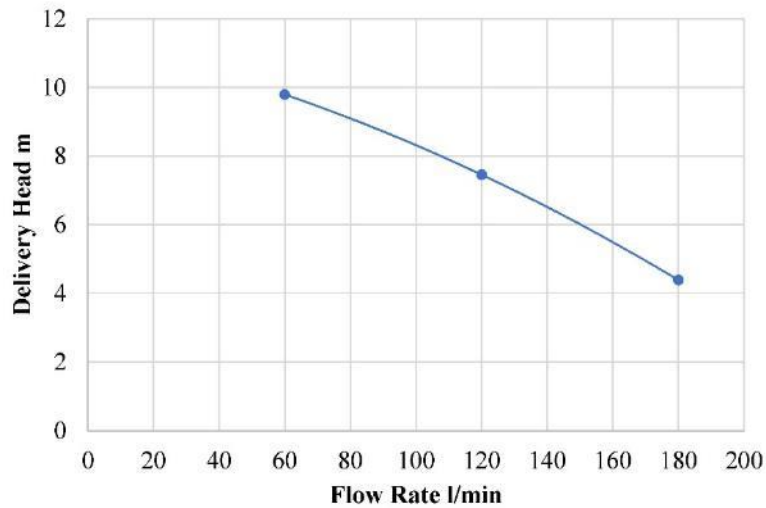


Figure 3.36. Delivery head (m) vs. flow rate graph of Pump-3 CFD results

Comparison of H-Q graph between theoretical prediction, experimental and CFD results of Pump-3 are shown in Figure 3.37.

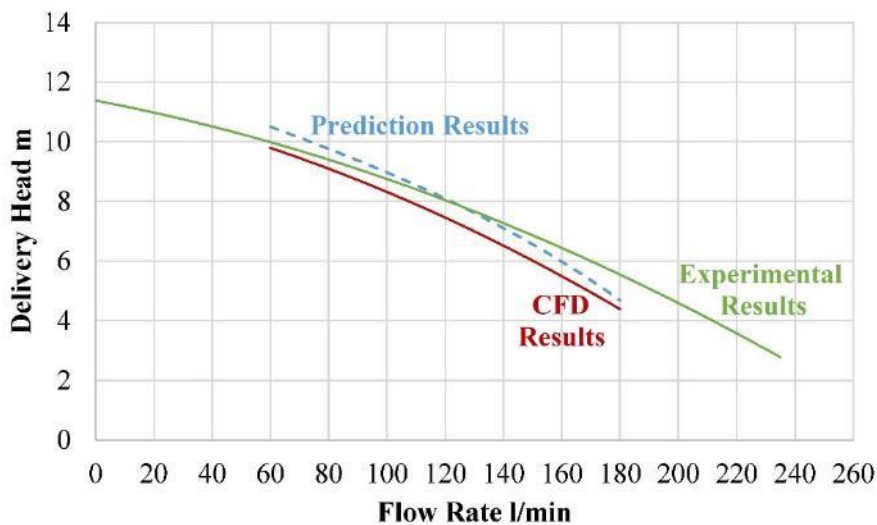


Figure 3.37. Comparison of loss results of Pump-3

At design point, theoretical predictions show excellent agreement with the experimental data however, considerable discrepancies are observed as the flow rate increases. Impeller of Pump-3 that is used in experiments has same blade geometry but has open gaps at the impeller exit that allows to fluid a passage at high flow rates. Therefore it causes discrepancies between the experiment, prediction and CFD results. Figure 3.38 shows that the actual impeller of Pump-2 and generated impeller for prediction and CFD. It is interesting to note that despite the visible discrepancies, the theoretical

predictions are in better agreement with the measurement at high flow rates compared to the CFD results, but at low flow rates, CFD results have better correspondence.



Figure 3.38. Impeller of (a) experimental Pump-3 and (b) predicted and CFD Pump-3

Results of theoretical prediction, CFD and experiments of Pump-1, Pump-2 and Pump-3 for 3 different flow rates and pump head values are shown in Table 3.4.

Table 3.4. Comparison of results at certain flow rates

| | Q (l/min) | Prediction (m) | Performance (m) | CFD (m) |
|---------------|----------------------------|---------------------------------|----------------------------------|--------------------------|
| Pump-1 | 390 | 21.05 | 20.9 | 20.71 |
| | 600 | 17.03 | 15.85 | 18.56 |
| | 850 | 8.90 | 6.51 | 11.22 |
| Pump-2 | 150 | 13.04 | 11.53 | 10.51 |
| | 300 | 9.52 | 8.99 | 8.77 |
| | 450 | 3.09 | 4.07 | 6.53 |
| Pump-3 | 60 | 10.48 | 9.78 | 9.79 |
| | 120 | 7.92 | 7.9 | 7.46 |
| | 180 | 4.66 | 5.46 | 4.39 |

4. CONCLUSION

A theoretical prediction procedure was developed to predict an off-design performance of the centrifugal pumps by applying the basic principles of the turbomachines and the empirical loss correlations.

The performance predictions are compared with CFD calculations and experimental measurements for the same pump geometry. For the range of flow rates studied here, delivery head predictions have been found to be in good agreement with experimental measurements and CFD results. The time required to construct the geometry and meshes, adjust solver settings, and CFD analysis takes at least 10-12 hours depending on the number and quality of meshes. It is possible to obtain the result takes less than 1 hour by developed program. Thus, the program provides a great advantage over CFD analysis in terms of time and effort. Therefore, the developed performance prediction code is highly reliable and can be used.

Predictions also showed that volute design has a significant effect on the pump performance. The pump head decreases considerably due to the increase in volute friction loss. The general structure of the developed code makes it a quick and effective tool and therefore it can successfully be used in the basic design of centrifugal pumps.

These present thesis approve that, prediction code is a powerful tool to predict the characteristics of a centrifugal pump with specific speed between 40 to 180. Predicted characteristics of three different pumps using mentioned loss correlations are in good agreement with performance curves at BEP and off-design points. Confirmity of predicted curves to the performance curves show that results of software is consistent and repeatable which is very important to develop a performance prediction software for a highly complicated flow in turbomachines. Therefore, prediction code proves to be a good supplement tool for the design of centrifugal pumps.

There is a need for future work in the sectional shape of the volute. Loss calculations of volute are performed assuming the volute has circular section. Trapezoidal section would be added to the calculations as an option. All the pump materials are assumed to be cast iron. A material library would be added to the calculations which effects the friction losses.

References

- [1] Dick E., Vierendeels J., Serbruyns S., Voorde J.V., (2001), Performance Prediction of Centrifugal Pumps with CFD-Tools, *Task Quarterly*, 5 (4), p. p579
- [2] Wang C., Shi W., Wang X., Jiang X., (2017), Optimal design of multistage centrifugal pump based on the combined energy loss model and computational fluid dynamics, *Journal of Applied Energy*, Vol. 187, pp. 10-26
- [3] Stel H., Ofuchi E.M., Sabino R.H.G., Ancajima F.C., Bertoldi D., (2018), Investigation of the Motion of Bubbles in a Centrifugal Pump Impeller, *ASME Journal of Fluids Engineering*, Vol 141(3).
- [4] Nocente A., Tufan A., Nielsen T.K., (2015), Numerical Prediction of a Multistage Centrifugal Pump Performance with Stationary and Moving Mesh, *Proceedings of the ASME 2015 Power Conference*,
- [5] Pfleiderer, C., (1961), *Die Kreiselpumpen für Flüssigkeiten und Gase.*, Springer Verlag, fifth Edition, ISBN 978-3-642-48170-3.
- [6] Gülich, J.F., (2014), *Centrifugal Pumps*, Third Edition, ISBN 978-3-642-40113-8.
- [7] Tuzson, J., (2000), *Centrifugal Pump Design*, John Wiley & Sons, ISBN 978-0-471-36100-8.
- [8] Hamkins, C., (1984), Correlation of One-Dimensional Centrifugal Pump Performance Analysis Method, *ASME Paper 84-WAFM-10*.
- [9] Dick E., Ammi M., (1991), Comparison between steady and unsteady one-dimensional performance analysis methods for centrifugal pumps. *European Journal of Mechanical Engineering*, Vol. 36, nr. 3.
- [10] Busemann A., (1928), Das Förderhohenverhältniss radialer Kreiselpumpen mit logarithmischspiraligen Schaufeln, *Z. Angew. Math. Mech.*, 372–384
- [11] Wiesner F.J., (1967), A Review of Slip Factors for Centrifugal Impellers, *ASME Journal Eng. Power* Vol. 89, n. 4.
- [12] Dixon S.L., Cesare H., (2010), *Fluid Mechanics and Thermodynamics of Turbomachinery*, Butterworth-Heinemann, Sixth Ed., ISBN: 978-18-561-7793-1

- [13] Dick E., (2015), Fundamentals of Turbomachines, Springer, First Ed., ISBN 978-94-017-9626-2
- [14] Pearsall I.S., (1978), Off design performance of pumps, Von Karman Institute Lecture Series vol.3.
- [15] Myles D.J., (1969), An Analysis of Impeller and Volute Losses in Centrifugal Fans, Archive Proceedings of the Institution of Mechanical Engineers 1847-1982 (vols 1-196) 184, 253-277.
- [16] ANSYS CFX Reference Guide (2018), ANSYS, Inc., Release 19.0
- [17] ANSYS Meshing User's Guide (2018), ANSYS, Inc., Release 19.0
- [18] ANSYS CFX-Solver Theory Guide (2018), ANSYS, Inc., Release 19.0
- [19] ANSYS CFX-Solver Modeling Guide (2018), ANSYS, Inc., Release 19.0
- [20] KSB Centrifugal Pump Handbook, (2015)
- [21] Baysal K., (1975), Tam santrifüj pompalar: Hesap, çizim ve konstrüksiyon özellikleri, İstanbul Teknik Üniversitesi Matbaası.
- [22] Lorett J. A., Gopalakrishnan S., (1986), Interaction between impeller and volute of pumps at off-design conditions, Journal of Fluids Engineering, vol. 108/1
- [23] The Centrifugal Pump Handbook, (2009), GRUNDFOS Research and Technology, Denmark
- [24] Stodola,A., (1927) Steam and Gas Turbines, McGraw-Hill Book Company, New York
- [25] Stanitz, J. D., (1952), Some Theoretical Aerodynamic Investigations of Impellers in Radial- and Mixed-Flow Centrifugal Compressors, Transactions of ASME, 74, pp. 473–476.
- [26] Backström T.W., (2006), A Unified Correlation for Slip Factor in Centrifugal Impellers, Journal of Turbomachinery, Vol. 128/1
- [27] Noorbakhsh A., (1973), Theoretical and Real Slip Factor in Centrifugal Pumps, von Karman Institute for Fluid Dynamics, Technical Note 93

- [28] Worster, R.C.,(1963), The flow in volutes and its effect on centrifugal pump performance. Proc. Inst. of Mech. Eng. 177(31), 843–875.-Noorbakhsh, A. (1973), A.
- [29] Finger R., (2013), The Java Virtual Machine (JVM): The Platform That Powers The World, <https://www.forbes.com/sites/richardfinger/2013/10/15/the-java-virtual-machine-jvm-the-platform-that-powers-the-world> (05.05.2018)
- [30] <http://www.oracle.com/technetwork/java/javase/overview/javafx-overview-2158620.html> (05.05.2018)

APPENDIX

A.1. Basic geometric calculations and loss calculations module

```
//First Calculations of Q-H-n
@FXML
public void calculate(ActionEvent event) throws Exception {

    double Qa, H, n, ns,Den, v;
    String nsstring;
    String Qstring = Q1.getText();
    String Hstring = H1.getText();
    String Denstring = Den1.getText();
    String nstring = n1.getText();
    String vstring = vis.getText();

    if (Q1.getText().isEmpty() || H1.getText().isEmpty() ||
n1.getText().isEmpty()
        || Den1.getText().isEmpty() || vis.getText().isEmpty()
        || n1.getText().matches("[a-zA-Z!'^+%&/()=?<>,-]*")
        || H1.getText().matches("[a-zA-Z!'^+%&/()=?<>,-]*")
        || Q1.getText().matches("[a-zA-Z!'^+%&/()=?<>,-]*")
        || Den1.getText().matches("[a-zA-Z!'^+%&/()=?<>,-]*")
        || vis.getText().matches("[a-zA-Z!'^+%&/()=?<>,-]*"))

    Qa = Double.parseDouble(Qstring);
    double Q = Qa/60000;
    H = Double.parseDouble(Hstring);
    Den = Double.parseDouble(Denstring);
    n = Double.parseDouble(nstring);
    v = Double.parseDouble(vstring);
    double g = 9.80665;

    ns = 3.65 * n * Math.pow(Q, 0.5) / Math.pow(H, 0.75) ;
    nsstring = String.format(Locale.ROOT,"% .2f", ns);
    ns1.setText(nsstring);

    double nsq = n * Math.pow(Q, 0.5) / Math.pow(H, 0.75) ;
    String nsqstring = String.format(Locale.ROOT,"% .2f", nsq);
    nsq1.setText(nsqstring);
```

```

double D0a = 4500 * Math.pow(Q/n, 0.3333333);
String D0astring = String.format(Locale.ROOT,"%0.2f", D0a);
D0_nom2.setText(D0astring);

double D0 = Math.round(D0a);
String D0string = String.format(Locale.ROOT,"%0.1f", D0);
D0_nom1.setText(D0string);

double nh = 100 * (1 - 0.42/ Math.pow(Math.log10(D0)-0.172,2));
String nhstring = String.format(Locale.ROOT,"%0.2f", nh);
nh_1.setText(nhstring);

double nv = 100 / (1 + 0.68 * Math.pow(ns,-0.6666666));
String nvstring = String.format(Locale.ROOT,"%0.2f", nv);
nv_1.setText(nvstring);

double nm = 97;
String nmstring = String.format(Locale.ROOT,"%0.1f", nm);
nm_1.setText(nmstring);

double no = nh*nv*nm / 10000;
String nostring = String.format(Locale.ROOT,"%0.2f", no);
no_1.setText(nostring);

double P_out = g*Den*Q *H / 1000;
String Poutstring = String.format(Locale.ROOT,"%0.2f", P_out);
P_out1.setText(Poutstring);

double P_in = P_out / (no / 100);
String Pinstring = String.format(Locale.ROOT,"%0.2f", P_in);
P_in1.setText(Pinstring);

double T = P_in * 1000 / (2 * Math.PI * n /60);
String Tstring = String.format(Locale.ROOT,"%0.2f", T);
T_1.setText(Tstring);

double Ds2 = Math.pow(16 * T / (0.012* Math.PI), 0.3333333);
String Ds2string = String.format(Locale.ROOT,"%0.2f", Ds2);
Ds_2.setText(Ds2string);

```

```

double Ds = Math.ceil(Ds2/2) * 2;
String Dsstring = String.format(Locale.ROOT,"%0.1f", Ds);
Ds_1.setText(Dsstring);

double Dh = Math.ceil(Ds*1.5);
String Dhstring = String.format(Locale.ROOT,"%0.1f", Dh);
Dh_1.setText(Dhstring);

double Qt = Q /nv*100;

double C0 = 4*Qt/(Math.PI *(Math.pow(D0/1000,2)- Math.pow(Dh/1000,2)));
String C0string = String.format(Locale.ROOT,"%0.2f", C0);
C0_1.setText(C0string);

double C1a = C0*1.05;
String C1astring = String.format(Locale.ROOT,"%0.2f", C1a);
C1_1.setText(C1astring);

double C1b = C0*1.1;
String C1bstring = String.format(Locale.ROOT,"%0.2f", C1b);
C1_2.setText(C1bstring);

// interpolation
double[] y_cm_1 = {0.109, 0.113, 0.118, 0.121, 0.124, 0.13, 0.1335, 0.138
,0.142, 0.145, 0.15, 0.154, 0.159, 0.162, 0.164, 0.169, 0.172, 0.176, 0.179, 0.182, 0.184,
0.187, 0.19, 0.192, 0.195, 0.199,0.202, 0.206, 0.209};
double[] y_cm_2 = {0.08, 0.083, 0.087, 0.09, 0.094, 0.098, 0.1, 0.104, 0.108,
0.11, 0.114, 0.117, 0.12, 0.122, 0.125, 0.129, 0.132, 0.134, 0.138, 0.14, 0.142, 0.145,
0.149, 0.15, 0.153, 0.155, 0.158, 0.16, 0.162};
//double[] y_ku_1 = {0.96, 0.965, 0.97, 0.975, 0.98, 0.983, 0.985, 0.99, 0.995,
0.998, 1, 1.005, 1.01, 1.02, 1.03, 1.04, 1.048, 1.05, 1.06, 1.07, 1.08, 1.085, 1.09, 1.095,
1.1, 1.11, 1.12, 1.13, 1.14};
double[] y_y_1 = {1.24, 1.22, 1.19, 1.17, 1.14, 1.12, 1.09, 1.075, 1.05, 1.03,
1.01, 0.99, 0.96, 0.94, 0.925, 0.9, 0.88, 0.87, 0.85, 0.83, 0.81, 0.8, 0.78, 0.76, 0.745,
0.73, 0.72, 0.71, 0.69};
double[] y_ns = {40, 45, 50, 55, 60, 65, 70, 75, 80, 85, 90, 95, 100, 105, 110,
115, 120, 125, 130, 135, 140, 145, 150, 155, 160, 165, 170, 175, 180};

double x_ns = Math.ceil(ns/5) * 5 ;
int i = 0 ;
for (i = 0; i<y_cm_1.length ; i++)

```

```

        {
            if (y_ns[i] == x_ns)
            {
                break;
            }
        }
        int XY = i-1;

        double k_cm1 = y_cm_1[XY] + (ns - y_ns[XY]) * (y_cm_1[XY+1] -
y_cm_1[XY]) / (y_ns[XY+1] - y_ns[XY]) ;
        double k_cm2 = y_cm_2[XY] + (ns - y_ns[XY]) * (y_cm_2[XY+1] -
y_cm_2[XY]) / (y_ns[XY+1] - y_ns[XY]) ;
        //double k_ku1 = y_ku_1[XY] + (ns - y_ns[XY]) * (y_ku_1[XY+1] -
y_ku_1[XY]) / (y_ns[XY+1] - y_ns[XY]) ;
        double k_y1 = y_y_1[XY] + (ns - y_ns[XY]) * (y_y_1[XY+1] - y_y_1[XY]) /
(y_ns[XY+1] - y_ns[XY]) ;

        double Cm1 = k_cm1 * Math.pow(2 * g * H, 0.5);
        String Cm1string = String.format(Locale.ROOT,"%0.2f", Cm1);
        Cm1_1.setText(Cm1string);
        double D1 = Math.round(D0*0.93);
        String D1string = String.format(Locale.ROOT,"%0.1f", D1);
        D1_1.setText(D1string);
        double D1d = D0 + 3;
        String D1dstring = String.format(Locale.ROOT,"%0.1f", D1d);
        D1d_1.setText(D1dstring);
        double D1i = 2 * D1 - D1d;
        String D1istring = String.format(Locale.ROOT,"%0.1f", D1i);
        D1i_1.setText(D1istring);
        double u1 = Math.PI * D1 * n / 60000;
        String u1string = String.format(Locale.ROOT,"%0.2f", u1);
        u1_1.setText(u1string);
        double u1d = Math.PI * D1d * n / 60000;
        String u1dstring = String.format(Locale.ROOT,"%0.2f", u1d);
        u1d_1.setText(u1dstring);
        double u1i = Math.PI * D1i * n / 60000;
        String u1istring = String.format(Locale.ROOT,"%0.2f", u1i);
        u1i_1.setText(u1istring);
        double B10 = Math.toDegrees(Math.atan(Cm1/u1));
        String B10string = String.format(Locale.ROOT,"%0.1f", B10);

```

```

B10_1.setText(B10string);
double B1 = Math.ceil(B10) + 3;
String B1string = String.format(Locale.ROOT,"%0.2f", B1);
B1_1.setText(B1string);
double B1d = Math.toDegrees(Math.atan(Cm1/u1d)) + (B1 - Math.ceil(B10)) ;
String B1dstring = String.format(Locale.ROOT,"%0.1f", B1d);
B1d_1.setText(B1dstring);
double B1i = Math.toDegrees(Math.atan(Cm1/u1i)) + (B1 - Math.ceil(B10)) ;
String B1istring = String.format(Locale.ROOT,"%0.1f", B1i);
B1i_1.setText(B1istring);
double b_1 = Qt / (Math.PI * D1/1000 * Cm1 * 0.65) * 1000 ;
String b_1string = String.format(Locale.ROOT,"%0.1f", b_1);
b1_2.setText(b_1string);
double b1s = Math.ceil(b_1) ;
String b1sstring = String.format(Locale.ROOT,"%0.1f", b1s);
b1_1.setText(b1sstring);
double u2a = Math.pow(2 * g * H / k_y1 , 0.5);
String u2astring = String.format(Locale.ROOT,"%0.2f", u2a);
u2a_1.setText(u2astring);
double D2a_1 = u2a * 60000 / (Math.PI * n);
String D2a_1string = String.format(Locale.ROOT,"%0.1f", D2a_1);
D2_2.setText(D2a_1string);
double D2 = Math.ceil(D2a_1) ;
String D2string = String.format(Locale.ROOT,"%0.1f", D2);
D2_1.setText(D2string);
double u2 = Math.PI * n * D2 / 60000 ;
String u2string = String.format(Locale.ROOT,"%0.2f", u2);
u2_1.setText(u2string);
double Cm2 = k_cm2 * Math.pow(2 * g * H , 0.5);
String Cm2string = String.format(Locale.ROOT,"%0.2f", Cm2);
Cm2_1.setText(Cm2string);
double Cu2 = g * H / (u2 * nh /100) ;
String Cu2string = String.format(Locale.ROOT,"%0.2f", Cu2);
Cu2_1.setText(Cu2string);
double Hmax = Math.pow(Math.PI * D2/1000 * n/60 , 2) / (2 * g);
String Hmaxstring = String.format(Locale.ROOT,"%0.2f", Hmax);
Hmax_1.setText(Hmaxstring);
double B20 = Math.toDegrees(Math.atan(Cm2/(u2- Cu2)));
String B20string = String.format(Locale.ROOT,"%0.1f", B20);
B20_1.setText(B20string);

```

```

int k = (int) Math.round(B20) ;
for (k++ ; k<50 ; k++ )
{
double Zi = 6.5 * ((D2+D1)/(D2-D1))* Math.sin((Math.toRadians(B1+k)/2));
double Zk = Math.round(Zi);
double K = 1 + (1.2*(1+Math.sin(Math.toRadians(k)))/(Zk*(1-Math.pow(D1/D2 , 2))))
;
double Cu2s = K * Cu2;
double B2k = Math.toDegrees(Math.atan(Cm2/(u2a- Cu2s)));
double m = Math.abs(k - B2k);
if (m <= 0.5)
    {
        break;
    }
}
double B2 = k ;
String B2string = String.format(Locale.ROOT, "%.2f", B2);
B2_1.setText(B2string);
double Zi = 6.5 * ((D2+D1)/(D2-D1))* Math.sin((Math.toRadians(B1+B2)/2));
double Zk = Math.round(Zi);
double K = 1 + (1.2*(1+Math.sin(Math.toRadians(B2)))/(Zk*(1-
Math.pow(D1/D2 , 2)))) ;
double Cu2s = K * Cu2;
double B2k = Math.toDegrees(Math.atan(Cm2/(u2a- Cu2s)));
String B2kstring = String.format(Locale.ROOT, "%.1f", B2k);
B22_1.setText(B2kstring);

//double Zi = 6.5 * ((D2+D1)/(D2-D1))* Math.sin((Math.toRadians(B1+B2)/2));
String Zistring = String.format(Locale.ROOT, "%.2f", Zi);
Z2_1.setText(Zistring);
double Z = Math.round(Zi);
String Zstring = String.format(Locale.ROOT, "%.2f", Z);
Z_1.setText(Zstring);
double e = 5;
String estring = String.format(Locale.ROOT, "%.1f", e);
e_1.setText(estring);
double l2 = 1 - (Z * e / Math.sin((Math.toRadians(B2)))/ Math.PI / D2) ;
String l2string = String.format(Locale.ROOT, "%.2f", l2);
l2_1.setText(l2string);
double b2 = Qt / (Math.PI * D2/1000 * l2/1000 * Cm2) ;

```

```

String b2string = String.format(Locale.ROOT,"%0.2f", b2);
b2_1.setText(b2string);
double l1 = 1 - (Z * e / Math.sin((Math.toRadians(B1)))/ Math.PI / D1) ;
String l1string = String.format(Locale.ROOT,"%0.2f", l1);
l1_1.setText(l1string);
double b1n = Qt / (Math.PI * D1/1000 * l1/1000 * Cm1) ;
String b1_1string = String.format(Locale.ROOT,"%0.2f", b1n);
b1_3.setText(b1_1string);
double b1 = Math.ceil(b1n) ;
String b1string = String.format(Locale.ROOT,"%0.1f", b1);
b1_1.setText(b1string);

double alfa1 = Math.toDegrees(Math.atan((b1-b2)/(D2- D1d)*2));
double alfa = Math.round(alfa1) ;
String alfastring = String.format(Locale.ROOT,"%0.1f", alfa);
angle_2.setText(alfastring);
b2_angle.setText(alfastring);
b2_angle1.setText(alfastring);
double b2_1 = b1 - Math.tan(Math.toRadians(alfa))*((D2-D1d)/2);
String b2_1string = String.format(Locale.ROOT,"%0.1f", b2_1);
b2_2.setText(b2_1string);

double T1 = 1 / (1- (Z * (e / 2) / (Math.PI * D1 * Math.sin(Math.toRadians(B1)))));
String T1string = String.format(Locale.ROOT,"%0.1f", T1);
//T1_1.setText(T1string);

double T2 = 1 / (1- (Z * e / (Math.PI * D2 * Math.sin(Math.toRadians(B2)))));
String T2string = String.format(Locale.ROOT,"%0.1f", T2);
//T2_1.setText(T2string);

//salyangoz hesapları
double t = 7 ;
String tstring = String.format(Locale.ROOT,"%0.1f", t);
t_1.setText(tstring);
double b3 = b2_1 + 2;
String b3string = String.format(Locale.ROOT,"%0.1f", b3);
b3_1.setText(b3string);
double A = Cu2* D2/2000 ;
double D3 = D2 + 2;
String D3string = String.format(Locale.ROOT,"%0.1f", D3);

```

```

D3_1.setText(D3string);
D3_2.setText(D3string);
double ee = D2 /60;
String eestring = String.format(Locale.ROOT,"% .1f", ee);
ee_1.setText(eestring);
ee_2.setText(eestring);
double df = D3 * 0.3;
double vdf = Q / (Math.PI* Math.pow(df/2000,2));
String vdfstring = String.format(Locale.ROOT,"% .1f", vdf);
v_df.setText(vdfstring);

```

```
//KAYIP HESAPLARI
```

```

public void calculate_loss(ActionEvent event) throws Exception {
//Theoretical Head
double E_loss = Math.exp(-8.16*Math.sin(Math.toRadians(B2))/Z2);
double Slip;
    if (R < E_loss ) {
Slip = (1-Math.pow(Math.sin(Math.toRadians(B2)),0.5)/Math.pow(Z2,0.7));
        }
    else {
Slip = (1-Math.pow(Math.sin(Math.toRadians(B2)),0.5)/Math.pow(Z2,0.7))*
        (1-Math.pow(((D1/D2-E_loss)/(1-E_loss)),3));
        }
double T2 = 1 - (e*z/(Math.sin(Math.toRadians(B2))*Math.PI*D2));
double Cm2 = Q / (Math.PI * D2/1000 * b2/1000 * T2 );
double Cu2 = Slip * u2 - Cm2/Math.tan(Math.toRadians(B2));
double H_th = u2 * Cu2 / g;
String Hth_string = String.format(Locale.ROOT,"% .2f", H_th);

```

```
//Inlet Loss
```

```

String C02 = C0_1.getText();
double C0 = Double.parseDouble(C02);
double H0 = 0.1* Math.pow(C0,2)/2 /g;
String H0_string = String.format(Locale.ROOT,"% .2f", H0);

```

```
//impeller loss
```

```

double T1 = 1 - (e*z/(Math.sin(Math.toRadians(B1))*Math.PI*D1));
double cm1 = Q / (Math.PI * D1/1000 * b1/1000 * T1 );
double cu1 = u1 - cm1 / Math.tan(Math.toRadians(B1));

```

```

//mismatching loss
double Hi_1 = 0.65* Math.pow(cu1, 2)/2/g;
String Hi1_string = String.format(Locale.ROOT,"% .2f", Hi_1);

//friction loss
double Li = (D2-D1)/1000/(2*Math.sin(Math.toRadians((B1+B2)/2)));
double a1 = Math.PI * D1/1000 * Math.sin(Math.toRadians(B1)) / z ;
double a2 = Math.PI * D2/1000 * Math.sin(Math.toRadians(B2)) / z ;
double Dh = 2 * (a1*b1/1000 + a2*b2/1000) / (a1+b1/1000+a2+b2/1000);
double Ef = Math.pow(1.138 + 2* Math.log10(Dh/1000/0.26) ,-2);
double w1 = cm1 / Math.sin(Math.toRadians(B1));
double Hi_2 = Ef * Li * Math.pow(w1,2) / (Dh*2)/g ;
String Hi2_string = String.format(Locale.ROOT,"% .2f", Hi_2);

//Blade loading loss
double w2 = Math.pow((Math.pow(Cm2, 2) + Math.pow((u2-Cu2), 2)), 0.5);
double s = z * Math.log(D2/D1) / (2 * Math.PI * Math.sin(Math.toRadians((B1+B2)/2))
);
double Dl = 1 - (w2/w1) + (((u1-cu1)-(u2-Cu2))/(2*s*w1)) ;
double Hi_3 = Math.pow(Dl, 2)*Math.pow(w2, 2) / 2/g ;

//Disc Friction Loss
double Re = u2 * D2/1000 / v * Math.pow(10,6);
double C = 0.15 * Math.pow(Re, -0.2);
double Pdf = C * Math.pow(u2, 3)* Math.pow(D2/2000,2)/2;
double Hdf = 0.3 * Pdf / Q /g ;
String Hdf_string = String.format(Locale.ROOT,"% .2f", Hdf);

//Volute Loss
//Mismatching
double Hv1 = Math.pow((D2*Cu2/D3-D4*c4/D3), 2)/2/g;
if (D2*Cu2 <= D4*c4 ) {
    Hv1 = 0;
}
String Hv1_string = String.format(Locale.ROOT,"% .2f", Hv1);

//Volute Friction Loss
double R3 = D3/2000 ;

```

```

double Av = (Math.PI * Math.pow(D4/1000,2)/4) *

Math.pow(1+Math.pow((2*Math.PI)/Math.log((R3+D4/2000)/R3),2),0.5) +

2*Math.PI*(D4/2000*(2*R3+D4/2000)/(2*Math.log((R3+D4/2000)/R3))-
Math.pow(D2/2000, 2));
double Lv = (D3/2000 - D2/2000 + Math.PI * D4 / 2000) /
Math.sin(Math.toRadians(8));
double Ef2 = Math.pow(1.89 + 1.62 * Math.log10(Lv/0.26) ,-2.5);
double Hv2 = Ef2 * Av * Math.pow(c4, 2) / (2*Math.PI *
Math.pow(D4/1000,2)/4)/g;
String Hv2_string = String.format(Locale.ROOT,"% .2f", Hv2);

//Diffusor Loss
double D5 = 1.15*D4;
double c5 = Q / Math.PI * (Math.pow(D5/1000,2) / 4);
double hd = (D5-D4)/ (2*Math.tan(Math.toRadians(8)));
double A1 = Math.PI*(D4+D5)/2000*Math.pow(Math.pow(D5/2000-
D4/2000,2)
+Math.pow(hd/1000,2),0.5);
double S1 = A1 + Math.PI * (Math.pow(D4/2000,2)+Math.pow(D5/2000,2));
double Kd = A1 / S1;
double Hdl= Kd * (Math.pow(c4,2)-Math.pow(c5, 2))/2/g ;
String Hd_string = String.format(Locale.ROOT,"% .2f", Hdl);

// Total H
double H = H_th - H0 - Hi_1 - Hi_2 - Hi_3 -Hv1 -Hv2 - Hdl + Hdf ;
String H_string = String.format(Locale.ROOT,"% .2f", H);

```

A.2. JavaFx code for the program interface

```
<?xml version="1.0" encoding="UTF-8"?>
<?import javafx.scene.control.Button?>
<?import javafx.scene.control.Label?>
<?import javafx.scene.control.Tab?>
<?import javafx.scene.control.TabPane?>
<?import javafx.scene.control.TextField?>
<?import javafx.scene.image.Image?>
<?import javafx.scene.image.ImageView?>
<?import javafx.scene.layout.AnchorPane?>
<?import javafx.scene.shape.Rectangle?>
<?import javafx.scene.text.Font?>

<AnchorPane prefHeight="655.0" prefWidth="1310.0" style="-fx-background-radius:
20;" xmlns="http://javafx.com/javafx/9.0.1" xmlns:fx="http://javafx.com/fxml/1"
fx:controller="application.MainController">
<children>
<Rectangle arcHeight="30.0" arcWidth="30.0" fill="TRANSPARENT" height="125.0"
layoutX="38.0" layoutY="15.0" stroke="BLACK" strokeType="INSIDE"
width="135.0" />
<Rectangle arcHeight="50.0" arcWidth="50.0" fill="TRANSPARENT" height="184.0"
layoutX="197.0" layoutY="8.0" stroke="BLACK" strokeType="INSIDE"
width="186.0" />
<Button fx:id="call" layoutX="261.0" layoutY="161.0" mnemonicParsing="false"
onAction="#calculate" text="Calculate" />
<Label fx:id="Flow" layoutX="226.0" layoutY="19.0" text="Flow Rate">
<font>
<Font name="Calibri" size="12.0" />
</font>
</Label>
<TextField fx:id="Q1" layoutX="287.0" layoutY="14.0" prefHeight="25.0"
prefWidth="45.0" />
<Label fx:id="l_min_text" layoutX="341.0" layoutY="18.0" text="l/min" />
<Label fx:id="Head" layoutX="206.0" layoutY="49.0" text="Delivery Head">
<font>
<Font name="Calibri" size="12.0" />
</font>
</Label>
<TextField fx:id="H1" layoutX="287.0" layoutY="43.0" prefHeight="25.0"
prefWidth="45.0" />
```

```

<Label fx:id="m_text" layoutX="341.0" layoutY="47.0" text="m" />
<Label fx:id="Speed_text" layoutX="243.0" layoutY="79.0" prefHeight="14.0"
prefWidth="34.0" text="Speed">
<font>
<Font name="Calibri" size="12.0" />
</font>
</Label>
<TextField fx:id="n1" layoutX="287.0" layoutY="73.0" prefHeight="25.0"
prefWidth="45.0" />
<Label fx:id="n_text" layoutX="341.0" layoutY="77.0" text="RPM" />
<Label fx:id="SpecSpeed_text1" layoutX="14.0" layoutY="199.0" prefHeight="17.0"
prefWidth="76.0" text="Specific Speed">
<font>
<Font name="Calibri" size="12.0" />
</font>
</Label>
<TextField fx:id="ns1" editable="false" layoutX="100.0" layoutY="196.0"
prefHeight="25.0" prefWidth="45.0">
<font>
<Font name="Calibri" size="12.0" />
</font>
</TextField>
<Label fx:id="SpecSpeed_nsq" layoutX="15.0" layoutY="228.0" prefHeight="17.0"
prefWidth="34.0" text="n sq">
<font>
<Font name="Calibri" size="12.0" />
</font>
</Label>
<TextField fx:id="nsq1" editable="false" layoutX="100.0" layoutY="225.0"
prefHeight="25.0" prefWidth="45.0">
<font>
</TextField>
<Label fx:id="D0nom_text" layoutX="14.0" layoutY="258.0" prefHeight="17.0"
prefWidth="76.0" text="D0 nominal">
<font>
<Font name="Calibri" size="12.0" />
</font>
</Label>
</children>
</AnchorPane>

```

A.3. JavaFx code for the interface of loss calculation

```
<?xml version="1.0" encoding="UTF-8"?>
<?import javafx.scene.control.Label?>
<?import javafx.scene.control.TableColumn?>
<?import javafx.scene.control.TableView?>
<?import javafx.scene.control.TextField?>
<?import javafx.scene.layout.AnchorPane?>
<?import javafx.scene.shape.Rectangle?>
<?import javafx.scene.text.Font?>

<AnchorPane          prefHeight="183.0"          prefWidth="541.0"
xmlns="http://javafx.com/javafx/9.0.1"          xmlns:fx="http://javafx.com/fxml/1"
fx:controller="application.LossController">
<children>
<AnchorPane layoutX="3.0" layoutY="3.0" maxHeight="-Infinity" maxWidth="-
Infinity" minHeight="-Infinity" minWidth="-Infinity" prefHeight="180.0"
prefWidth="538.0">
<children>
<Rectangle arcHeight="20.0" arcWidth="20.0" fill="TRANSPARENT" height="67.0"
layoutX="23.0" layoutY="99.0" stroke="BLACK" strokeType="INSIDE"
width="130.0" />
<Rectangle arcHeight="20.0" arcWidth="20.0" fill="TRANSPARENT" height="141.0"
layoutX="357.0" layoutY="12.0" stroke="BLACK" strokeType="INSIDE"
width="168.0" />
<Rectangle arcHeight="20.0" arcWidth="20.0" fill="TRANSPARENT" height="158.0"
layoutX="172.0" layoutY="11.0" stroke="BLACK" strokeType="INSIDE"
width="175.0" />
<Label fx:id="Hdf_text" layoutX="71.0" layoutY="61.0" prefHeight="17.0"
prefWidth="25.0" text="Hdf">
<font>
<Font name="Calibri" size="12.0" />
</font>
</Label>
<TextField fx:id="_HdfLossTextField" editable="false" layoutX="96.0"
layoutY="57.0" prefHeight="25.0" prefWidth="45.0">
<font>
<Font name="Calibri" size="12.0" />
</font>
</TextField>
<Label fx:id="text225" layoutX="144.0" layoutY="63.0" text="m">
<font>
```

```

</font>
</TextField>
<Label fx:id="Hi1_text" layoutX="255.0" layoutY="68.0" prefHeight="17.0"
prefWidth="25.0" text="Hi1">
</font>
</Label>
<TextField fx:id="_Hi2LossTextField" editable="false" layoutX="279.0"
layoutY="98.0" prefHeight="25.0" prefWidth="45.0">
<font>
<Font name="Calibri" size="12.0" />
</font>
</TextField>
<Label fx:id="Hi2_text" layoutX="255.0" layoutY="101.0" prefHeight="17.0"
prefWidth="25.0" text="Hi2">
<Font name="Calibri" size="12.0" />
</font>
</Label>
<TextField fx:id="_Hi3LossTextField" editable="false" layoutX="280.0"
layoutY="132.0" prefHeight="25.0" prefWidth="45.0">
<font>
</Label>
<TextField fx:id="_HTotalTextField" editable="false" layoutX="68.0"
layoutY="129.0" prefHeight="25.0" prefWidth="45.0">
<font>
<Font name="Calibri Bold" size="14.0" />
</font>
</Label>
<TextField fx:id="_Hv1LossTextField" editable="false" layoutX="458.0"
layoutY="38.0" prefHeight="25.0" prefWidth="45.0">
<font>
<Font name="Calibri" size="12.0" />
</font>
</TextField>
<Label fx:id="Hv1_text" layoutX="434.0" layoutY="41.0" prefHeight="17.0"
prefWidth="25.0" text="Hv1">
</Label>
<Label fx:id="Hv2_text1" layoutX="362.0" layoutY="71.0" prefHeight="35.0"
prefWidth="63.0" text="Volute Friction Loss" wrapText="true">
<font>
<Font name="Calibri" size="12.0" />
</font>

```

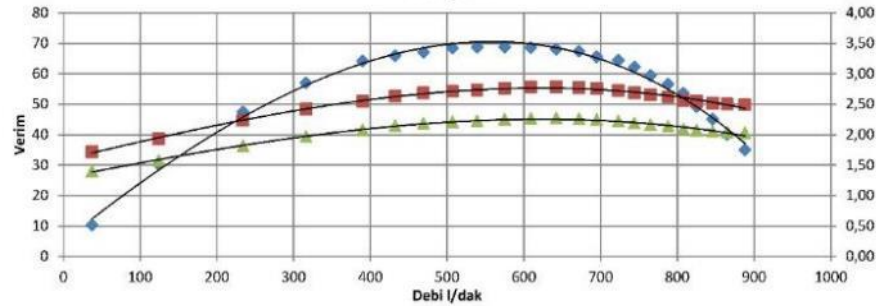
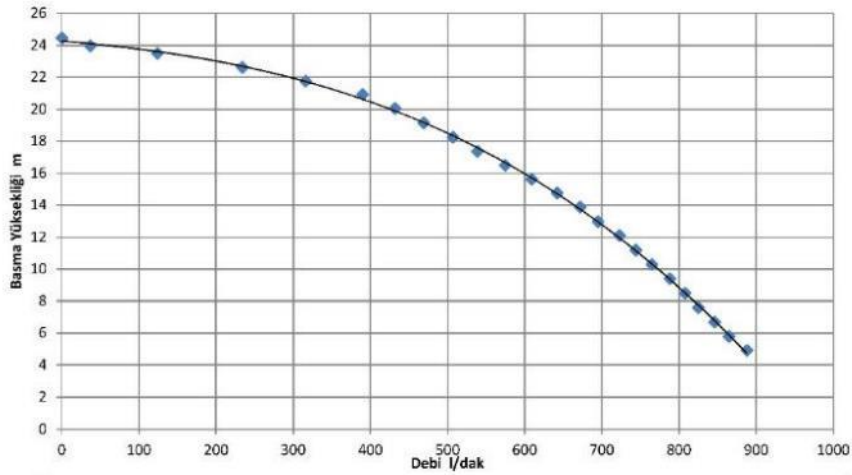
```

</Label>
<Label fx:id="Hd_text1" layoutX="362.0" layoutY="110.0" prefHeight="35.0"
prefWidth="50.0" text="Diffusor Loss" wrapText="true">
<font>
</font>
</Label>
</children>
</AnchorPane>
<TableView fx:id="myTableView" layoutX="6.0" layoutY="183.0"
prefHeight="275.0" prefWidth="530.0">
<columns>
<TableColumn fx:id="col1" prefWidth="137.0" text="Losses" />
<TableColumn fx:id="col2" prefWidth="65.0" text="Q1" />
<TableColumn fx:id="col3" minWidth="0.0" prefWidth="65.0" text="Q2" />
<TableColumn fx:id="col4" minWidth="6.0" prefWidth="65.0" text="Q3" />
<TableColumn fx:id="col5" minWidth="0.0" prefWidth="65.0" text="Q4" />
<TableColumn fx:id="col6" prefWidth="65.0" text="Q5" />
<TableColumn fx:id="col7" minWidth="0.0" prefWidth="65.0" text="Q6" />
</columns>
</TableView>
</children>
</AnchorPane>


```

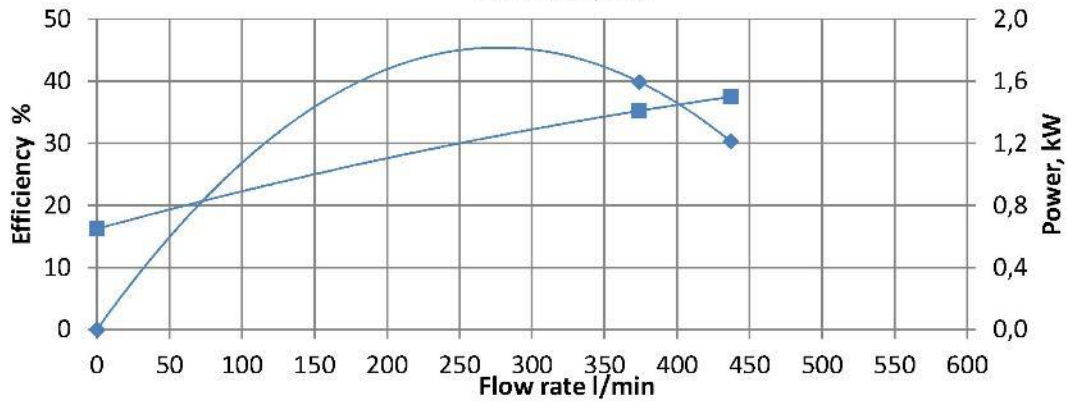
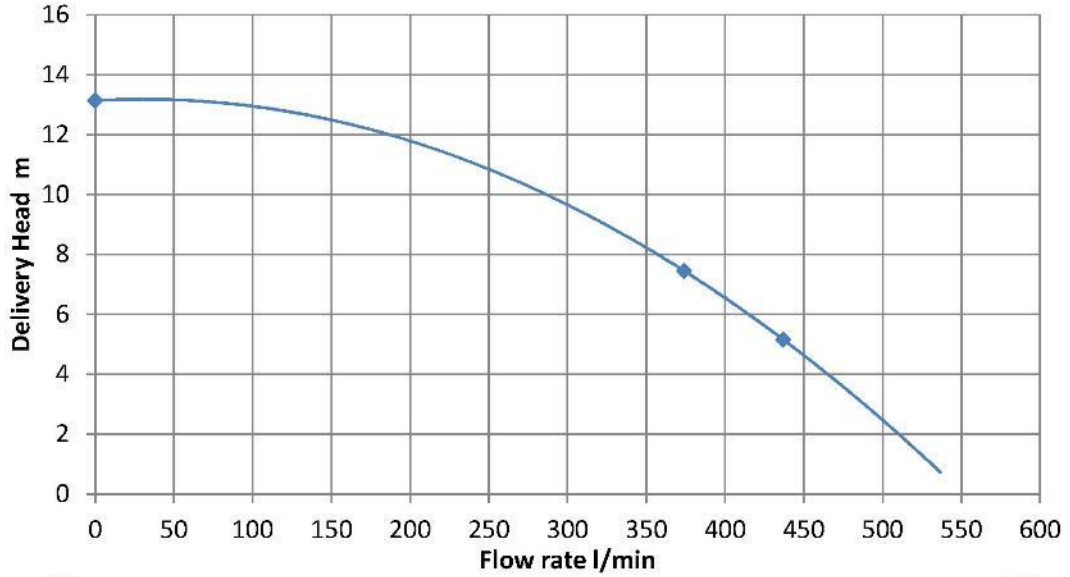
B.1. Pump-1 performance test report

| miksan MOTOR | | POMPA TEST RAPORU | | | Tarih : | 29.02.12 | | |
|-------------------|-----------|-------------------|---------|---|----------|----------|--------------|----------|
| | | | | | İmza : | O.MERCAN | | |
| Pompa Modeli : | JPA | Motor : | 100 | Not : Döküm açık çark ile test yapıldı. Gerilim 390-395V aralığındaydı. 2B Salyangoz bağlandı. Maksimum debi 940 lt/dk | | | | |
| Hmax (m) : | | P (kW) : | 3 | | | | | |
| Qmax (m) : | | U (V) : | 400 | | | | | |
| Verim (%) : | | I (A) : | 6,9 | | | | | |
| Basma Çapı (mm) : | 50 | Cos Φ : | 0,77 | | | | | |
| Çark Çapı (mm) : | 142 | Verim (%) : | 81,5 | | | | | |
| Z2-Z1 (m) : | 1 | n (d/d) : | 2870 | | | | | |
| Q lt/dak. | Hb Bar | v2/2g m | Hm m | I A | P1 kW | P2 kW | η pompa % | n d/d |
| 888,0 | 0,10 | 2,90 | 4,9 | 5,43 | 2,50 | 2,03 | 35,1 | 2925 |
| 865,0 | 0,20 | 2,75 | 5,8 | 5,41 | 2,50 | 2,04 | 40,1 | 2921 |
| 846,0 | 0,30 | 2,63 | 6,7 | 5,42 | 2,51 | 2,05 | 45,2 | 2922 |
| 825,0 | 0,40 | 2,50 | 7,6 | 5,42 | 2,55 | 2,07 | 49,3 | 2923 |
| 808,0 | 0,50 | 2,40 | 8,5 | 5,48 | 2,57 | 2,09 | 53,7 | 2921 |
| 788,0 | 0,60 | 2,28 | 9,4 | 5,51 | 2,62 | 2,14 | 56,6 | 2916 |
| 765,0 | 0,70 | 2,15 | 10,3 | 5,50 | 2,65 | 2,16 | 59,5 | 2917 |
| 744,0 | 0,80 | 2,03 | 11,2 | 5,58 | 2,69 | 2,19 | 62,2 | 2912 |
| 723,0 | 0,90 | 1,92 | 12,1 | 5,62 | 2,72 | 2,22 | 64,4 | 2914 |
| 695,0 | 1,00 | 1,77 | 13,0 | 5,66 | 2,76 | 2,25 | 65,6 | 2913 |
| 672,0 | 1,10 | 1,66 | 13,9 | 5,73 | 2,77 | 2,26 | 67,5 | 2913 |
| 642,0 | 1,20 | 1,51 | 14,8 | 5,78 | 2,79 | 2,27 | 68,1 | 2913 |
| 609,0 | 1,30 | 1,36 | 15,6 | 5,78 | 2,78 | 2,27 | 68,6 | 2913 |
| 575,0 | 1,40 | 1,21 | 16,5 | 5,71 | 2,76 | 2,25 | 68,8 | 2915 |
| 539,0 | 1,50 | 1,07 | 17,4 | 5,74 | 2,73 | 2,23 | 68,7 | 2914 |
| 507,0 | 1,60 | 0,94 | 18,3 | 5,67 | 2,71 | 2,21 | 68,4 | 2916 |
| 469,0 | 1,70 | 0,81 | 19,1 | 5,62 | 2,68 | 2,19 | 67,1 | 2917 |
| 432,0 | 1,80 | 0,69 | 20,0 | 5,55 | 2,63 | 2,15 | 66,0 | 2919 |
| 390,0 | 1,90 | 0,56 | 20,9 | 5,48 | 2,55 | 2,08 | 64,3 | 2922 |
| 316,0 | 2,00 | 0,37 | 21,8 | 5,40 | 2,42 | 1,97 | 57,0 | 2925 |
| 234,0 | 2,10 | 0,20 | 22,6 | 5,29 | 2,23 | 1,82 | 47,5 | 2932 |
| 124,0 | 2,20 | 0,06 | 23,5 | 5,00 | 1,93 | 1,58 | 30,2 | 2944 |
| 37,0 | 2,25 | 0,01 | 24,0 | 4,91 | 1,72 | 1,40 | 10,4 | 2953 |
| 0,0 | 2,30 | 0,00 | 24,5 | 4,83 | 1,74 | 1,41 | 0,0 | 2953 |




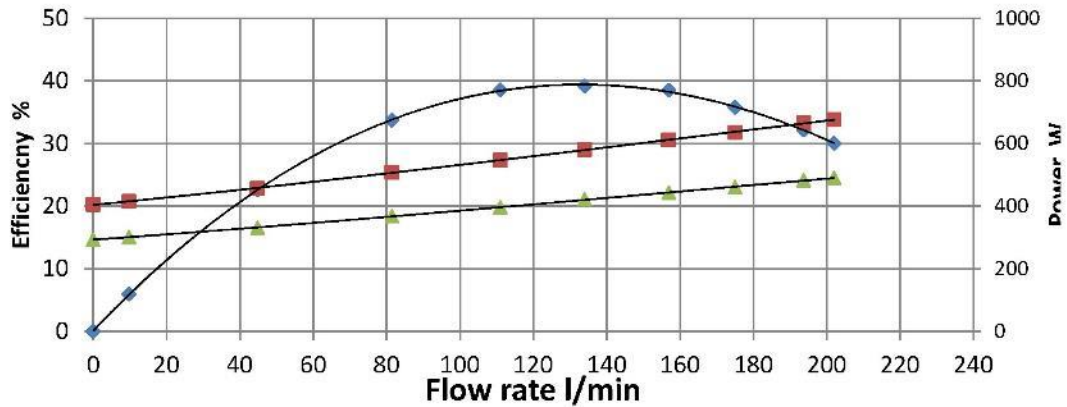
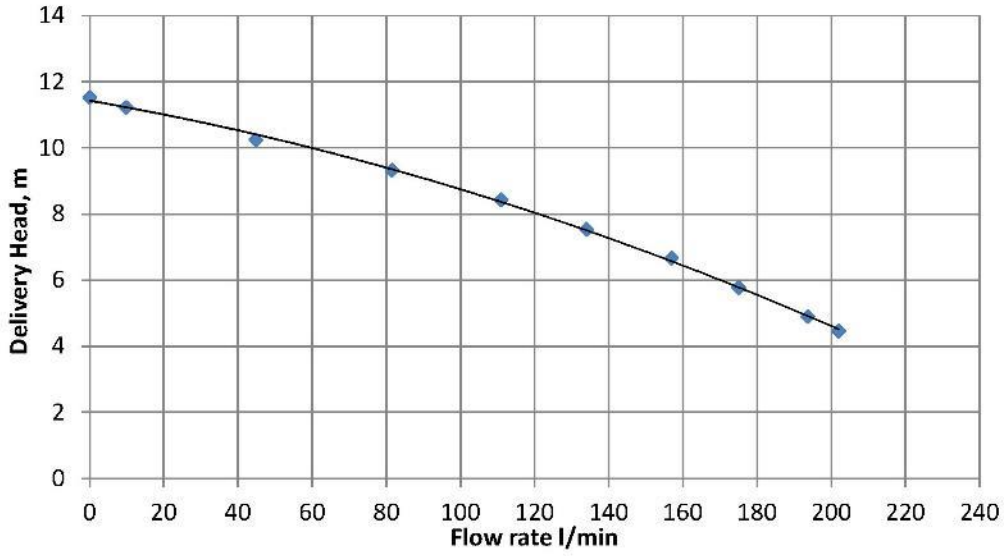
B.2. Pump-2 performance test report

|  | | POMPA TEST RAPORU | | | | Tarih : | 18.03.16 | | |
|---|------|-------------------|------|--|------|---------|----------|-----|--|
| | | | | | | İmza : | D.DEVELI | | |
| Pompa Modeli : | IP 1 | Motor : | 90 | Not : 1 kademe pompa 3" hatta test edildi. Transmitter ile pompa çıkışından ölçüm yapıldı. Seviye farkı 1,10 m. Pompa önce 400V 50Hz değerlerinde test edildi, daha sonra aynı düzenekte 460V 60Hz değerlerinde ölçüm yapıldı. | | | | | |
| Hmax (m) : | | P (kW) : | 2,2 | | | | | | |
| Qmax (m) : | | U (V) : | 400 | | | | | | |
| Verim (%) : | | I (A) : | 4,8 | | | | | | |
| Basma Çapı (mm) : | 40 | Cos Φ : | 0,82 | | | | | | |
| Çark Çapı (mm) : | 106 | Verim (%) : | 81 | | | | | | |
| Z2-Z1 (m) : | 1,1 | n (d/d) : | 2850 | | | | | | |
| Q | Hb | v2/2g | Hm | I | P1 | P2 | η pompa | n | |
| lt/dak. | Bar | m | m | A | kW | kW | % | d/d | |
| 437,0 | 0,23 | 1,71 | 5,2 | - | 1,50 | 1,22 | 30,3 | - | |
| 374,0 | 0,50 | 1,25 | 7,5 | - | 1,41 | 1,14 | 39,9 | - | |
| 0,0 | 1,18 | 0,00 | 13,1 | - | 0,65 | 0,53 | 0,0 | - | |
| 60 Hz Sonuçlar | | | | | | | | | |
| 538,0 | 0,40 | 2,60 | 7,8 | - | 2,42 | 1,96 | 34,9 | - | |
| 522,0 | 0,50 | 2,44 | 8,6 | - | 2,39 | 1,94 | 38,1 | - | |
| 450,0 | 0,85 | 1,82 | 11,6 | - | 2,25 | 1,82 | 46,8 | - | |
| 338,0 | 1,20 | 1,02 | 14,4 | - | 2,03 | 1,64 | 48,3 | - | |
| 0,0 | 1,77 | 0,00 | 19,2 | - | - | - | 0,0 | - | |



B.3. Pump-3 performance test report

|  | | POMPA TEST RAPORU | | | Tarih : | 07.03.13 | | |
|---|-----------|-------------------|---------|---|---------|----------|--------------|----------|
| | | | | | İmza : | D.DEVELİ | | |
| Pompa Modeli : | EP 251 | Motor : | 71/2 | Not : Emme Çapı Ø35mm , derinliği 14,5mm olan döküm salyangoz, kanat yüksekliği 17,5mm , hub yüksekliği 10mm olan döküm çark, 27 gövde (kömürsüz) ve 0,55kW motor ile test edildi. En son ölçülere göre işlendi. Çark gövdeye 0,5mm boşluk bırakılarak bağlandı. Gerilim değerleri 398-403V. Açık vana: h=0,35bar - Q=202lt/dk - P=676. | | | | |
| Hmax (m) : | | P (kW) : | 0,55 | | | | | |
| Qmax (m) : | | U (V) : | 380 | | | | | |
| Verim (%) : | | I (A) : | 1,35 | | | | | |
| Basma Çapı (mm) : | 32 | Cos Φ : | 0,82 | | | | | |
| Çark Çapı (mm) : | 94 | Verim (%) : | 72,5 | | | | | |
| Z2-Z1 (m) : | 0 | n (d/d) : | 2752 | | | | | |
| Q lt/dak. | Hb Bar | v2/2g m | Hm m | I A | P1 W | P2 W | η pompa % | n d/d |
| 235,0 | 0,15 | 1,21 | 2,7 | - | 717 | 520 | 20,2 | - |
| 202,0 | 0,35 | 0,89 | 4,5 | 1,23 | 676 | 490 | 30,1 | - |
| 193,7 | 0,40 | 0,82 | 4,9 | 1,24 | 666 | 483 | 32,1 | - |
| 175,0 | 0,50 | 0,67 | 5,8 | 1,20 | 636 | 461 | 35,8 | - |
| 156,9 | 0,60 | 0,54 | 6,7 | 1,17 | 611 | 443 | 38,5 | - |
| 134,0 | 0,70 | 0,39 | 7,5 | 1,14 | 581 | 421 | 39,2 | - |
| 111,0 | 0,80 | 0,27 | 8,4 | 1,10 | 547 | 397 | 38,6 | - |
| 81,5 | 0,90 | 0,15 | 9,3 | 1,06 | 508 | 368 | 33,7 | - |
| 44,8 | 1,00 | 0,04 | 10,2 | 1,01 | 457 | 331 | 22,6 | - |
| 9,8 | 1,10 | 0,00 | 11,2 | 0,97 | 415 | 301 | 6,0 | - |
| 0,0 | 1,13 | 0,00 | 11,5 | 0,95 | 405 | 294 | 0,0 | - |



OĞUZCAN MERCAN

| | |
|--|--|
| Permanent Address: Bahcelievler Mah. Kirazlı Sok. Yucel Apt. 16/2 Bahcelievler 34180 Istanbul / Turkey Mobile: +90 555 972 54 34 E-Mail: mercanoguz@gmail.com | Birth Date: 11/11/1986 Birth Place: Beyoglu/Istanbul Citizenship: T.C. Military Service: Completed (2014) |
|--|--|

Education

| | |
|--------------------|--|
| on-going | MSc, Inst. of Pure and App. Sci., Mechanical Engineering (EN) Marmara University, Istanbul/TURKEY Current GPA: 3.79 / 4.00 |
| 2005 - 2010 | BSc, Faculty of Engineering, Mechanical Engineering (English) Marmara University, Istanbul/TURKEY GPA: 2.64 / 4.00 |
| 2004 - 2005 | Marmara University, Istanbul/TURKEY School of Foreign Languages, Professional |

Experience

05/2014 – on-going Miksan Motor San. ve Tic. A.S Istanbul/TURKEY

Management and monitoring of projects supported by official institutes. Design and development of centrifugal pumps for machine tools using engineering software ANSYS and open source CFD software OpenFOAM. Assembly and performance testing of first prototype pumps.

12/2011 – 10/2013 Miksan Motor San. ve Tic. A.S Istanbul/TURKEY

- 08-09/2008 Mercedes-Benz Türk A.S Istanbul/TURKEY**
ME400 Summer trainee – 5 weeks of training in Central Procurement – Chassis Procurement.
- 07-08/2008 Grundig Elektronik A.S Istanbul/TURKEY**
ME400 Summer trainee – 5 weeks of training in Quality Assurance and Quality Control.
- 07-08/2007 Sistem Reklamcılık A.S Istanbul/TURKEY**
ME300 Summer trainee – 6 weeks of training on machining

Skills

| | | |
|-------------------------|--------------------|---------------------|
| Software Skills: | AutoCAD (well) | ANSYS (well) |
| | Solid Edge (well) | MATLAB (medium) |
| | Solid Works (well) | OpenFOAM (beginner) |
| | Catia (medium) | MS Office (well) |
| Language Skills: | Turkish (native) | |
| | English (fluent) | |

Publications and Conferences

- Mercan O., Develi D., Ayder E., Effects of Inducer on the Performance of Centrifugal Pump, 9th Pump-Valve-Compressor Conference, Istanbul, 2016
- Kentli, A. & Mercan, O., Application of Different Algorithms to Optimal Design of Canal Sections. *Journal of Applied Research and Technology*. Vol. 12, pp 762-768, 2014
- Ekici B., Ak E., Mercan O., “The Role of Finite Element Method in the Stent Design Methodology”, ISCSE2011 International Symposium Gediz University Izmir, 2011